Electrochemical Co-Deposition of Metals Coating

A Thesis
Submitted to the College of Engineering of
Al-Nahrain University in Partial Fulfillment of the
Requirements for the Degree of Master of Science
in Chemical Engineering

by
Ahmed Yaqdhan Mousa Al-Shaybi
(B.Sc. in Chemical Engineering 2002)

Rabee ii 1426
April 2005

CERTIFICATION

We certify that the preparation of this thesis titled **"Electrochemical Co-Deposition of Metals Coating"** was made by **Ahmed Yaqdhan Mousa Al-Shaybi** under our supervision at Al-Nahrain University, College of Engineering, in partial fulfillment of the requirement for the degree of Master of Science in Chemical engineering.

Signature:
Name: Prof. Dr. Qasim J.M Slaiman
(Supervisor)
Date: 4/ 6/2005

Signature:
Name: Dr. Naseer A. Habobi
(Supervisor)
Date: 1 / 6 /2005

Signature:
Name : Prof. Dr. Qasim J.M Slaiman
Head of Chemical Engineering Department
Date: / /

CERTIFICATE

We certify, as an examining committee, that we have read the thesis entitled **"Electrochemical Co-Deposition of Metals Coating"** and examined the student **Ahmed Yaqdhan Mouse Al-Shaybi** in its content and found it meets the standard of thesis for the degree of Master of Science in Chemical Engineering.

Signature: Naseer
Name : Dr. Naseer A.Habobi
(Supervisor)
Date : 1/6/2005

Signature:
Name : Prof. Dr. Qasim J.M.Slaiman
(Supervisor)
Date : 4/6/2005

Signature:
Name : Dr. Saad A.Jafar
(Member)
Date : 24/5/2005

Signature:
Name : Dr. Nawal E.Abd Al lateef
(Member)
Date : 28/6/2005

Signature:
Name : Prof. Dr. Albert Elia Yousif
(Chairman)
Date : 1/6/2005

Approval of the College of Engineering.

Signature:
Prof. Dr. **Fawzi M. AL-Naima**
(Dean)
Date : 12/7/2005

Abstract

The present work has been mainly aimed to find a relationship between current densities of individual copper and zinc anodes with percentages of brass alloy plating in certain solutions .The influence of various variables on the individual plating of copper and zinc that would provide good plating on graphite bar (cathode) using copper and zinc as anodes has been investigated. The cathodic current efficiencies are also investigated under various values of temperature, time, cathodic current density, and concentrations of CuCN in copper bath and ZnO in zinc bath.

The important factor in alloy deposition is the deposition potential determined by polarization processes occurring on cathode rather than the standard potential of the two metals as determined by the e.m.f series. The use of complex solutions (cyanide) is to bring the deposition potential of two different metals closer together than is possible in aqueous solution.

The performance of cathodic current efficiency has been tested for four major factors that affect the plating process. These were temperature, , time of plating process, cathodic current density and concentration of CuCN in copper plating and ZnO in zinc plating.

The results showed that the cathodic current efficiency increasing with increasing temperature, time of plating and concentration of both CuCN in copper bath and ZnO in zinc bath and decreases with increasing cathodic current density.

An empirical equation expressing the relationship between copper current density(i_{Cu}) and zinc current density(i_{Zn}) with percentages of brass alloy(Cu%, Zn%) plating has been obtained as follows:

$$\mathbf{i_{Cu}/i_{Zn} = 0.719735 + 0.005395 * \exp(0.082058 * Cu\ \%) - 0.001086 * \exp(0.082123 * Zn\ \%)}$$

The conditions of equation above are bath temperature 50 ^{0}C and 200RPM, in a solution of 17.5 g/l CuCN, 12.5 g/l ZnO, 38 g/l NaCN and 96.1 g/l NaOH.

List of Contents

Chapter One

Introduction

Chapter Two

Literature Survey and Theory of Electroplating

Chapter Three

Experimental Work

Chapter Four
Results and Interpretation

Chapter Five

Discussion

Chapter Six

Conclusions and Recommendations for Future work

List of Symbols

Symbol	**Definition**	**Unit**
$A_{cath.}$	Surface area of cathode	cm^2
Conc.	Concentration	g/l
Cu%	Copper percentage	-
Eff. %	Cathodic current efficiency	-
E	Deposition potential	V
E^0	Standard potential	V
$E_{corr.}$	Corrosion potential	V
F	Faraday constant 96487	Coulomb/equiv.
I	Total current	mA
i	Current density	mA/cm^2
i_{Cu}	Copper current density	mA/cm^2
i_{Zn}	Zinc current density	mA/cm^2
P	Rate factor	V
Q	Amount of electricity passed through cell	Coulomb
R	Universal gas constant	8.314 j/mol.K
SCE	Saturated Calomel Electrode	-
t	Exposure time	min.
T	Temperature	^oC
w	Experimental weight of deposit	g
w_t	Theoretical weight of deposit	g
w_{iCu}	Theoretical weight of copper deposit	g
w_{iZn}	Theoretical weight of zinc deposit	g
W_{act}	Actual weight	
ΔW	Weight loss	g
z	The charge number	-
Zn%	Zinc percentage	-

Chapter one

Introduction

1.1 Electroplating

Electroplating is an electrochemical process by which metal is deposited on a substrate by passing a current through the bath. Usually there is an anode (positively charged electrode), which is the source of the material to be deposited; the electrochemistry which is the medium through which metal ions are exchanged and transferred to the substrate to be coated; and a cathode which is the substrate (the negatively charged electrode) to be coated [1].

The process of metal deposition generally consists of several partial processes:

1. Transport of ions to be deposited from the bulk of the solution to the cathode surface through migration and diffusion.
2. Charge transfer reaction: the simple metallic ions are then discharged at the electric double layer.
3. Electrocrystallization process: the discharged metal atoms are then changed into crystalline state [2].

In the case of materials such as gold, the anode is not sacrificial (gold does not dissolve easily), but it is made out of material that does not dissolve in the electrolyte, such as titanium. The deposited gold comes out of the solution. Plating is an oxidation-reduction reaction, where one material gives up electrons (gets oxidized) and the other material gains electrons (gets reduced). The anode is the electrode at which oxidation occurs, and the cathode is the electrode at which reduction occurs [1].

The electroplating process depends on a great number of factors affecting the nature and properties of deposits, among these factors are current density, conductivity of the solution, presence of addition agents, agitation, temperature and the nature of the base metal (substrate) [2].

The first plating comes from Sumerian Battery which is a device found in Baghdad, Iraq with age 2,000 years old and consists of an earthenware shell, with a stopper composed of asphalt. Sticking through the top of the stopper is an iron rod. Inside the jar the rod is surrounded by a cylinder of copper [3], which is believed to be a crude battery used for electroplating [4].

Practically the first alloy electroplates were made in the decade 1835-1845, the same era when electrodeposition of individual metals began. They were alloys of the noble metals and brass (Cu-Zn). Also alloy deposition is governed by the same variables and parameters as individual metal plating [5].The first plating solution is made from the sulfates of copper and zinc converted to carbonates and dissolved in potassium cyanide operating at low current densities [5]. Many alloys are commercially electrodeposited and these depositions generally involve complex solutions such as cyanides or pyrophosphates. The important factor in alloy deposition is the deposition potential which is determined by the polarization processes occurring at the cathode rather than the standard potentials of the two metals as determined by the e.m.f. series [6].

Complexing of metals alters the deposition potential as they are usually used to bring the deposition potentials of two different metals closer together than is possible in aqueous solution [6]. The present work is plating binary alloy (brass) onto a cathode bar by taking two separated anodes (Cu &Zn) in cyanide bath and by applying different optimum currents for each anode to gain different percentages of brass being plated at cathode bar.

1.2 Scope of the work:

1. Study the effect of
    a. Agitation speed (100, 200 and 300 RPM) on polarization process.
    b. Temperature (40, 50 and 60°C) on polarization process and current efficiency.
    c. Current density (10, 20, 30 and 40 mA/cm^2) on current efficiency.
    d. Concentrations on polarization process and current efficiency.

2. Cathodic polarization curves for copper and zinc deposition to show the behaviour under different temperatures and agitations.

The production of a thin coating of one metal on another by electrodeposition is very extensively used in industry and is continuing to enlarge its useful functions. Various plated metals and combinations thereof are being used for different purposes as illustrated below [7]:

1. Decoration and protection of metals against corrosion.... nickel and chromium.

2. Protection against corrosion……………………………………cadmium or zinc

3. Protection against wear……………………………………..chromium

4. Build-up of a part or parts undersize…………………………..chromium or nickel

5. Plate for rubber adhesion………………………………………brass

6. Protection against carburization and for brazing operations…...copper and nickel

Chapter two

Literature Survey and Theory of Electroplating

2.1. History of electroplating

The early history of electrodeposition of precious metals onto lesser metal can be reliably traced back to around 1800. Italian chemist and university professor Luigi Brugnatelli, is considered by many as the first person to utilize gold in the electroplating process. Brugnatelli was a friend of Allisandro Volta, who had just discovered the chemical principles that would later lead to the development of "voltaic"electrical batteries. Volta's first practical demonstration of this was called a "Voltaic Pile." As a result, Brugnatelli's early work using voltaic electricity enabled him to experiment with various metallic plating solutions. By 1805, he had refined his process enough to plate a fine layer of gold over large silver metals. Brugnatelli wrote: *"I have lately gilt in a complete manner two large silver medals, by bringing them into communication by means of a steel wire, with a negative pole of a voltaic pile, and keeping them one after the other immersed in ammoniuret of gold newly made and well saturated"* [8].

From the early 1800's to about 1845, two main commercial processes for coating objects in gold were utilized. For low costs, immersing an object in a diluted form of gold chloride solution (water gilding) allowed a very thin flash of gold to be deposited onto inexpensive objects. For objects where durability and value were required, a dangerous process utilizing mercury amalgam and gold leaf (fire gilding) was the main technique for achieving a thick, durable gold plate over a surface. By 1839, scientists in Great Britain and Russia had independently devised metal deposition a process similar to Brugnateli's, for the copper electroplating of printing press plates [8].

In Russia, large scale gold plating for cathedral domes, icons and religious statues were being successfully completed. Electroplating baths and equipment based on the patents of the Elkingtons were scaled up to accommodate the plating of numerous large scale objects. Eventually the use of old techniques such as mercury amalgam gold gilding and water gilding were largely displaced by the electroplating process. As knowledge of electrochemistry broadened, its relationship to the electroplating process became more widely known [8].

Electroplating processes for bright nickel, brass, tin, and zinc were adapted for commercial purposes by the 1850's. Many of these types of platings were utilized for specific manufacturing and engineering applications [8].

As the industrial age and financial capital expanded from Great Britain to the rest of the world, electroplating processes would find more usages in the manufacturing of goods and services [8].

Despite the expansion of electroplating processes to other industries, no significant scientific developments were discovered until the emergence of the electronic industry in the mid-1940. With the exception of some technical improvements to direct current (D.C.) power supplies, the late 1940's witnessed the rediscovery of heavy gold plating for electronic components. By the mid-

1950's, the utilization of new and safer plating baths based on acid formulas, began to displace some of the traditional cyanide based formulas in large scale commercial use. The 1970's led to numerous regulatory laws for waste water emissions and disposal that set the direction for the electroplating industry for the next 30 years. Improvements in chemical formulas and technical hardware allowed for the rapid and continuous plating of wire, metal strips, semiconductors and complex metal shapes [8].

Today, chemical developments and a greater understanding of their underlying electrochemical principles, have led to sophisticated plating bath formulas. Greater control over the working characteristics, layer thickness, and performance of electroplated finishes are being achieved. New chemical developments have enabled greater plating speed, throwing power and high quality reliable plated finishes [8].

The electroplating of exotic materials such as platinum, ruthenium and osmium are now finding broader usages on electronic connectors, circuit boards and contacts. Many experts believe that the expansion of the telecommunication industry will be increasingly dependent on new and innovative electroplating technology. The electronic industry and the need to support the expansion of their underlying infrastructure continue to drive improvements worldwide in the electroplating industry [8].

Future progress in waveform technologies for (D.C.) power supplies may lead to even greater achievements for the electroplating and metal finishing industry. In addition, safer "closed loop" manufacturing processes and waste water recycling will continue to reduce work related exposure to harmful chemicals and waste byproducts [8].

Electroplating processes for all types of decorative and technical plating applications will continue to find new applications as manufacturing capabilities expand into emerging global markets [8].

2.2. The Deposition Process…

2.2.1 Metal Deposition Mechanisms:

According to the modern concepts, a metal crystal or grain consists of metal ions located in regular lattice position, togather with a cloud of moving electrons, equal in number to the charge of metals ions. These electrons are more or less free to distribute themselves among the ions according to the certain distribution laws. Each ionic charge is neutralizing by the electronic charge when averaged over a period of time or over a number of ions according to Pauling [9]. This arrangement gives rise to resonating bond forces responsible for cohesion and the resulting physical properties of the metal crystal [5].

As an electrode normally carries an electric charge, when in solution it attracts water molecules, which are dipoles, as well as ions carrying charges of the opposite sign. Water molecules may be held by adsorption forces which are often quite strong. Ions are held near the metal surface by electronic attraction, forming an electrical double layer with a measurable capacitance. From this layer metal ions may reach the metal surface, eventually finding their way to stable position in the metal lattice, releasing their ligands, with overall charge neutralization [5].

This process constitutes a spontaneous flow of cathodic current. Simultaneously, lattice ions in neighboring localities may be sufficiently loosened from lattice forces to coordinate with some of the adsorbed water molecules, eventually moving into the ionic side of the double layer as hydrated ions, and then into the solution. This outward movement of positive charge constitutes an anodic or dissolution current [5].

When the electrode potential is at its equilibrium value, the anodic and cathodic currents are precisely equal, and there is no net change. The current flowing is called the *exchange current*. In single salt solutions, metals such as tin and lead have very high exchange current; if the metal is in an amalgam, they exceed 200mA/cm^2 [10]. For copper and zinc, exchange current is about 0.02mA/cm^2, and for transition metals such as nickel, 2×10^{-6}mA/cm^2 [11]. The relative magnitudes of these exchange currents place the metals in the same groups as the relative rates at which their respective ions undergo ordinary chemical reaction involving exchange of ligands, as expected, since electrode reactions involved exchange of solvent ligands with metallic coordination bonds. The presence of adsorbed impurities or addition agents sharply decreases the exchange currents, because these substances tend to bond preferentially and more strongly than the water ligands [5].

If one considers the overall changes as an ion is deposited, energy must be expended to strip the ligand water molecules from the metal ion, but energy is released as the ion finds its place in the metal lattice. The relative magnitudes of these two energies determine the potential for the reaction [5].

2.2.2 Current efficiency:-

The ratio of the weight of metal actually deposited to that would have resulted if all the current had been used for depositing it is called the *current efficiency* with respect to metal deposition. An efficiency of 96% in nickel plating means that 4% of the current was used in depositing hydrogen or in other reductions (such as that of Fe^{3+}). With respect to sum of all electrolytic processes occurring at an electrode, the efficiency is, of course, 100%, in accordance with Faraday's laws. Similar efficiency quotients apply also to the anode [5].

Besides containing the desired weight of metal, deposits should be distributed in an acceptable fashion on the cathode surfaces. Generally uniform thickness is sought, though as a rule it can only be approximated; or leveling of a rough surface is wanted. Pores, cracks, and other discontinuities are usually undesirable. The deposits should have the specific brightness, hardness, ductility, internal stress, and resistance to corrosion. Baths are formulated to permit achieving these objectives at reasonable rates and costs [5].

The cathodic current efficiency (Eff %) is calculated simply according to Faraday's laws from the relation:

$$\text{Eff}\ \% = w/w_t \times 100 \qquad \ldots 2.1$$

where (w) is the experimental weight of the deposit and (w_t) is the theoretical weight of the deposit. The theoretical weight of the individual metal deposited can be calculated as follows:

$$w_t = \frac{Q}{Faraday's\,Const.} \times Equivalent\ Weight\ of\ metal \qquad \ldots.\ 2.2$$

where (Q = I x t) is the amount of electricity passed through the cell and expressed in ampere second and Faraday's constant is 96485 [2].

2.2.3 Complex ions:-

If a metal ion in solution is associated with chemical groups, or ligands (other than water), thus forming a complex ion, its activity is very much lower than when it is merely hydrated ("free" or "simple" ion) and, accordingly, its standard potential is shifted to more negative value. The changes may be as great as 0.6 to 0.8 V, and alter the relative positions of metal in the so-called electromotive or activity series [5]. For example, in simple salt solutions, zinc has a standard potential 1.1V more negative than copper. In cyanide baths, the standard potential of zinc is still about 0.8V more negative than that of $Cu/[Cu(CN)_2]$. But as the cyanide content increases, the copper potential becomes still more negative as copper is converted largely to higher complexes, $[Cu(CN)_3]^{2-}$ and $[Cu(CN)_4]^{3-}$, where that of zinc shows little change[12]. Eventually the copper potential becomes more negative than that of zinc. Accordingly, brass may be plated out as an alloy [5].

2.2.4 Effect of Temperature:

The advantage of higher temperature for decorative coatings include higher plating speeds, improved anode corrosion, and ability to operate more dilute baths with no less in performance. For protective coatings, the ability to use higher currents with the accompanying increase in deposition rates is of greatest importance [5], as shown in Fig 2.1.

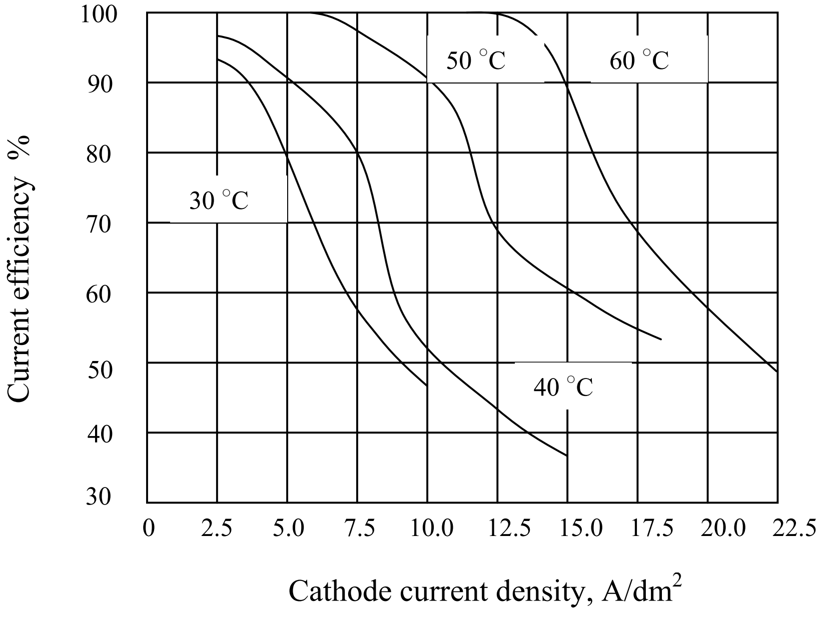

Fig. 2.1.The effect of Temperature on current efficiency in zinc plating [5].

2.3 Copper electrodeposition:

Copper electrodepositions have variety of applications in a metal finishing but the primary uses are as detailed below [6]:

1. An undercoat for surface finishes such as nickel-chromium electrodeposits on steel, aluminum and zinc-base die castings.

2. Electroforming of precision components and moulds for polymeric material.
3. Thick deposit for the restoration or build- up of worn or damaged surface not subject to heavy mechanical loading.
4. Thick deposit applied to steel as a stop-off coating in case- hardening processes such as carburizing and nitrating.
5. In the production of electronic printed circuits, and of electrotypes and printing surfaces.
6. As a base for oxidised or coloured finishes on a steel and other metals.
7. For metallisation of plastics and protection for silvered mirrors.

Copper can be electrodeposited from variety of solutions although the main baths are the acid sulfate, cyanide, pyrophosphate and more recently, fluoborate. Dull or matt, semi-bright and bright deposit of copper are possible and many proprietary solutions are also self-leveling. The inherent softness of the deposit, which facilitates mechanical polishing, is a useful attribute when copper is used as an undercoat for nickel-chromium electrodeposits, although this procedure is now less favored than brightened copper deposits [6].

2.3.1 Acid Copper Sulfate Bath

The simplest copper electrodeposition solution is the acid copper sulfate bath based on copper sulfate and sulfuric acid. The concentrations are not critical and typically can be 200-250 g/L $CuSO_4$ and 50-70 g/L $H2SO_4$, the bath can operate at temperatures 20-50 $^{\circ}C$ and current densities up to 20 A/dm^2 without agitation (and higher current densities are possible in agitated solution). Lower sulfuric acid content is used in semi-bright deposition solution whilst decreased copper sulfate levels are common in bright deposition solution. A large number of proprietary solutions are available which yield deposits that are bright and that have good leveling properties. The sulfite baths are very stable and have cathode current efficiencies of 100% although the throwing power is lower than that for cyanide and pyrophosphate solutions [6].

2.3.2 Copper cyanide Baths:

The most widely used copper electrodeposition solution is that based on copper cyanide, the solution containing sodium cyanide in order that a cuprocyanide complex is formed in solution together with some excess or free sodium cyanide. The free sodium cyanide that is present in excess of the stoichiometric requirement for complexing the copper cyanide is necessary for solution stability and reduced anode polarization. At low cyanide level the cathode efficiency increases with increase in copper cyanide content of the solution but at high free cyanide levels, the cathode efficiency decreases. The copper cyanide baths have a good throwing power and therefore are very useful for the electrodeposition of complex shaped articles [6]. Three types of cyanide baths are known, namely the strike, the Rochelle and high-efficiency cyanide baths as shown in Table 2.1.

Table 2.1. Cyanide copper bath formulations [5].

Bath No.	**1**	**2**		**3**	
Bath type	**Strike g/L**	**Rochelle g/L**		**High-Efficiency g/L**	
		Typical	**Limits**	**Typical**	**Limits**
CuCN	15	26	19-45	75	49-127
NaCN or KCN	23	35	26-53	93	62-154
				115	76-178
Na2CO3	15	30	15-60		
NaOH or KOH				30	22-37
				42	31-52
Rochelle salt($KNaC_4H_4O_6.4H_2O$)		45	30-60	optional	
*Sodium and potassium cyanide and the corresponding hydroxide and carbonates may be used interchangeably in equivalent molecular amounts.					

2.3.2.1 Strike baths:

Strike baths are used extensively to apply relatively thin coatings of copper as undercoating for other metals. Deposits from this bath vary from dull to semi-bright; the brightness or luster is not of major importance in most of its applications [5].

Copper strike baths are used primary for applying a thin coating of copper on zinc die casting before plating with other metals. The adherent copper coating prevents chemical attack when the die casting subsequently plated with a heavier coating of copper from the alkaline high efficiency baths. The thickness of strike deposits normally varies from about 0.5 to 1μm, although it may some times be as high as 2.5μm. The heavier strike deposits must be used when the subsequent plating operation is from an acid electrolyte. For instance, the copper strike deposit on zinc die casting must be three to five times as heavy for subsequent acid copper plating as compared with cyanide copper plating [5].

In addition to show a good adhesion of subsequent electrodeposits, the copper strike from cyanide baths is an additional cleaning operation. Furthermore, a thin copper strike(1.3μm) under lead coatings over steel has shown improved protective value in atmospheric exposure tests compared to lead coatings alone[13], [14]. A thin copper strike is also used over zinc die castings before bright zinc plating and bright dipping to produce a commercial bright zinc finish. This eliminates the nonuniform coverage of the heterogeneous surface composition of the castings which occurs when trying to produce the finish without the copper strike [5].

2.3.2.2 Rochelle baths:

Rochelle baths, in general, are not as sensitive to contamination as the high-efficiency baths and are used in applications where an intermediate thickness of copper is applied. Deposits from this bath vary from dull to semi-bright; the brightness or luster is not of major importance in most of its applications [5].

Rochelle baths are used for plating zinc die casting and other metals when heavy coatings of copper are not required. Good deposits in the thickness range 2.5 to 7.5μm are obtained without a copper strike. This feature, the plating of copper in one step in contrast to the two step process of striking with copper followed by plating from high efficiency baths is a major factor in the continued commercial use of this type of bath [5].

2.3.2.3 High-efficiency cyanide baths

Baths that are formulated and operated under conditions which give essentially 100% anode and cathode efficiencies are classified in this category. The rates of deposition are appreciably higher than can be obtained form strike and Rochelle baths [5].

Many of high-efficiency cyanide copper baths are used for plating of automotive bright trim parts. As pointed out earlier, Rochelle baths may be used for plating zinc die castings. Most of the installations, however, use high-efficiency baths in order to obtain the required thickness relatively quickly. The brightness of deposits from the high-efficiency baths is also an important factor [5].

Copper is also plated from high-efficiency baths on selected surfaces of ferrous metals parts to prevent carbon penetration during case hardening. Thickness requirements vary from 13 to 25 mμ, depending on the type of carburizing medium used, time of treatment in the carburizing bath, and type of surface finish on the steel. Commercial experience has shown that the newer propriety high-efficiency cyanide copper plating processes produce coatings which are superior for this application; this may be attributed to their reduced porosity [5].

2.3.3 Operating conditions:

The operating conditions of strike, Rochelle and high-efficiency baths are given in table below.

Table 2.2. Operating conditions for typical baths [5].

Bath No.	1	2	3
Bath type	**Strike**	**Rochelle**	**High-Efficiency**
Temperature, °C	41-60	55-70	60-80
Cathode current density A/dm^2	1.0-3.2	1.6-6.5	1.0-11.0
Anode current density A/dm^2	0.5-1.0	0.8-3.3	1.5-4.0
Efficiencies range Cathode %	10-60	30-70	99+
Anode%	95-100	50-70	99+
Ratio of anode to cathode area	3:1	2:1	3:2
Agitation			
Cathode rod	Optional	Preferred	Either or both
Air			
Bath voltage, V	6	6	0.75-4
Limiting thickness, mμ	2.5	1.3	Unlimited

2.4 Zinc electrodeposition:

Zinc electrodeposition is, after nickel and chromium electrodeposition, the most widely applied coating system. Zinc is applied to ferrous substrates primarily for corrosion protection but zinc electrodeposition as a corrosion protection system is economic only for coatings of 30µm or less in thickness. Above this thickness, other systems such as hot dip galvanizing and metal spraying are more suitable. Electrodeposited zinc coatings however, have certain advantages over the other processes, notably greater deposit density and ductility (due to the application of a pure zinc coating), close control of coating thickness and reduced metal wastage [6].

Several electrodeposition solutions are used for zinc, notably those based on cyanide baths, acid sulfate and chloride baths, the fluoborate solutions as well as alkaline zincates and pyrophosphate baths. Pure zinc anodes are used in all processes although the anode efficiency exceeds the cathode efficiency and for some proprietary baths zinc-magnesium or nonreactive stainless steel anodes in conjunction with zinc anodes are recommended [6].

2.4.1 Acid Zinc Sulfite Bath:

The acid sulfate solutions are popular for their faster deposition rates compared to the cyanide solution, although the throwing power is inferior and the deposits are coarser grained [6].

Deposits from the acid sulfate solution are generally whiter in color than those from cyanide baths and more malleable whilst there is a decreased tendency to hydrogen embrittlement of spring steel components. The acid sulfate solutions have higher deposition rates and greater current efficiencies (98-100%) than the cyanide baths for zinc electrodeposition. A variety of acid sulfate solutions exist and they are based on zinc sulfate with ammonium chloride, ammonium sulfate or aluminum sulfate as shown in Table 2.2, the chloride and aluminum being added to improve solution conductivity and to provide a whiter deposit. Various organic additives, such as licorice, glucose, gelatin and others are added to improve the deposit smoothness [6].

Table 2.2 Zinc electrodeposition solutions (Acid zinc sulfate solutions) [6].

Baths No.	**1**	**2**	**3**	**4**
Zinc sulfate	400	225-350	350	375
Ammonium chloride	22	14-23		
Ammonium sulfate			30	
Sodium sulfate	75			75
Aluminum sulfate		23		
Magnesium sulfate				60
Operation temperature, °C	20-30	35-50	38-55	55-65
Current density, A/dm^2	1-3	1-3	10-30	25-40

2.4.2 Zinc cyanide Baths:

The cyanide baths are most widely used and are based on zinc oxide, sodium cyanide and sodium hydroxide. A wide range of cyanide solutions are in common use and a typical bath is given in Table 2.3. The cathode efficiency of cyanide baths lies in the range 75-95% and is affected by the metal content, the sodium hydroxide (that is, the zincate) content, the sodium cyanide/zinc ratio, the solution temperature and the current density [6].

The exact relationships are fairly complex but, in general, the current efficiency increases with increase in zinc content and NaOH content, but decreases with increase in the NaCN:Zn ratio(the optimum ratio 2-2.5:1) [15] as shown in Fig.2.2.

Table 2.3 Zinc electrodeposition solution (Cyanide solutions)[6].

Bath type	**Conventional**	**Low cyanide**
Zinc as metal	60	9
Sodium cyanide	40	4
Sodium hydroxide	80	90
Operating temperature, ^0C	20-35	20-25
Current density, A/dm^2	1-10	0.1-3

The cyanide solutions may be operated in both vats and barrels although for the latter, slightly higher total cyanide and sodium hydroxide levels are used. A low cyanide bath is also used, having good throwing power and is advantageous where cyanide pollution is a problem. Careful control of metal content of the solution, however, is necessary for satisfactory operation [6]. Reaction equation when using zinc as metal [16]:

$Zn^{++}\ + 2\ NaOH \longrightarrow \underset{\downarrow}{\underline{Zn(OH)_2}}\ + 2Na^{++}$ …..2.3

$\underset{\downarrow}{\underline{Zn(OH)_2}} + 2\ NaOH \longrightarrow Na_2[Zn(OH)_4]$ ….2.4

$Zn^{++}\ + 4\ NaOH \longrightarrow Na_2[Zn(OH)_4] + 2Na^{++}$ ……2.5

Reaction equation when using zinc oxide [16]:

$ZnO\ \ +4\ NaOH \ \text{———}\ H_2O \longrightarrow Na_2[Zn(OH)_4]\ + 2\ NaOH$ ….. 2.6

At pH values around 9.5

$Na_2[Zn(OH)_4] \longrightarrow Zn(OH)_2\ + 2NaOH$ …..2.7

At pH values below 9

$$Zn(OH)_2 \longrightarrow Zn^{++} \quad + 2\ OH \quad .....2.8$$

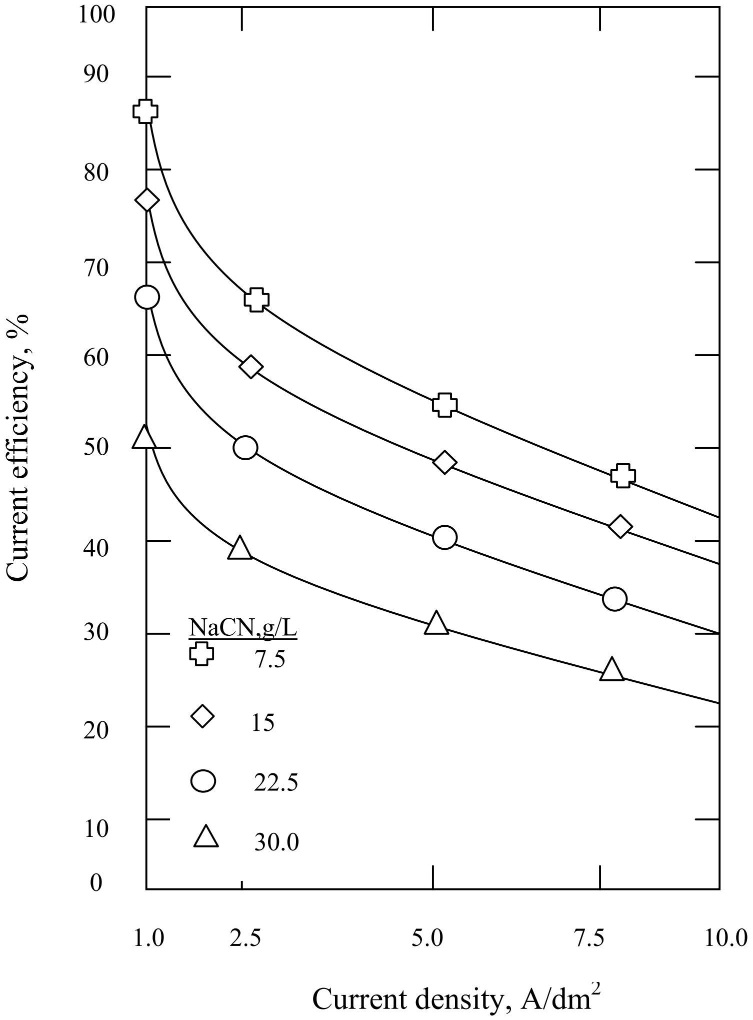

Fig.2.2 The effect of NaCN content on current efficiency in zinc plating [5].

2.5 Alloy Deposition

In any electrodeposition process there is usually more than one cathodic reaction occurring. For example, metal deposition will often occur with concomitant hydrogen evolution. The position of the individual cathodic polarization curves will determine the magnitude of the partial current densities corresponding to the individual cathodic reactions. This is illustrated in Fig.2.3. If a metal A has a more noble polarization curve than some other metal B in Fig. 2.3a, then only deposition of metal A will occur and the deposition potential of B is not attained. At cathode potential E_1, current density i_1 is found which corresponds only to the deposition of metal A. if, however, the current density is increased then deposition of metal B will also occur as the cathode potential became more active (that is , more negative). When the polarization curves or the deposition potentials of the two metal are close together in Fig. 2.3b, then at some potential E_1 the current density i_1 corresponds to deposition of both metals A and B although even at low current density the proportion of A deposited will be greater than that of metal B.The most favorable conditions for codeposition for both metals A and B occur when the polarization curves of the two metals are identical. This situation, however, is rarely found in practice. More commonly, polarization curves intersect in Fig. 2.3c, under these conditions there will be simultaneous and equal deposition of metal A and B at the intersection potential E_1, at potential more noble than E_1 the proportion of B deposition will exceed that of metal A, whilst at potentials active or negative to E_1, a greater proportion of metal A will be deposited [6].

It is common to find some intersection of the partial polarization curves. Typically the deposition of more noble metals can occur at less noble cathode potentials than that observed for discharge of the noble metal on its own.

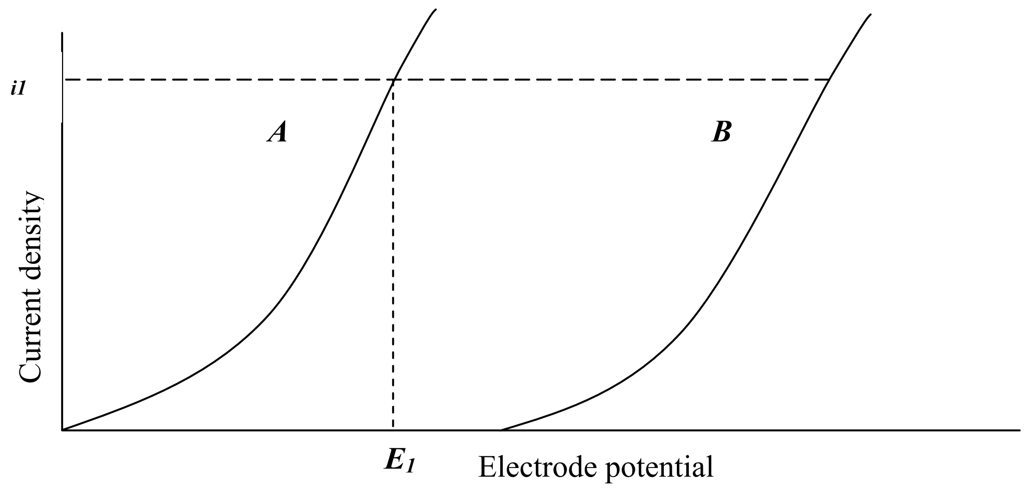

Fig.2.3a Schematic polarization curves for two metals A and B [6].

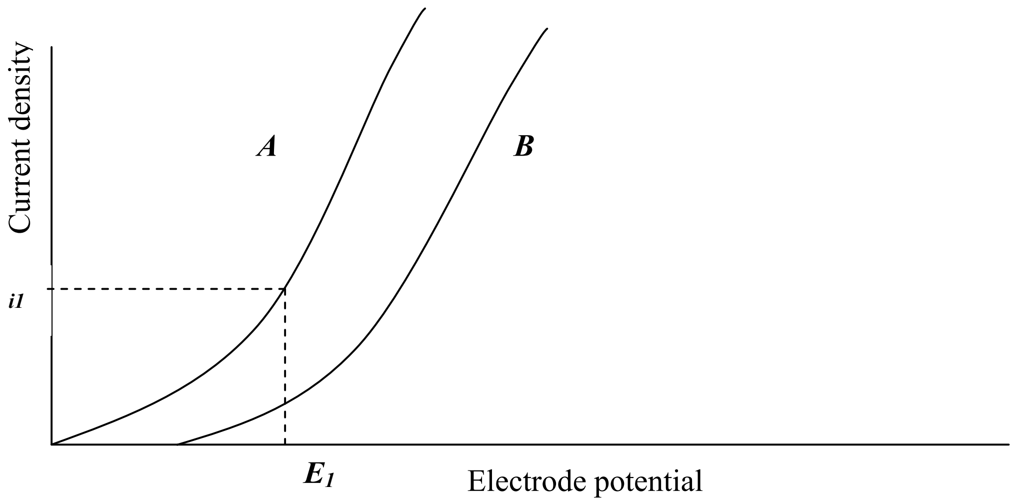

Fig.2.3b Schematic polarization curves for two metals A and B [6].

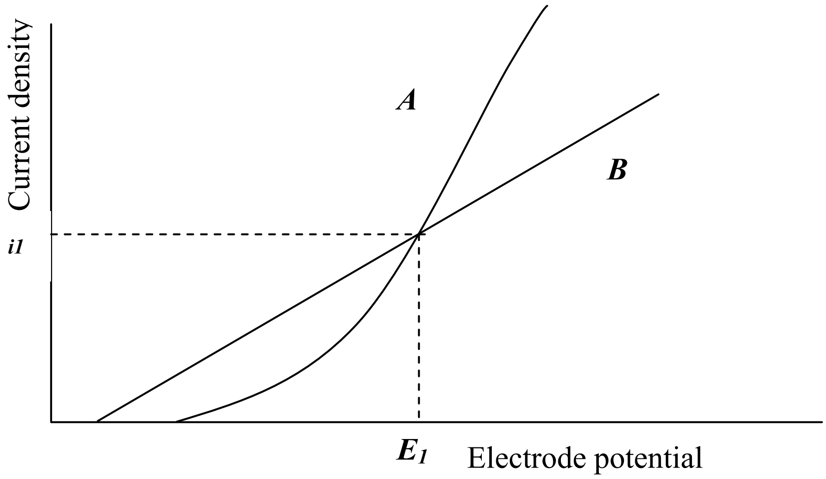

Fig.2.3c Schematic polarization curves for two metals A and B [6].

Conversely, the less noble metal can be deposited at nobler cathode potentials than when deposited alone. For a given electrolyte composition and operating conditions, the position of the cathode polarization curves for alloy relative to the curves of the separated metals will depend on the composition and electrochemical properties of the alloy to be deposited. It can be found, for example that the less noble metal will deposit preferentially (that is it functions as a more noble metal) during simultaneous deposition of the two metals. This can be found with nickel-zinc alloys. The general rule for codeposition of alloys is that the metal which is, nobler under the electrolysis conditions and which is favored during discharge is preferentially deposited to a greater degree the lower the polarization existing during deposition. All factors that increase the polarization will shift the deposition ratio in favor of the less noble metal such that its proportion in the deposit is increased. Similarly, an increase in the ratio of the less noble metal deposited is produced by a decrease in the solution temperature and in static solution. Conversely, a decrease in polarization favors discharge of the more noble metal. Thus a high solution temperature, a low current density and solution agitation will lead to the deposit having greater proportion of the more noble metal [6].

There are, however , exceptions, as for example, in gold-copper deposition where the gold is always preferentially deposited although an increase in the temperature will lead to the greater proportion of copper will be deposited. This is due to a shift in the equilibrium [6].

$$Cu(CN)_2^- + CN^- \rightarrow Cu(CN)_3^- \qquad \ldots 2.9$$

to the left so that the concentration polarization for copper is decreased [6].

Many alloys are commercially electrodeposited and these depositions generally involve complex solution such as cyanide or pyrophosphates, simple solutions are, however, also known. For example, cadmium-nickel alloys may be deposited from sulfate solution. The important factor in alloy deposition is the deposition potential which is determined by the polarization processes occurring at the cathode rather than the standard potentials of the two metals as determined by the e.m.f. series [6].

2.5.1 Principle of alloy plating

In order for two metals to codeposit, they must be in an electrolyte that provides a cathode film in which the individual deposition potentials can be the same or nearly the same. In an alloy plating bath, the static electrode potential E of a metal is given by Nernst equation [5].

The Nernst equation is named after the German physical chemist Walther Nernst who first formulated it. Its derivation is from thermodynamic principles, but for the present purposes we need consider only the equation itself. The Nernst equation links the actual (measurable) reversible potential of an electrode, *E*, to the standard reversible potential of the electrode couple, E^0 [17].

$$E = E^\circ + \frac{RT}{ZF} \ln a^{Z+} \qquad \text{.....2.10}$$

where $a^{Z+} = (a(\mathrm{RED})/a(\mathrm{OX}))$, the factor a^{Z+} is the activity of the depositing action in the film of plating bath at the cathode face [5]. E° is the "standard" equilibrium electrode potential;*R* is the universal gas constant, *T* is the absolute temperature, *Z* is the charge number of the electrode reaction (which is the number of moles of electrons involved in the reaction as written), and *F* is the Faraday constant. The notation *a*(RED) represents the chemical activities of all of the species which appear on the reduced side of the electrode reaction and the notation *a*(OX) represents the chemical activities of all of the species which appear on the oxidized side of the electrode reaction [17].

The equation refers to a condition of reversible equilibrium. Since deposition usually occurs in an irreversible process, equation (2.10) cannot indicate the potential of deposition, which is a dynamic value associated with the discharge of cations at a definite rate in an irreversible process [5].

The deposition potential *E*, as given by the equation

$$E = E^{\circ} + \frac{RT}{ZF} \ln a^{Z+} + P \quad ......2.11$$

Includes a term P, which equals E - E^{O}. P can be called a rate factor expressed as the extra potential required to keep the deposition going at the given speed under the conditions existing in the cathode film. Calculation of a metal deposition potential by equation (2.11) requires knowledge of the values of a^{Z+} and P for the given plating conditions, that is, current density, temperature, concentration and valence of all ions, ion mobility, and pH.
For example:

The $E°$ values for copper and zinc are far apart in the standard emf series and codeposition prospects would appear to be remote. This difference in potential can be eliminated or even reversed by changing the values of a^{Z+}as would result from a large change in concentration of the ions of the depositing metals, such as by complex ion formation. Calculations show, For instance, that the copper ion concentration can be made much smaller than the zinc ion concentration in cyanide solutions used for Zn-Cu alloy plating. In a solution containing simple salts of zinc and copper, the ion concentrations and the activity coefficients of the two metals are so close together that the large difference between $E°$ for copper and $E°$ for zinc cannot be reduced enough to permit good alloy plating. In a solution of the complex cyanide, the Cu^{+} concentration can be reduced to the order of 10^{-18} mole/i and the ion concentration ratio of Zn^{2+} /Cu^{+} will be very large. Calculation illustrates this for general use in consideration of alloy plating solutions for which data on the molecular composition and the dissociation constant of complex ions are employed. The copper cyanide complex is taken to be $Cu(CN)_3^{2-}$, for which the dissociation constant is $5.6x10^{-28}$and the zinc cyanide complex is taken as $Zn(CN)_4^{2-}$, for which dissociation constant is $1.3\ x\ 10^{-17}$. [5] Then

$$\frac{(Cu^{+})(CN^{-})^{3}}{Cu\ (CN)_{3}{}^{2-}} = 5.6x10^{-28} \qquad \text{.....}\ 2.12$$

$$\frac{(Zn^{2+})(CN^{-})^{4}}{Zn\ (CN)_{4}{}^{2-}} = 1.3x10^{-17} \qquad \text{......}2.13$$

To simplify, the following abbreviations are used:

$(C^{2-}) = [Cu(CN)_3^{2-}]$ and $(Z^{2}) = [Zn(CN)_4^{2-}]$

In equation (2.12), let $(Cu^{+}) = X$ and $(CN^{-}) = 3X$ and neglect the value of X in $Cu(CN_3)^{2-} = (0.05 - X)$. Then

$(X)\times(3X)^3 = (0.05)\times(5.6\ x\ 10^{-28})$

from which

$$X= 4.19\ x\ 10^{-8}$$

therefore

$$(Cu^{+})= 4.19\ X\ 10^{-8}$$

in the copper solution, and

$$(CN)^{-} = 9.57\ x10^{-8}$$

A similar calculation for the concentration of (Zn^{2+}) and (CN^{-}) in the zinc solution [using equation (2.13)] gives

$$(Zn^{2+})= 6.62\ x\ 10^{-5}$$

$(CN^-) = 2.65 \times 10^{-4}$

After the two solutions are mixed, the CN^- ion concentration would be approximately that in the zinc solution, that is, $(CN^-) = 2.65 \times 10^{-4}$, since the value in the copper solution is so much lower. Then an approximation of the copper ion concentration is again given by equation (2.12), or

$$\frac{(Cu^+)(2.65x10^{-4})^3}{0.05} = 5.6x10^{-28}$$

$$(Cu^+) = 1.5x\ 10^{-18}$$

These calculated molar concentrations of Zn^{2+} and Cu^+ can be use in equation (2.10) instead of a^{Z+} for an approximation of the two equilibrium electrode potentials, respectively, for the 0.025 M $Zn(CN)_4^{2-}$ solution and the 0.05 M $Cu(CN)_3^{2-}$ solution. At 25°C, $E°$ for copper in equilibrium with Cu^+ is +0.52 V, and $E°$ for zinc in equilibrium with Zn^{2+} is -0.76V accordingly, at 25°C, for Cu: [5].

$$E = 0.52 + \frac{0.0592}{1}\log 3.9x10^{-8}$$

$$=0.08\ \text{V}$$

for Zn:

$$E = 0.76 + \frac{0.0592}{2}\log 6.62x10^{-5}$$

$$= -\ 0.85\ \text{V}$$

Although the calculation reveals that the zinc and copper potentials have been brought nearer together, there is still a spread that might appear too great to allow codeposition. When the solutions are mixed, the Cu^+ Concentration is 1.5 x 10^{-18}. Then for copper [5].

$$E = 0.52 + \frac{0.0592}{1} \log 1.5x10^{-18}$$

$$= -0.54V$$

At an ion concentration of the order of 10^{-18}, the activity of that ion will be at least that small and probably smaller, so the actual value of E for copper will be more negative than -0.54 V. Thus, owing to the effect of $Zn(CN)_4^{2-}$,E for copper approaches much more closely that of zinc in the mixed solution. From such calculations using ion concentrations, it could be reasoned that codeposition of copper and zinc is a possibility and depends on the term P in equation (2.11), so that the codeposition potential is less than those of copper and zinc. The results may clarify the relative magnitudes of P for deposition of pure metals on themselves and for codepositing metals on their alloys [5].

2.5.2 Brass Deposition:

The most important commercial alloy deposition is that of brass, copper-zinc plating, which is not possible in aqueous sulfate solutions. The schematic polarization curves for copper, zinc, and a solution containing both metals is given in Fig.2.4. It can be seen in Fig.2.4 that the near vertical curves for copper and zinc indicate that there is a low overpotential for deposition of these two metals from solution but the deposition potentials are approximately 1V apart. Consequently, it is not possible to codeposit copper and zinc from aqueous solution. In a cyanide electrolyte, however, the two deposition potentials shift more closely together such that the polarization curves become far less noble (curve c and d in Fig.2.4) and furthermore, intersection of the two curves is found. It should be noted here that there is a greater displacement of the deposition potential of the more noble metal, copper, than is found for the baser metal zinc. The polarization curve for a brass electrodepositing solution curve e in Fig.2.4 is similar to the curves for the individual metals in cyanide solution but differs in that the deposition potential is rather nobler than that of either of the two individual metals and it has a much longer limiting current region [6].

With all brass cyanide solutions, the copper content of the deposit varies with applied current density and it is found that with increase in current density the copper content of the deposit first falls to a minimum value then increase a gain. The minimum copper content in the deposit occurs at a limiting current density of 0.5-1.0 A/dm^2. Above this limiting current density, hydrogen is evolved at the cathode and with hydrogen evolution the copper content of deposit increases again [6].

At current densities below the limiting value, copper behaves as a noble metal whilst at current densities in excess of the limiting value; zinc is the more noble metal. This behavior is due to the fact that as hydrogen evolved, the pH at the cathode increases so that the deposition potential of zinc becomes more noble whitest that of copper is unaffected. Consequently, an increase in current density and thus an increase in polarization results in an increase in the proportion of copper in the electrodeposit. Brass electrodeposition is usually performed for decorative purposes onto ferrous substrates and the deposit generally consists of

70-80% copper and 30-20% zinc. Deposition is usually, but not necessarily always, carried out with a bright brass nickel undercoat, and both matt or dull as well as bright brass electrodeposits may be produced. Furthermore, there has been some use of brass as an undercoat for nickel -cadmium deposition onto aluminum. A white brass, zinc-25-30% copper, has also been used as a bonding coat for rubber on a number of metals as well as a substitute for nickel – chromium deposits. White brass electrodeposits, however, must be of low thickness since deposits greater than 8μm thick are susceptible to cracking [6].

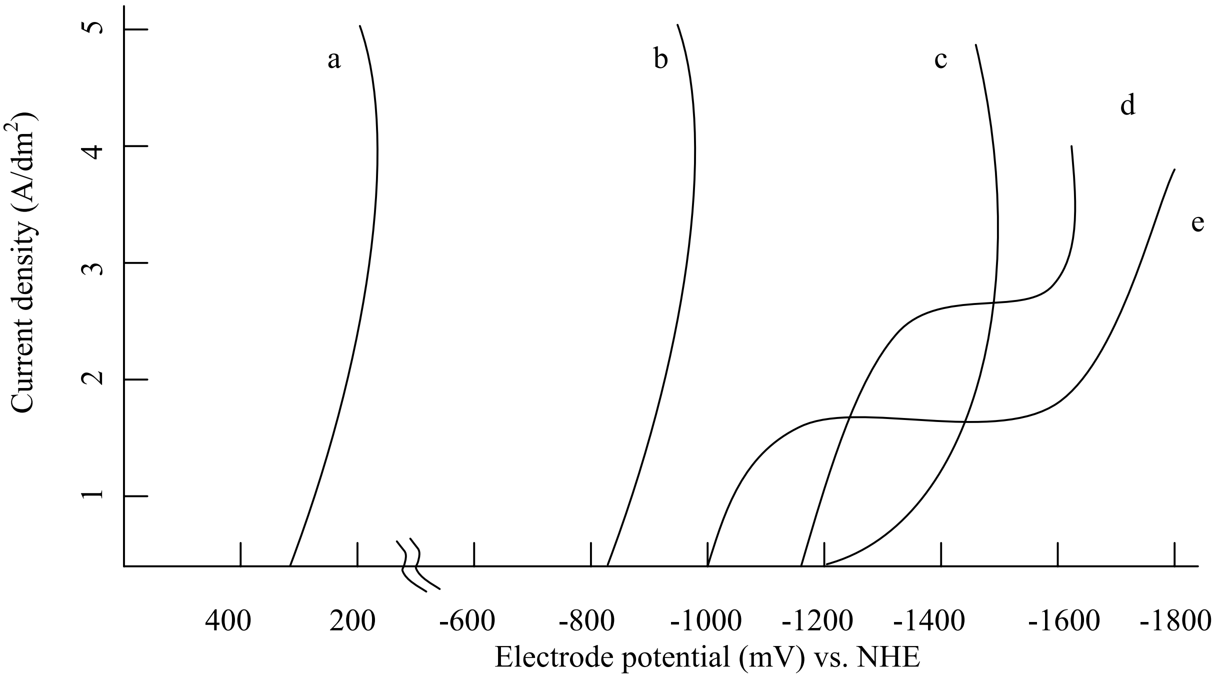

Fig.2.4 Schematic polarization curves for copper and zinc in sulfate and cyanide solution. (a) Copper in sulfate solution. (b) Zinc sulfate solution. (c) Copper in cyanide solution. (d) Zinc in cyanide solution. (e) Copper and zinc in cyanide solution (brass electrodeposition solution) [6].

2.6 Influence of common variables in alloy plating:

The independent variables such as current density, agitation, temperature, pH, and the concentration of the bath constituents influence the ratio in which two or more metals codeposit, the physical character of the plate, and the rate of deposition. An appreciable change in any one variable may be required for an appreciable and compensating change in another variable or combination of variables in order to maintain a given plate composition or physical properties, yet each variable can be considered with regard to its general effect [5].

1. Current Density:

An increase in current density tends to increase the proportion of the less noble metal in alloy plate. The extent of change is likely greater in simple primary salt solutions than in complex primary salt solutions and greater when the codepositing metals are in complex ions with common anion than when the anions of the complex ions are different. In the later case, when the metals are associated with different complex ions, an appreciable change in a current density can be permitted with little change in plate composition [5].

The limiting current density for codeposition in commercially acceptable physical form is likely to differ from the limiting current density for the influence of the physical properties of plates. Limiting current densities can be altered by using appropriate addition agents. Agitation, temperature, pH, and the like influence the current density effects. If addition agents are used, their influence on the plate composition must be considered when judging current density effects [5].

2. Agitation:

An increase in agitation usually increases the amount of more noble metal in alloy plate, thus tending to offset the effect of an increase in current density. The primary ion ratio established at the cathode face in a still bath depends on the degree of dissociation and the concentration of the primary salt or complex ion, the relative ion diffusion velocities at the given temperature, and for some complex ions, the rate of dissociation. By mechanically bringing fresh bath to the cathode film and decreasing the film thickness, agitation offsets the normal tendency for more rapid depletion of the more noble metal ions in the deposition zone [5].

The relative effect of agitation is likely to be less pronounced when the primary metal ions are associated with complex ions rather than with simple anions, and more pronounced when the two or more metals are associated with like anions rather than with unlike anions [5].

3. Temperature:

An increase in temperature usually tends to increase the proportion of more noble metal in the alloy plate, thus having the same effect as increase in agitation and the opposite effect to an increase in current density. Exception can be found in cases where the temperature effect on the degree of ionization and ion activity is relatively greater for the less noble metal. It is conceivable that temperature change in either direction from an optimum value (or narrow optimum range) can reverse the relative nobility of two codeposition metals. In such cases, an increase in current density or agitation will have a different effect on plate compositions deposited at different temperature [5].

4. pH:

The pH is generally accepted as a more factor in physical property control than in plate composition control. This is practically so in brass, Ni-Co, Ni-Zn, Ag-Pb, Cu-Sn, and Ag-Cd deposition. There have been divergent reports on the effect of pH change on plate codeposit .The differences observed could be caused by the unintentional overlooking of the effect of a change in some other variable[5].

A specific influence for pH is to be expected in determining the most efficacious addition agent, particularly where bright alloy plating is the goal, especially if bath operation is near the isoelectric point of a colloidal addition agent [5].

5. The current efficiency:

There are instances on record where the codeposition current efficiency exceeds that of the single deposition of one or both metals form the type of bath in question. When this occurs, the current efficiency depends on alloy composition. For this reason the thickness distribution of an alloy plate may differ from that expected according to the current efficiency [5].

Alloy plating has effected codeposition of some metals not depositable singly; thus the current efficiency for that metal is raised from zero to some significant value [5].

6. Throwing Power in alloy deposition:

Since current density change can alter the composition of an alloy plate, there is a question of uniform plate composition associated with throwing power. Whenever the plate composition is critically dependent on current density, the “throwing power composition” will be critical. Fortunately, alloy deposition baths can often be developed for which the current density range is wide enough to permit a good throwing power of composition over fairly irregular shapes. Knowledge of the current density effect on composition and current efficiency will give a good indication of expected throwing power, covering power, and plate composition uniformly over a surface for the particular type of bath being used [5].

7. The influence of bath concentration in alloy plating:

The ratio of primary ion concentrations M1/M2 of the depositing metals has the most determinant effect on the composition of the alloy electroplate. Increasing the ratio usually increases the ratio of the two metals in the alloy plate, but not necessarily to the same degree.

The bath concentrations in alloy deposition are usually similar to those for the single deposition of the individual metals from the same type of bath. Since the essential conditions for alloy plating are based on ion ratios, dilution or concentration of the bath has an effect only as the ion ratios are changed. A change in ion ratios with dilution or concentration depends on the relative effect on the degree of ionization, the primary salt concentration, and diffusion rates. The question of limiting concentration and of conductivity of the bath versus concentration is the same as for any metal deposition [5].

Chapter Three

Experimental Work

The present chapter illustrates the laboratory design of electroplating system as well as the experimental work.

3.1 System specifications:

a) Working cathode:

The cathode was a bar of graphite (taken from battery type JB, 777, size D), the cathode placed vertically with length of 5.5 cm and 0.6 cm in diameter. The length of cathode bar in the solution was 2cm and 0.5cm above the bottom of the solution container.

b) Working anode:

The anode was a plate of pure metal (copper or zinc); the length of the anode was 4 ×2 ×0.1 cm, located vertically opposite the counter cathode.

c) Reference electrode:

The cathodic potential was determined with respect to a Saturated Calomel Electrode (SCE) .A lugging capillary bridge leading to the reference electrode was mounted near the center along the cathode length to within (≅ 1mm) from the side of the cathode. The opening of the capillary tube near sample metal (cathode) was equal to (≅ 1mm) in diameter.

d) Glass bath: A bath was made of glass with the dimensions (30 x 14.5 x 12cm).

e) Thermometer: This is made of glass to measure temperature up to 100 °C.

f) Water bath: water bath with heater range 0-100 °C of type Memmert.

g) Insulation: A perspex separator was used with dimensions 22*12*2.5cm place in middle of the glass bath.

3.2 The electrolyte:

1. Copper bath:

- **Copper Cyanide:** 17.5 g/l CuCN.
- **Sodium Cyanide:** 23 g/l NaCN.
- **Sodium Hydroxide:** 11.1 g/l NaOH.
- **Distilled Water**

2. Zinc bath:

- **Zinc Oxide:** 12.5 g/l ZnO.
- **Sodium Cyanide:** 15 g/l NaCN.
- **Sodium Hydroxide:** 85 g/l NaOH.
- **Distilled Water**

Hydrochloric acid: HCl, Technical Hydrochloric acid of concentration 32%, supplied by *Rayon State Establishment, Saddat AL-Hindiyah* . As a cleaning electrolyte for the metal specimen (before each test) an HCl of 3% concentration is used, which had been prepared according to dilution law:

$$C_1 V_1 = C_2 V_2 \qquad \ldots (3.1)$$

C_1 : initial concentration.

V_1 : initial volume.

C_2 : final concentration.

V_2 : final volume.

As example; in order to preparing 0.5liter of an HCl of 3% concentration from 32% HCl concentration, according to dilution law we need 0.046 liter of 32% HCl, added to 0.464 liter of distilled water. A 20% HCl is needed as a cleaning electrolyte for the metal specimens (after each test), which had been prepared using the dilution procedure.

3.3 Solvents used:

These are used to clean the metal specimens.

1. **Acetone :** C_3H_6O of concentration ≅ 99% supplied by FLUKA.
2. **Ethanol :** C_2H_4O of concentration ≅ 99% supplied by FLUKA.

3.4 The electrical circuit:

The electrical circuit consisted of the following (see details in Figs.3.1, 3.2).

a) D.C Power supply: A filtered *D.C* power supply which is equipped with current and voltage limiters offers better stability and control and can be used for applying galvanostatic boundary condition. *It is type Leybold-heraeusA, with a range 0-15V and 1A).*

b) Multirange ammeter: A digital Multirange ammeter *(type DT830A, digital millimeters with range 0-0.2A)* was used to measure the total current passing through the cathodic system.

c) Multirange voltmeter: Two of Multirange voltmeter were used, one of these is to measure the working electrode/reference potential difference *(type DT830A, digital millimeters with range (0-120V)*, and the other to measure the overall voltage of the electroplating system, made by *(type DT830A, digital millimeters with range (0-120V)*

d) Multirange resistor (Resistance Box): A variable resistance *(DECADE resistance box type DR5/CDEFG with range (0-0.1 MΩ)*
with accuracy of 0.1 Ω .

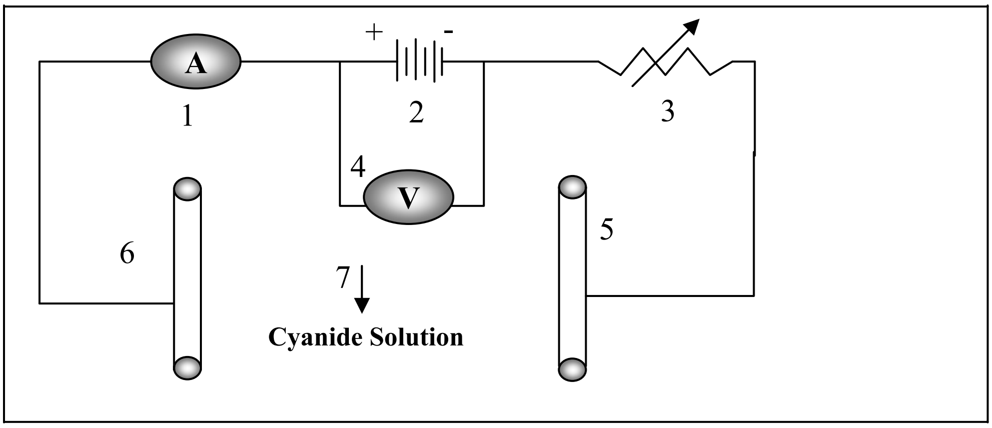

Fig.3.1.The Electrical Circuit for current efficiency.

Table 3.1 The item numbers with details as illustrated in Fig.3.1.

Item No.	Details
1	*Multirange Ammeter.*
2	*D.C Power Supply.*
3	*Resistance Box.*
4	*Multirange Voltmeter.*
5	*Cathode(graphite)*
6	*Anode(copper or zinc)*
7	*Cyanide Solution*

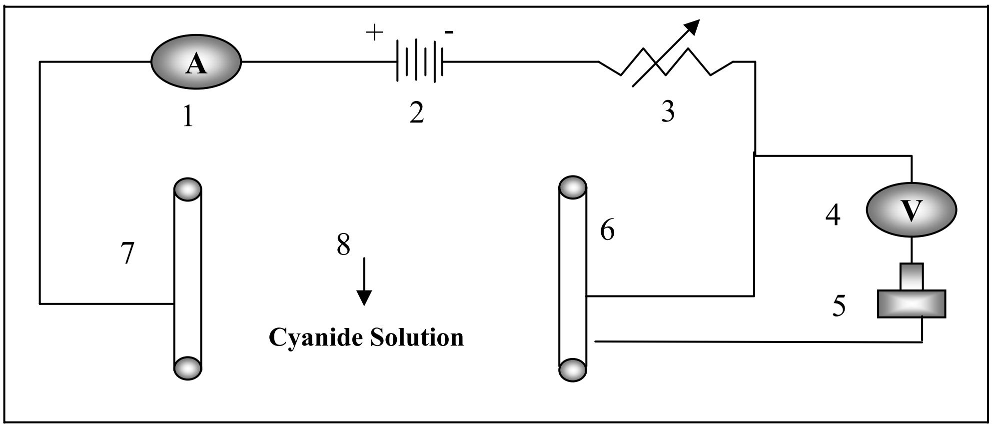

Fig.3.2.The Electrical Circuit for polarization.

Table 3.2 The item numbers with details as illustrated in Fig.3.2.

Item No.	Details
1	*Multirange Ammeter.*
2	*D.C Power Supply.*
3	*Resistance Box.*
4	*Multirange Voltmeter.*
5	*Saturated Calomel Electrode (SCE)*
6	*Cathode(graphite)*
7	*Anode(copper or zinc)*
8	*Cyanide Solution*

3.5 Experimental procedure:

3.5.1 The current efficiency procedure:

The cathode bar (graphite) was 5.5cm long with diameter 0.6 cm from dry battery(A size) and the anode plate (copper or zinc) was 3cm long with 2 cm width in order to use it in the current efficiency experiments. Before each experimental run, the metal specimen was immersed in 3% HCl for two minutes, then washed with distilled water, dried with paper tissue followed by immersing in analar methanol for two minutes, then dried and immersed in analar acetone for two minutes, and finally left to dry for 12 hour in the disscater over silica gel . Weighing the cathode (graphite) and anode (copper or zinc) were carried out using digital balance to 0.1 mg accuracy. (Analytical balance type AE260 Delta RANGE, mettler).

3.5.1.1 The current efficiency procedure for copper (anode):

a) Measuring the cathode current efficiency with concentration of copper cyanide, CuCN:

10g of CuCN, 23g NaCN and 11.1g NaOH were added to the beaker and diluted by using distilled water to 1 liter to obtain a cyanide bath solution .The electrolyte was stirred by using a magnetic mixer (Harvard / LTE) in order to obtain a homogenous solution, then the heater controller in bath was set to the required temperature 50 ^{o}C to achieve thermal equilibrium before starting the experimental run.

Before starting each run, the cathode (graphite) and the anode electrode (copper) were fixed into aluminum tube (out of solution) with the plastic stands as shown in Fig.3.3.The area of the anode electrode was 3:1 to the area of the cathode for each case.

According to references the voltage of the D.C power supply was held constant at 6 V and changing the resistance of the circuit until obtaining a total current 81 mA. The experimental run lasted 10 minutes, then the cathode was washed with distillated water and finally left to dry for 12 hour in the desiccators over silica gel. Weighing the cathode (graphite) and recorded.
The above procedure was repeated for different concentrations 12.5, 15, 17.5 and 20g of CuCN, and weighing the anode (copper) in concentration of 10, and 20g of CuCN.

b) Measuring the cathode current efficiency with current density:

17.5g of CuCN, 23g NaCN and 11.1g NaOH were added to the beaker and diluted by using distilled water to 1 liter to obtain a cyanide bath solution.

The above procedure and specifications were repeated for different total currents of 40, 120, and 160 mA. and weighing the anode (copper) at total current of 40, and 160 mA.

c) Measuring the cathode current efficiency with time:

17.5g of CuCN, 23g NaCN and 11.1g NaOH were added to the beaker and diluted by using distilled water to 1 liter to obtain a cyanide bath solution.

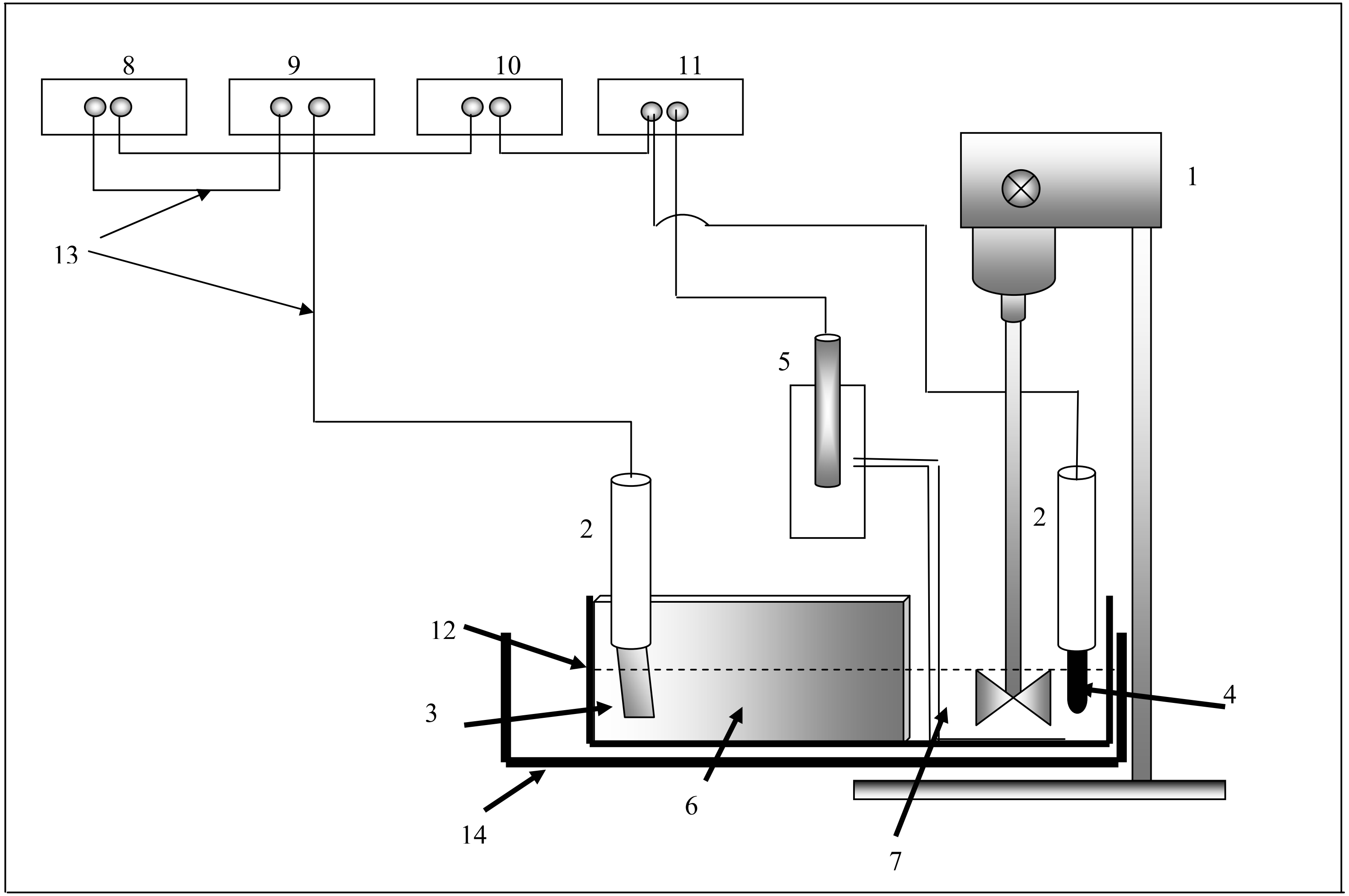

Fig.3.3 A simple sketch showing the details of the laboratory current efficiency System and its identification is given in Table 3.3

Table 3.3. The item numbers with details as illustrated in Fig.3.3.

Item No.	Details
1	*Stirrer*
2	*Aluminum stand*
3	*Anode(copper or zinc)*
4	*Cathode(graphite)*
5	*Saturated Calomel Electrode(SCE)*
6	*Insulation (Perspex)*
7	*Solution*
8	*D.C Power supply*
9	*Multirange Ammeter*
10	*Resistance Box.*
11	*Multirange Voltmeter*
12	*Glass Bath of solution*
13	*Connecting Wires*
14	*Water Bath*

The above procedure and specifications were repeated for different times 5, 15, and 20 minutes, and weighing the anode (copper) after 10 and 20 minutes.

d) Measuring the cathode current efficiency with temperature:

17.5g CuCN, 23g NaCN and 11.1g NaOH were added to the beaker and diluted by using distilled water to 1 liter to obtain a cyanide bath solution.

The above procedure and specifications were repeated for temperatures of 40 and 60 ^{o}C and weighing the anode (copper) at temperatures of 40, 50 and 60 ^{o}C. Each run was repeated twice with a third run when reproducibility was in doubt.

3.5.1.2 The current efficiency procedure for zinc (anode)

a) Measuring the cathode current efficiency with concentration of zinc oxide, ZnO:

6.25g of ZnO, 15g NaCN and 85g NaOH were added to the beaker and diluted by using distilled water to 1 liter to obtain a cyanide bath solution.

The above procedure and specifications were repeated for concentration of 12.5, 18.5, and 25g of ZnO; and weighing the anode (zinc) in concentration of 6.25, and 25g of ZnO.

b) Measuring the cathode current efficiency with current density:

12.5g of ZnO, 15g NaCN and 85g NaOH were added to the beaker and diluted by using distilled water to 1 liter to obtain a cyanide bath solution.

The above procedure was repeated for different total current of 40, 120, and 160 mA and weighing the anode (zinc) at total current of 40, and 160 mA.

c) Measuring the cathode current efficiency with time:

12.5g of ZnO, 15g NaCN and 85g NaOH were added to the beaker and diluted by using distilled water to 1 liter to obtain a cyanide bath solution.

The above procedure and specifications were repeated for times of 5, 15, and 20 minutes, and weighing the anode (zinc) after 10 and 20 minutes.

d) Measuring the cathode current efficiency with temperature:

12.5g of ZnO, 15g NaCN and 85g NaOH were added to the beaker and diluted by using distilled water to 1 liter to obtain a cyanide bath solution.

The above procedure and specifications were repeated for temperatures of 40 and 60 ^{o}C and weighing the anode (zinc) at temperature of 40, 50 and 60 ^{o}C. Each run was repeated twice with a third run when reproducibility was in doubt.

3.5.2 Cathodic Polarization Investigation Procedure:

After the solution (17.5g/l CuCN, 23g/l NaCN and 11.1g/l NaOH) preparation, the electrolyte was stirred by using a a magnetic mixer (Harvard / LTE) in order to obtain a homogenous solution, then the heater controller in bath was set to the required temperature 40 ^{o}C to achieve thermal equilibrium before starting the experimental run. The length of cathode bar in the cyanide bath was 2cm and 0.5cm above the bottom of the solution container as shown in Fig.3.3. The electrical circuit was connected to the reference electrode (SCE) after checking all the electrical connections. When the bath reached the required temperature, then the stirrer controller was set to the required RPM (200), the polarization electrical circuit was set to the (ON) position in order to draw the curve of any given condition, according to galvanostatic technique by making the voltage of the D.C power supply constant at 6V and changing the current by altering the resistance of the circuit. At each setting of the resistance two parameters were recorded (potential and cathodic current) by the voltmeter and the ammeter respectively, i.e, to measure the cathodic portion of the polarization curve. Two minutes at least were allowed in order to record the steady state values of the polarization process (see Fig.3.3).

After reaching ($E_{corr.}$) of the metal specimen used, the run was ended by putting off the power supply and water bath emptied from the used electrolyte. The system was then washed entirely by using distilled water to make sure that there was no electrolyte left in the system.

The above procedure was repeated exactly for temperatures of 50 and 60 ^oC. For other conditions of high-efficiency cyanide bath, RPM (100, 200 and 300 RPM) of stirrer and temperature (40, 50 and 60 ^oC) of solution were employed.

Also this procedure was repeated exactly for zinc with solution of 12.5g/l ZnO, 10g/l NaCN and 85g/l NaOH at different temperatures of 40, 50 and 60 ^oC. And for other conditions of cyanide bath (18.5 g/l ZnO, 15NaCN, 100 NaOH), RPM (100, 200 and 300 RPM) of stirrer and temperature (40, 50 and 60 ^oC) of solution were used. Each run was repeated twice with a third run when reproducibility was in doubt.

3.6 Brass plating with individual anodes (Cu, Zn) on cathode (graphite) procedure:

After the solution (17.5g/l CuCN, 23g/l NaCN and 11.1g/l NaOH) and (12.5 g/l ZnO, 15g/l NaCN and 85g/l NaOH) preparation, the electrolytes were blended together to obtain brass solution, stirred by using a a magnetic mixer (Harvard / LTE) in order to obtain a homogenous solution, then the heater controller in bath was set to the optimum temperature 50 ^{o}C to achieve thermal equilibrium before starting the experimental run. The cathode (graphite) and the anode electrodes (copper and zinc) were fixed into aluminum tube (out of solution) with the plastic stands as shown in Fig.3.4.The area of the anode electrodes was 3:1 to the area of the cathode for each case. The length of cathode bar in the brass bath was 2cm and 0.5cm above the bottom of the solution container as shown in Fig.3.4. When the bath reached the required temperature, then the stirrer controller was set to the required RPM (200), the electrical circuit was set to the (ON) position, with the voltage of both D.C power supply constant at 6V and changing the current by altering both resistance of the circuit in order to obtain certain current for copper and zinc respectively. The electrical circuit was set to the (OFF) position after 15 minutes. Then the cathode was washed with distillated water and finally left to dry for 12 hours in the desiccators over silica gel. Weighing the cathode (graphite) before and after by digital balance to 0. 1 mg accuracy (Analytical balance type DF625 Beta RANGE, franker) and was recorded. The cathode bar is analyzed by the *Abn-Sina company for chemical industries*

The above procedure was repeated for time of 20 and 25 minutes for each current density. The current densities were taken from polarization curve Fig5.15 tabulated in Table 3.4.

Table 3.4 The current densities at certain potential taken from Fig.5.15

Potential, mV	Current density for copper, mA/cm^2	Current density for zinc, mA/cm^2
-1026	0.4	0.12

-1050	0.55	0.55
-1100	0.7	1.8
-1207	1.84	1.84
-1300	5.5	2.7

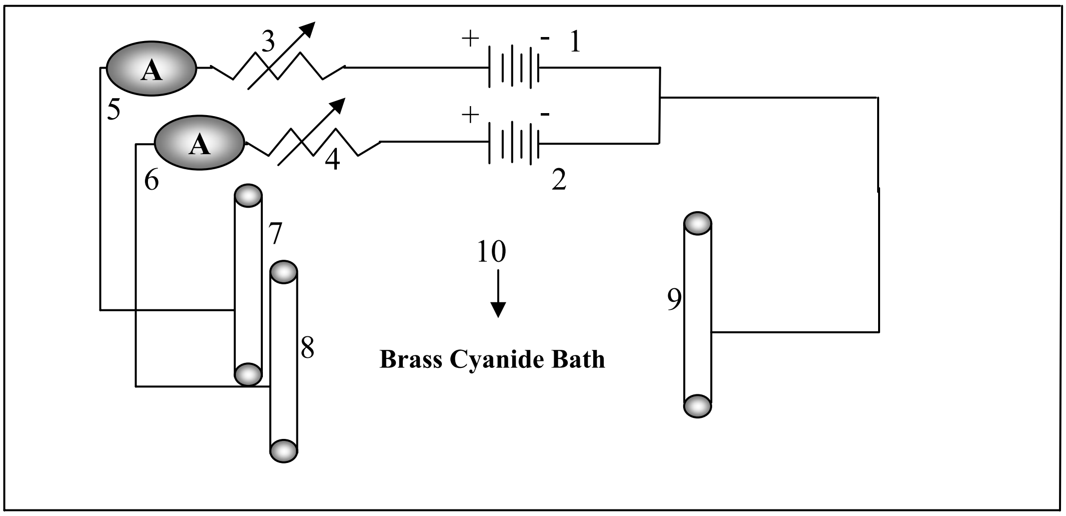

Fig.3.4.The Electrical Circuit for Brass plating with individual anodes (Cu, Zn) on Cathode (graphite)

Table 3.5 The item numbers with details as illustrated in Fig.3.4.

Item No.	**Details**
1	***D.C Power Supply1***
2	***D.C Power Supply2***
3	***Resistance Box1***
4	***Resistance Box2***
5	***Multirange Ammeter 1***
6	***Multirange Ammeter 2***
7	***Anode(copper)***
8	***Anode(zinc)***
9	***Cathode(graphite)***
10	**Brass Cyanide Bath**

Chapter Four

Results and Interpretation

4.1 Introduction:

The present work has been mainly aimed to find a relationship between current densities of individual copper and zinc anodes with percentages of brass alloy plating in certain solutions on graphite at different current densities and find relationship between copper and zinc current density with percentage of brass (copper and zinc) alloy plating. Also it is required to show the effect of concentration of CuCN and ZnO at constant temperature as described in chapter three in order to find a relationship between cathodic current efficiency, current density, time, temperature and CuCN or ZnO concentration.

Polarization (using galvanostatic technique) was used in this study under mass transfer control (copper) and under activation control (zinc) in the cathodic region of hydrogen evolution at different concentrations of different stirred solutions and temperatures. The electrode potentials are presented with reference to saturated calomel electrode (SCE). The current values reported in Appendix (A, B) are expressed per unit area, i.e., current densities. The reported results are the average values of duplicated experimental runs obtained with satisfactory repeatability.

Tables of experimental runs, classified as groups, including the experimental conditions are presently reported. Polarization curves for selected conditions are presented, while the data for the remaining experiments are tabulated in Appendix (A) for copper and Appendix (B) for zinc.

4.2 Parameters studied:

In the present work five major parameters have been studied as follows:

1. Concentration CuCN and ZnO.
2. Temperature.
3. Current density.
4. Time.
5. Agitation.

4.3 Experimental results:

4.3.1 Cathodic current efficiency:

The best indication for electroplating is cathodic current efficiency, which is calculated from equations 2.1 and 2.2 (as shown in Appendix C) with equivalent weight 31.773g for Cu and 32.69g for Zn [5].

4.3.1.1 Effect of concentration:

The effect of concentration of CuCN or ZnO on cathodic current efficiency is shown in Table 4.1a for copper and Table 4.1b for zinc. It is to be noticed that an increase in concentration of CuCN or ZnO will increase the cathodic current efficiency in both systems, Fig. 4.1a and Fig. 4.1b

Table 4.1a Cathodic current efficiency, total current (I), experimental weight of the deposit (ΔW), and the theoretical weight of deposit (Wt) for different concentrations of CuCN at time period of 10 min., T=50 °C, 200 RPM, and $A_{cath.}$ = 4.0526 cm^2 for copper solution.

Conc. CuCN g/L	$\Delta W_{act.}$(g)	I (mA)	Wt(g)	Eff%
10.0	0.0001	81	0.016004	0.62
12.5	0.0033	81	0.016004	20.61
15.0	0.0081	81	0.016004	50.61
17.5	0.0126	81	0.016004	78.73
20.0	0.0147	81	0.016004	91.85

Table 4.1b Cathodic current efficiency, total current (I), experimental weight of the deposit (ΔW), and the theoretical weight of deposit (Wt) for different concentrations of ZnO at time period of 10 min., T=50 °C, 200 RPM , and $A_{cath.}$ = 4.0526 cm^2 for zinc solution.

Conc. ZnOg/L	$\Delta W_{act.}$(g)	I (mA)	Wt(g)	Eff%
6.25	0.0119	81	0.016466	72.27
12.5	0.0130	81	0.016466	78.95
18.5	0.0141	81	0.016466	85.56
25	0.0153	81	0.016466	92.91

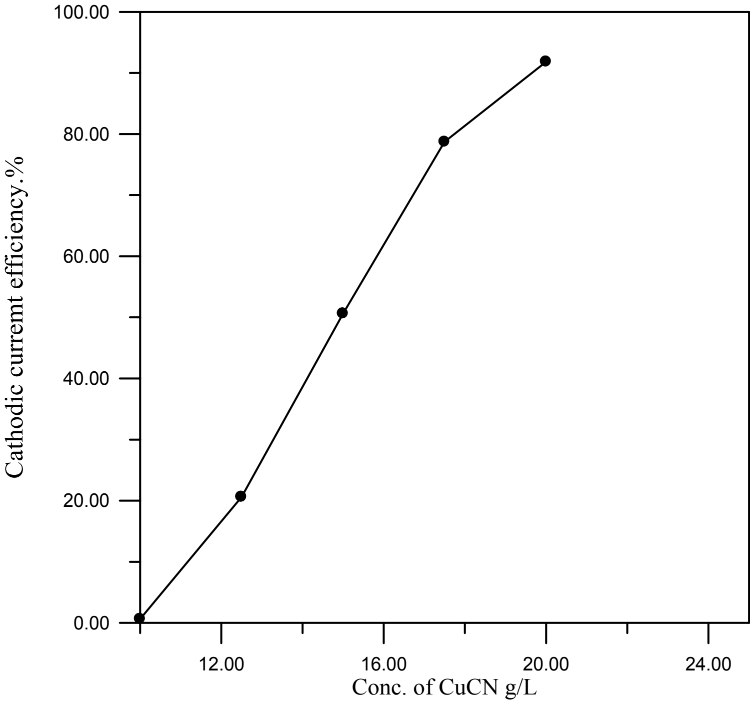

Fig.4.1a Cathodic current efficiency vs. concentrations, CuCN, of 23 g/l NaCN and 11.1g/l NaOH

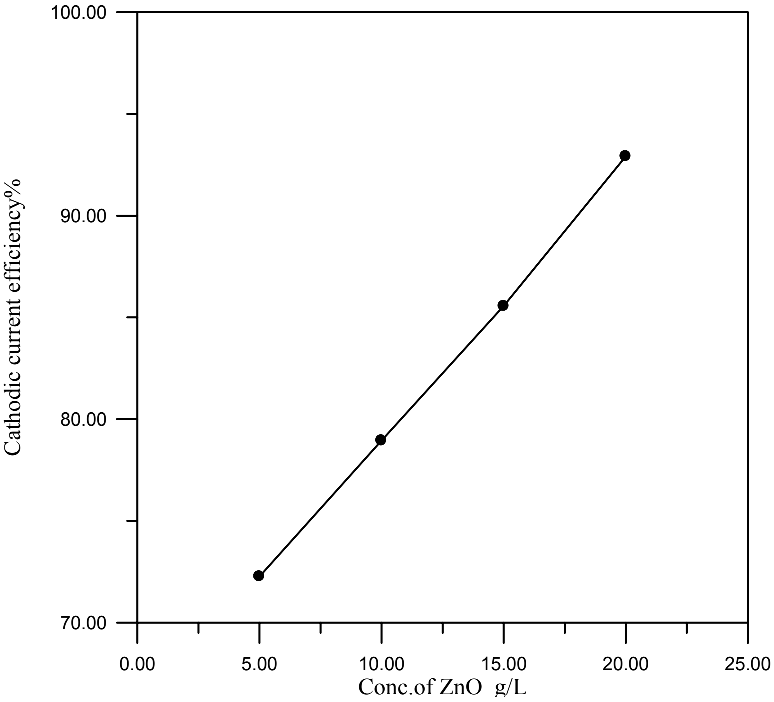

Fig.4.1b Cathodic current efficiency vs. concentrations of ZnO, 10 g/l NaCN and 85 g/l NaOH

4.3.1.2 Temperature of solution

Effect of solution temperature (copper or zinc) on cathodic current efficiency is shown in Table 4.2a for copper and Table 4.2b for zinc. The increase in temperature of both solutions will lead to an increase in cathodic current efficiency, Fig. 4.2a and Fig. 4.2b.

Table 4.2a Cathodic current efficiency, total current (I),experimental weight of the deposit (ΔW),and the theoretical weight of deposit (Wt) for different solutions temperatures for copper deposition at time period of 10 min., CuCN 17.5 g/l, 200 RPM, and $A_{cath.}$ = 4.0526 cm^2.

Temp. ^{O}C	$\Delta W_{act.}$(g)	I (mA)	Wt(g)	Eff%
40	0.0111	81	0.016004	69.35
50	0.0126	81	0.016004	78.73
60	0.0144	81	0.016004	89.97

Table 4.2b Cathodic current efficiency, total current (I), experimental weight of the deposit (ΔW),and the theoretical weight of deposit (Wt) for different solutions temperatures for zinc deposition at time period of 10 min., ZnO 12.5 g/l, 200 RPM, and $A_{cath.}$ = 4.0526 cm^2.

Temp. ^{O}C	$\Delta W_{act.}$(g)	I (mA)	Wt(g)	Eff%
40	0.0115	81	0.016466	69.84
50	0.0129	81	0.016466	78.34
60	0.0146	81	0.016466	88.66

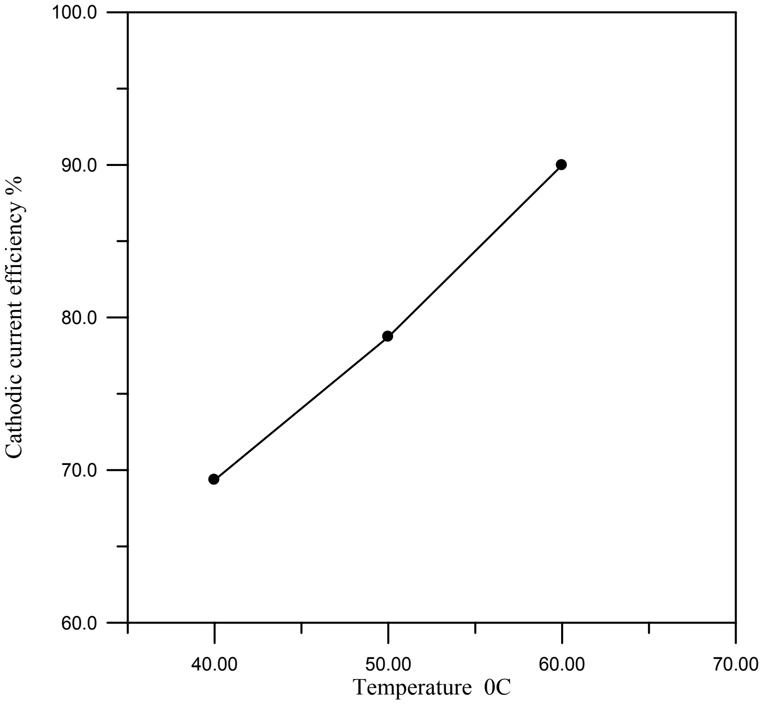

Fig4.2a Cathodic current efficiency vs. temperature in 17.5g/l CuCN, 23 g/l NaCN and 11.1g/l NaOH solution.

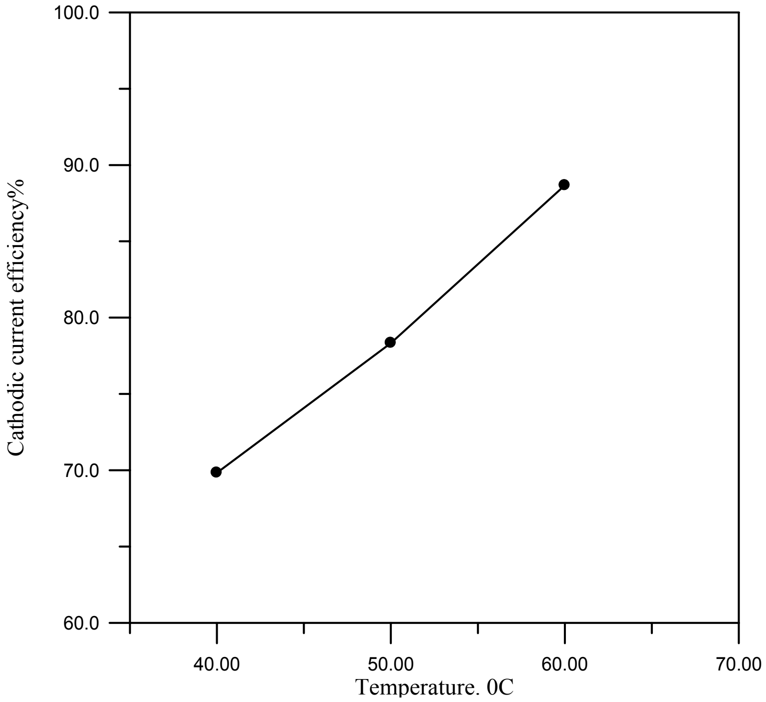

Fig4.2b Cathodic current efficiency vs. temperature in 12.5 g/l ZnO, 10 g/l NaCN and 85 g/l NaOH solution

4.3.1.3 Effect of plating time:

The effect of plating time (copper or zinc) on cathodic current efficiency is shown in Table 4.3a for copper and Table 4.3b for zinc. The increase in plating time of both solutions increased the cathodic current efficiency of both systems, Fig. 4.3a and Fig. 4.3b.

Table 4.3a Cathodic current efficiency, total current (I), experimental weight of the deposit (ΔW),and the theoretical weight of deposit (Wt) for different time periods of copper electroplate at T=50 ^{o}C , CuCN 17.5 g/l, 200 RPM, and $A_{cath.}$ = 4.0526 cm^2.

Time(min)	$\Delta W_{act.}$(g)	I (mA)	Wt(g)	Eff%
5	0.0053	81	0.008002	66.23
10	0.0124	81	0.016004	77.48
15	0.0206	81	0.024006	85.81
20	0.0286	81	0.032008	89.35

Table 4.3b Cathodic current efficiency, total current (I), experimental weight of the deposit (ΔW),and the theoretical weight of deposit (Wt) for different time periods of zinc electroplate at T=50 ^{o}C , ZnO 12.5 g/l, 200 RPM, and $A_{cath.}$ = 4.0526 cm^2.

Time(min)	$\Delta W_{act.}$(g)	I (mA)	Wt(g)	Eff%
5	0.0053	81	0.008233	64.37
10	0.0129	81	0.016466	78.34
15	0.0219	81	0.024699	88.66
20	0.0314	81	0.032932	95.34

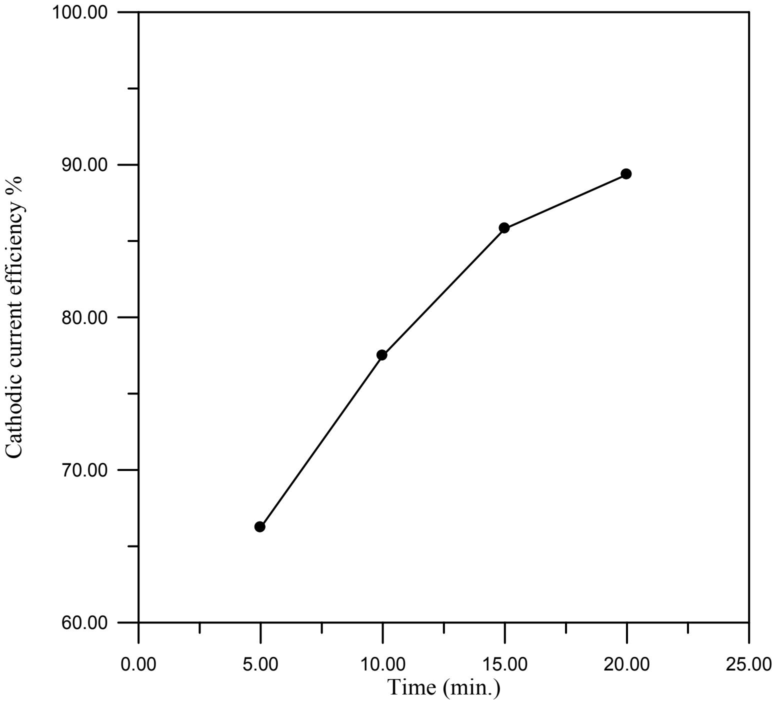

Fig4.3a Cathodic current efficiency vs. time in 17.5 g/l CuCN, 23 g/l NaCN and 11.1 g/l NaOH solution

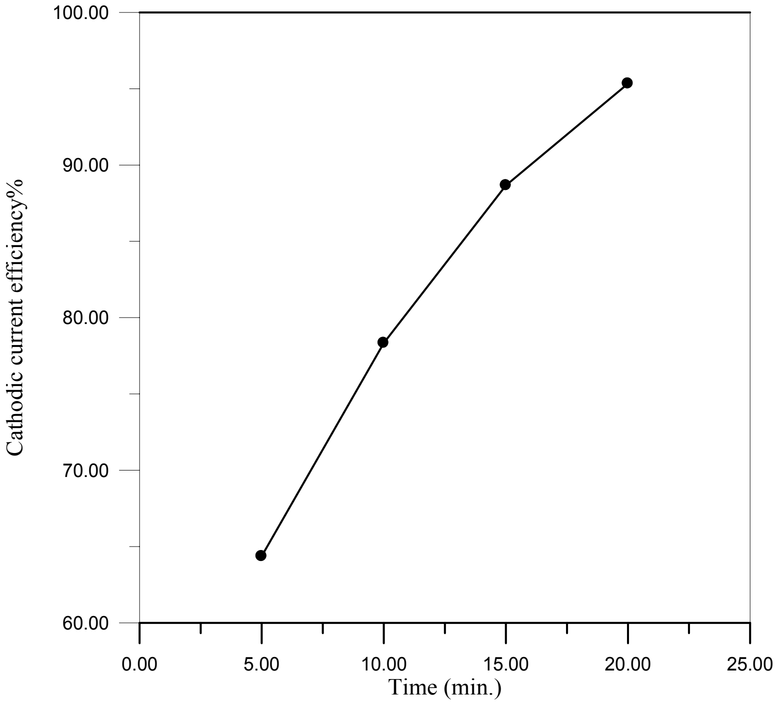

Fig4.3b Cathodic current efficiency vs. time in 12.5 g/l ZnO, 10 g/l NaCN and 85 g/l NaOH solution.

4.3.1.4 Effect of cathodic current density:

The effect of cathodic current density (for copper or zinc plating) on cathodic current efficiency is shown in Table 4.4a for copper and Table 4.4b for zinc. An increase in cathodic current density in both solutions will lead to decrease the cathodic current efficiency, see Figs. 4.4a and 4.4b.

Table 4.4a Cathodic current efficiency, experimental weight of the deposit (ΔW), and the theoretical weight of deposit (Wt) for different cathodic current densities at time periods 10 min. at T=50 ^{o}C , CuCN 17.5 g/l, 200 RPM and $A_{cath.}$ = 4.0526 cm^2 for copper plating.

C.D mA/cm^2	$\Delta W_{act.}$(g)	I (mA)	Wt(g)	Eff%
10	0.0071	40	0.007903	89.83
20	0.0125	81	0.016004	78.1
30	0.0155	121	0.023908	64.83
40	0.0178	162	0.032008	55.61

Table 4.4b Cathodic current efficiency, experimental weight of the deposit (ΔW), and the theoretical weight of deposit (Wt) for different cathodic current density at time periods 10 min. at T=50 °C , ZnO 12.5 g/l, 200 RPM, and $A_{cath.}$ = 4.0526 cm^2 for zinc plating

C.D mA/cm^2	$\Delta W_{act.}$(g)	I (mA)	Wt(g)	Eff%
10	0.0070	40	0.008131	86.09
20	0.0130	81	0.016466	78.95
30	0.0162	121	0.024598	65.85
40	0.0198	162	0.032932	60.12

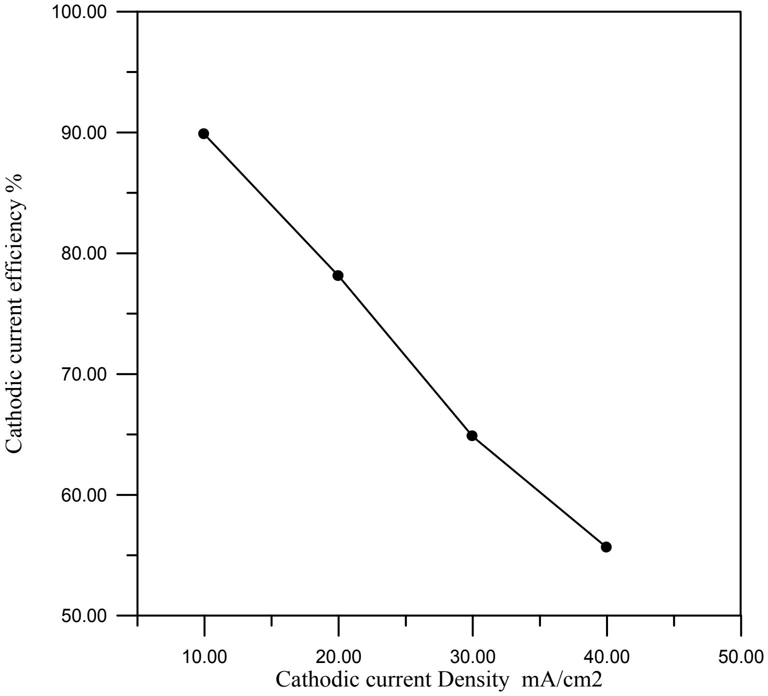

Fig4.4a Cathodic current efficiency vs cathodic current density on 17.5 g/l CuCN, 23 g/l NaCN and 11.1 g/l NaOH solution

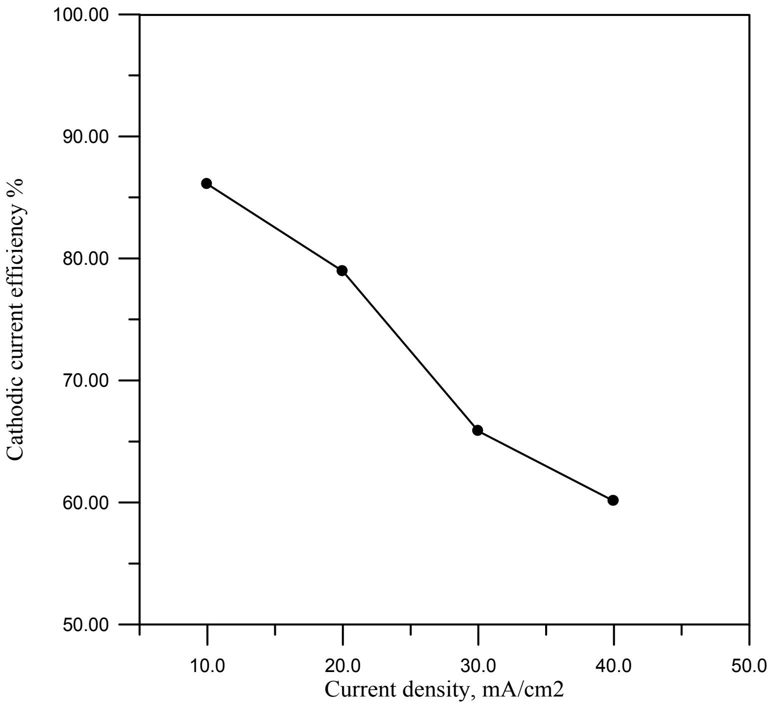

Fig4.4b Cathodic current efficiency vs cathodic current density on 12.5 g/l ZnO, 10 g/l NaCN and 85 g/l NaOH solution.

4.3.2 Anodic current efficiency:

The effect of concentration of CuCN or ZnO, temperature, time and current density on anodic current efficiency is shown in Tables 4.5a, 4.5b, 4.5c and 4.5d for copper and Tables 4.6a, 4.6b, 4.6c and 4.6d for zinc. An increase in concentration, temperature and time in both copper solution or in zinc solution will lead to increase slightly the anodic current efficiency while an increase in current density in both solutions decreased anodic current efficiency.

Table 4.5a Anodic current efficiency, total current (I), experimental weight loss of anode (ΔW), and theoretical weight of copper electroplating (Wt) for different concentrations of CuCN , time period of 10 min.,T=50 °C, 200 RPM , and $A_{cath.}$ = 4.0526 cm^2 for copper plating

Conc. CuCNg/L	$\Delta W_{act.}$(g)	I (mA)	Wt(g)	Eff%
10	0.0146	81	0.016004	91.22
20	0.0147	81	0.016004	91.85

Table 4.5b Anodic current efficiency, total current (I),experimental weight loss of anode (ΔW),and theoretical weight of copper electroplating (Wt) at different temperatures for time period of 10 min., CuCN 17.5 g/l, 200 RPM, and $A_{cath.}$ = 4.0526 cm^2 for copper plating.

Temp. °C.	$\Delta W_{act.}$(g)	I (mA)	Wt(g)	Eff%
40	0.0146	81	0.016004	91.22
50	0.0150	81	0.016004	93.72
60	0.0158	81	0.016004	98.72

Table 4.5c Anodic current efficiency, total current (I), experimental weight loss of anode (ΔW), and theoretical weight of copper electroplating (Wt) for different time period copper electroplating at T=50 °C , CuCN 17.5 g/l, 200 RPM, and $A_{cath.}$ = 4.0526 cm^2 for copper plating.

Time (min.)	$\Delta W_{act.}$(g)	I (mA)	Wt(g)	Eff%
10	0.0149	81	0.016004	93.1
20	0.0305	81	0.032008	95.28

Table 4.5d Anodic current efficiency, experimental weight loss of anode (ΔW), and theoretical weight of copper electroplating (Wt) for different current densities at time period 10 min. at T=50 °C , CuCN 17.5 g/l, 200 RPM , and $A_{cath.}$ = 4.0526 cm^2 for copper plating

C.D mA/cm^2	$\Delta W_{act.}$(g)	I (mA)	Wt(g)	Eff%
10	0.0075	40	0.007903	94.90
40	0.0232	162	0.032008	72.48

Table 4.6a Anodic current efficiency, total current (I), experimental weight loss of anode (ΔW), and theoretical weight of copper electroplating (Wt) for different concentrations of ZnO at time period of 10 min. T=50 °C, 200 RPM, and $A_{cath.}$ = 4.0526 cm^2 for zinc plating

Conc. ZnO g/L	$\Delta W_{act.}$(g)	I (mA)	W_t(g)	Eff%
6.25	0.0150	81	0.016466	91.09
25	0.0151	81	0.016466	91.70

Table 4.6b Anodic current efficiency, total current (I), experimental weight loss of anode (ΔW),and theoretical weight of zinc electroplating (Wt) at different temperatures solution for time period of 10 min., ZnO 12.5 g/l, 200 RPM, and $A_{cath.}$ = 4.0526 cm^2 for zinc plating.

Temp. °C.	$\Delta W_{act.}$(g)	I (mA)	Wt(g)	Eff%
40	0.0147	81	0.016466	89.27
50	0.0151	81	0.016466	91.70
60	0.0157	81	0.016466	95.34

Table 4.6c Anodic current efficiency, total current (I), experimental weight loss of anode (ΔW), and theoretical weight of zinc electroplating (Wt) for different time period of plate zinc at T=50 °C , ZnO 12.5 g/l, 200 RPM , and $A_{cath.}$ = 4.0526 cm^2

Time (min.)	$\Delta W_{act.}$(g)	I (mA)	Wt(g)	Eff%
10	0.0152	81	0.016466	92.31
20	0.0315	81	0.032932	95.65

Table 4.6d Anodic current efficiency, experimental weight loss of anode(ΔW), and the theoretical weight of zinc electroplating (Wt) for different cathodic current density at time period 10 min. at T=50 °C , ZnO 12.5 g/l, 200 RPM , and $A_{cath.}$ = 4.0526 cm^2 for zinc plating

C.D mA/cm^2	$\Delta W_{act.}$(g)	I (mA)	Wt(g)	Eff%
10	0.0076	40	0.008131	93.46
40	0.0251	162	0.032932	76.21

4.3.3 Cathodic Polarization curves:

The cathodic polarization curves with a well-defined limiting current plateau were obtained under different conditions.

4.3.3.1 Effect of concentration:

The effect of concentration on cathodic current –potential curves is shown in Figs.4.5a.and 4.5b.for copper and 4.6a. 4.6b. for zinc. From these figures one can notice that potential ($E_{i.}$) is less negative with increasing CuCN or ZnO concentration, due to the complex action of cyanide[20].

4.3.3.2 Effect of agitation:

The effect of agitation on cathodic current –potential curves is shown in Figs. 4.7a. , 4.7b and 4.7c.for copper and 4.8a., 4.8b., and 4.8c. for zinc. It can be noticed that current density decreased with increasing agitation (100, 200, and 300) RPM only in copper bath and little effect in zinc bath which may be negligible.

4.3.3.3 Effect of temperature:

The effect of temperature on cathodic current –potential curves is shown in Figs. 4.9a., 4.9b. and 4.9c.for copper and 4.10a., 4.10b., and 4.10c. for zinc which show that the curves are shifted to higher current densities with increasing of temperature (40, 50, and 60 ^{o}C) in both baths (Cu and Zn)

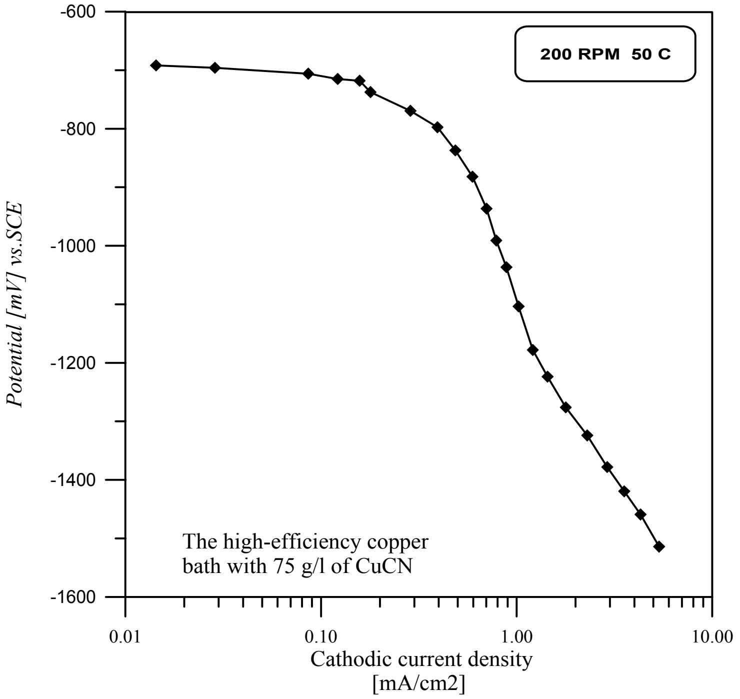

Fig4.5a Cathodic polarization curve on copper

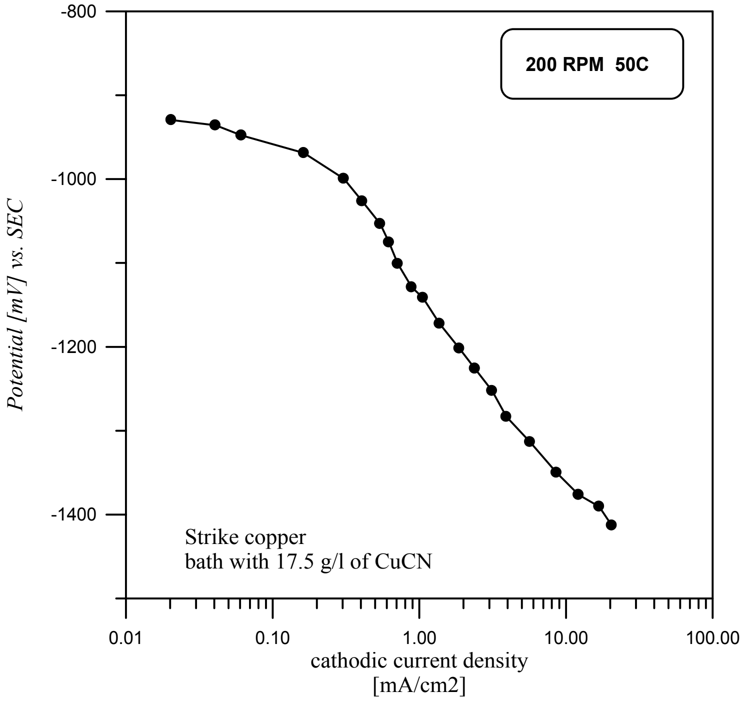

Fig4.5b Cathodic polarization curve on copper

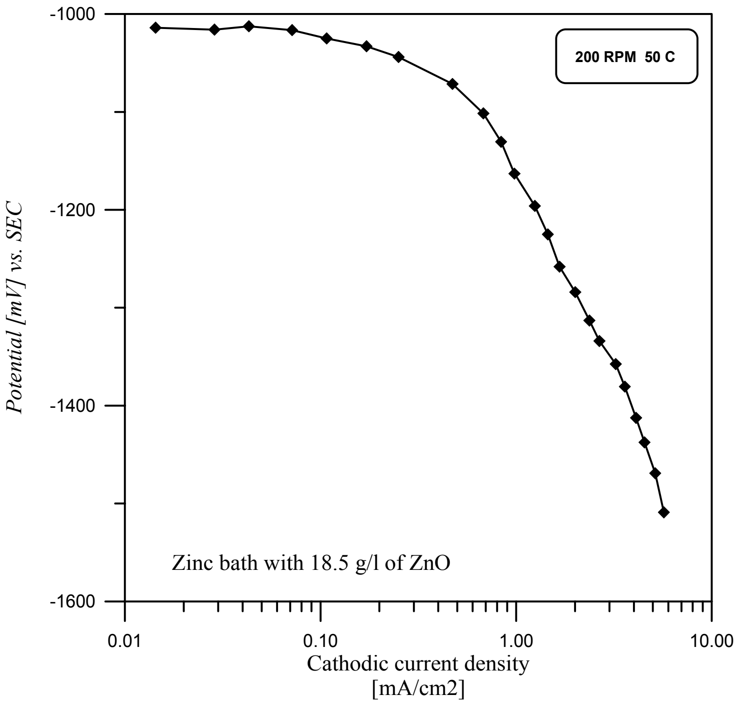

Fig4.6a Cathodic polarization curve on zinc

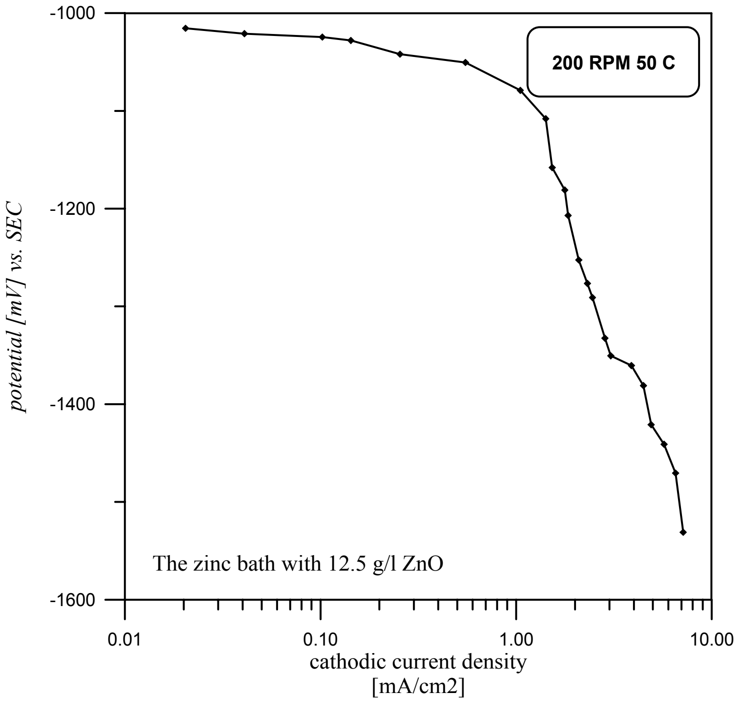

Fig4.6b Cathodic polarization curve on zinc

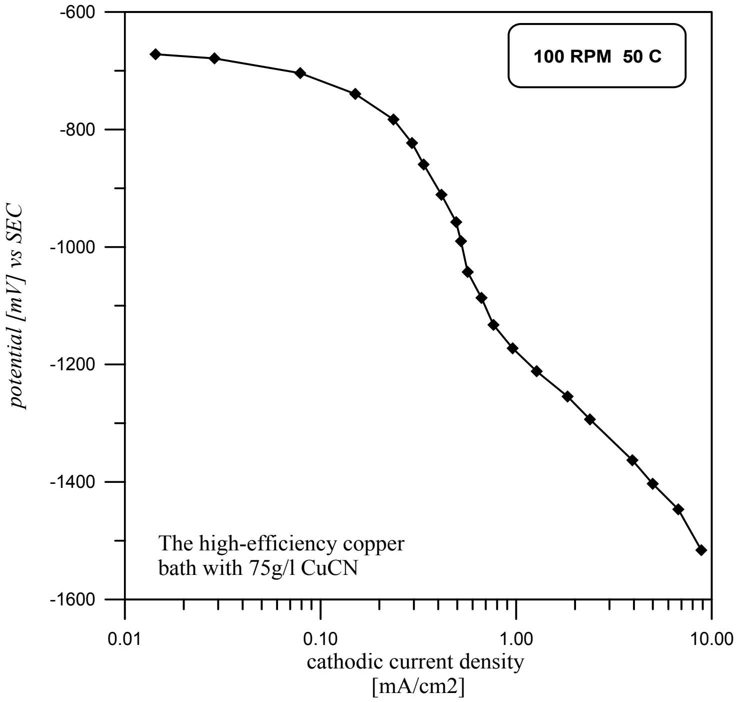

Fig4.7a Cathodic polarization curve on copper

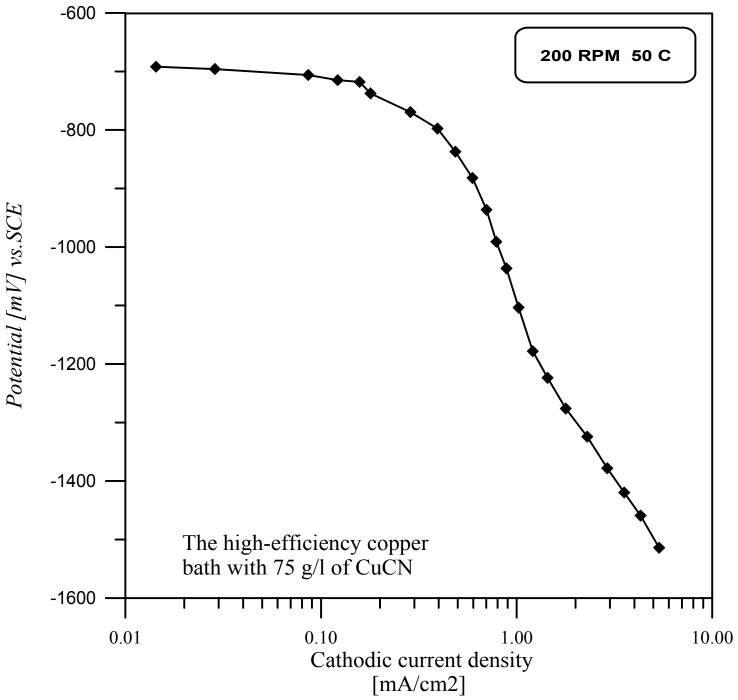

Fig4.7b Cathodic polarization curve on copper

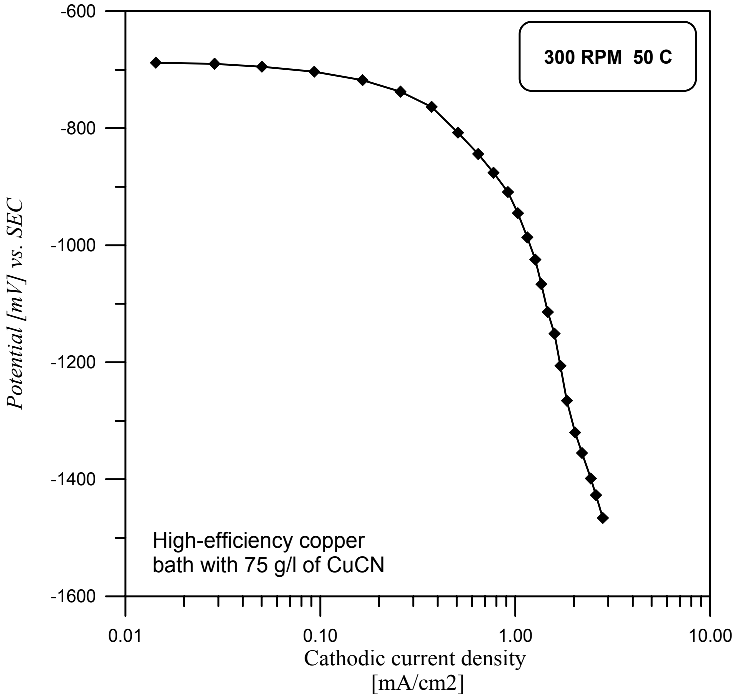

Fig4.7c Cathodic polarization curve on copper

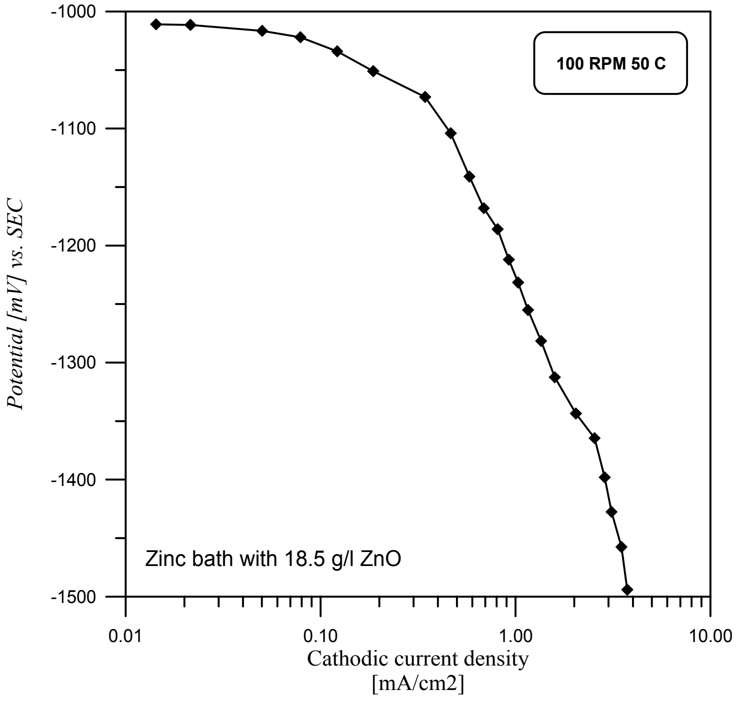

Fig4.8a Cathodic polarization curve on zinc

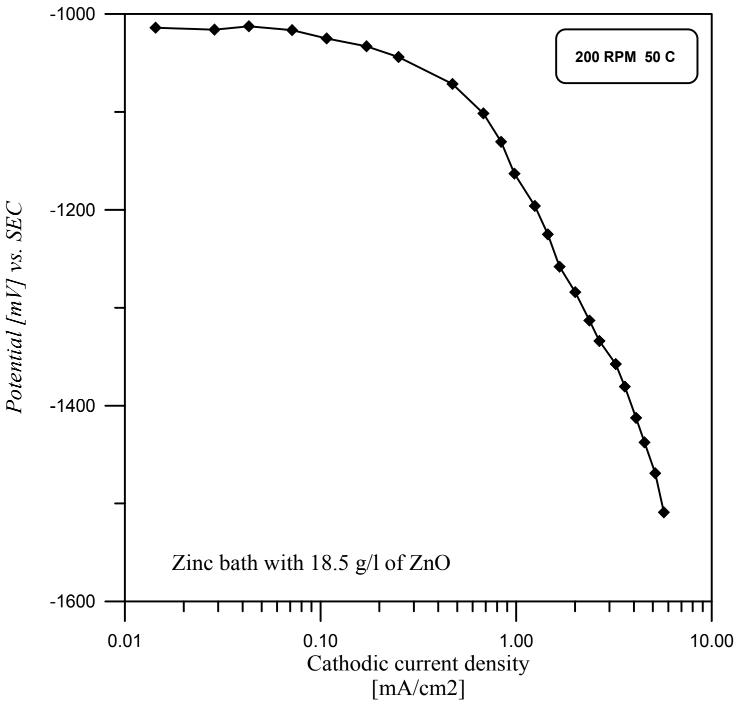

Fig4.8b Cathodic polarization curve on zinc

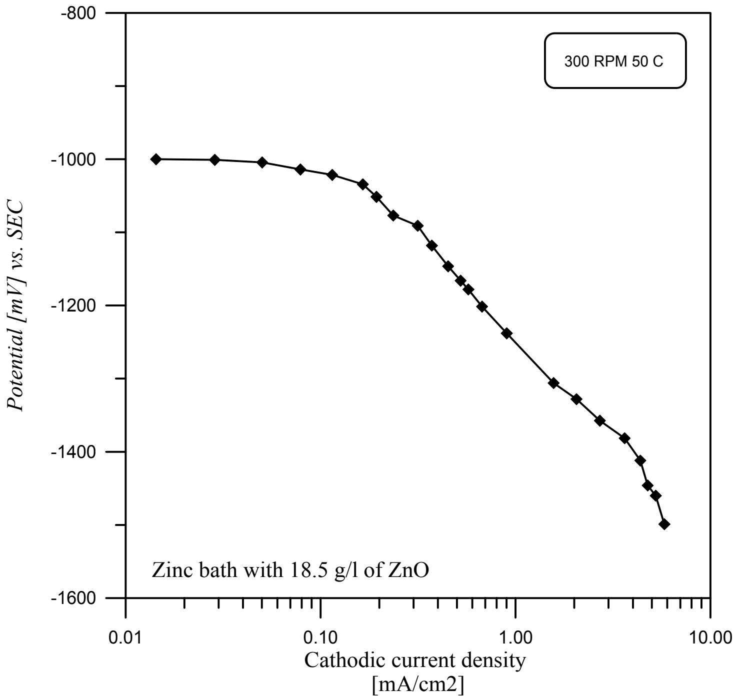

Fig4.8c Cathodic polarization curve on zinc

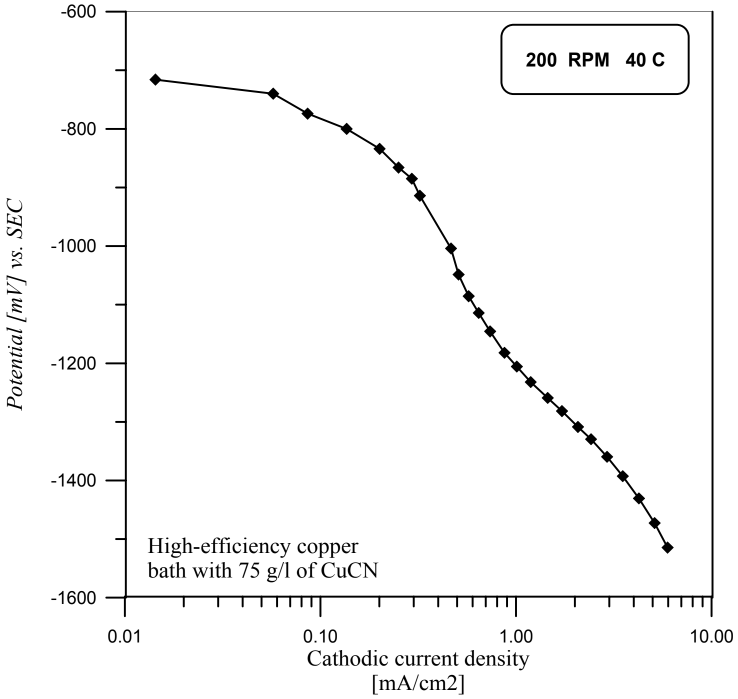

Fig4.9a Cathodic polarization curve on copper

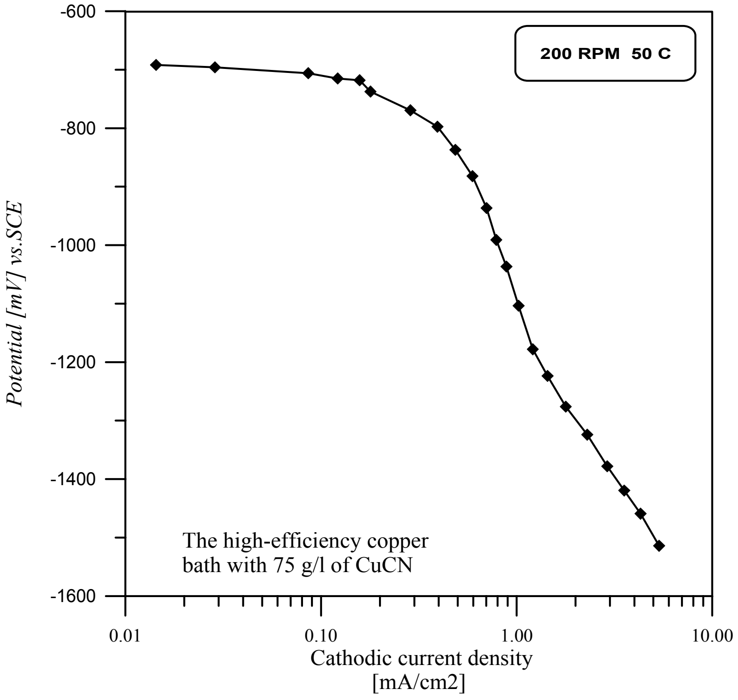

Fig4.9b Cathodic polarization curve on copper

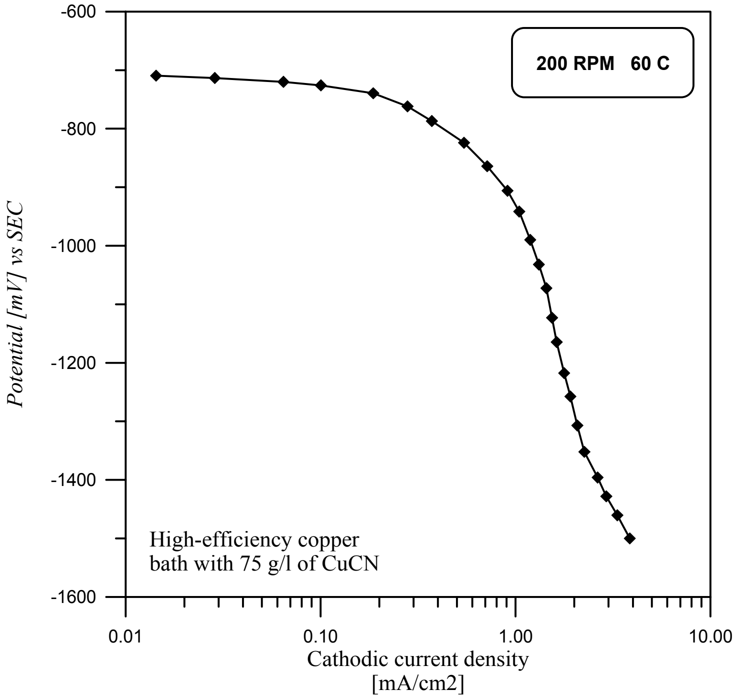

Fig4.9c Cathodic polarization curve on copper

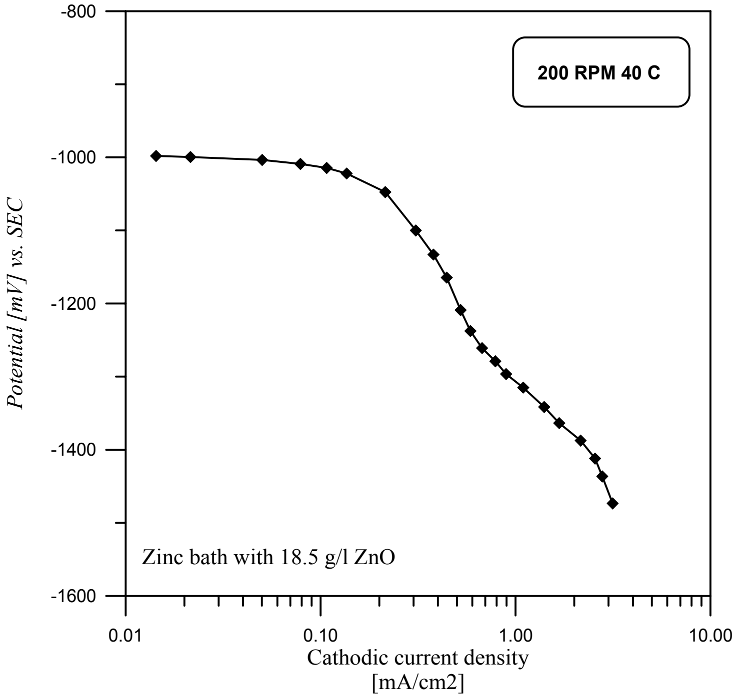

Fig4.10a Cathodic polarization curve on zinc

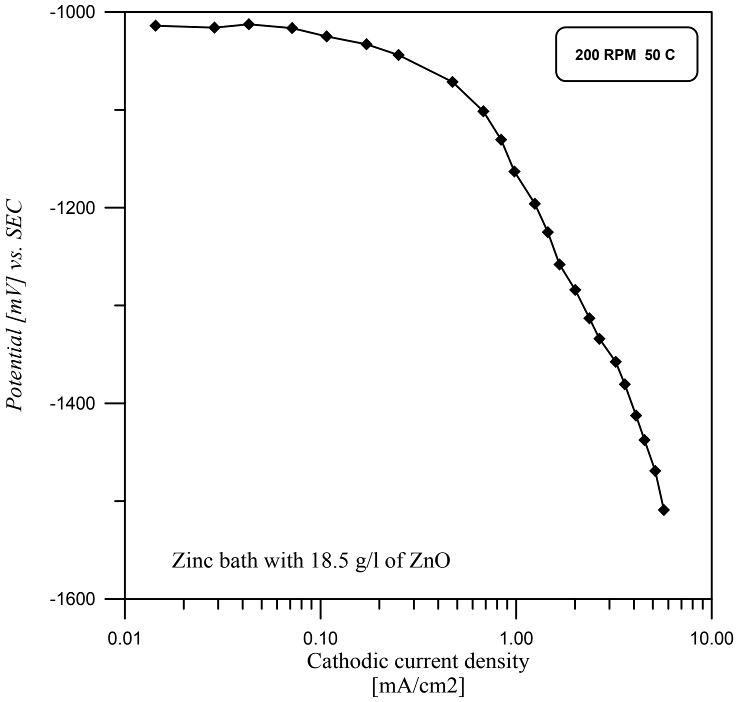

Fig4.10b Cathodic polarization curve on zinc

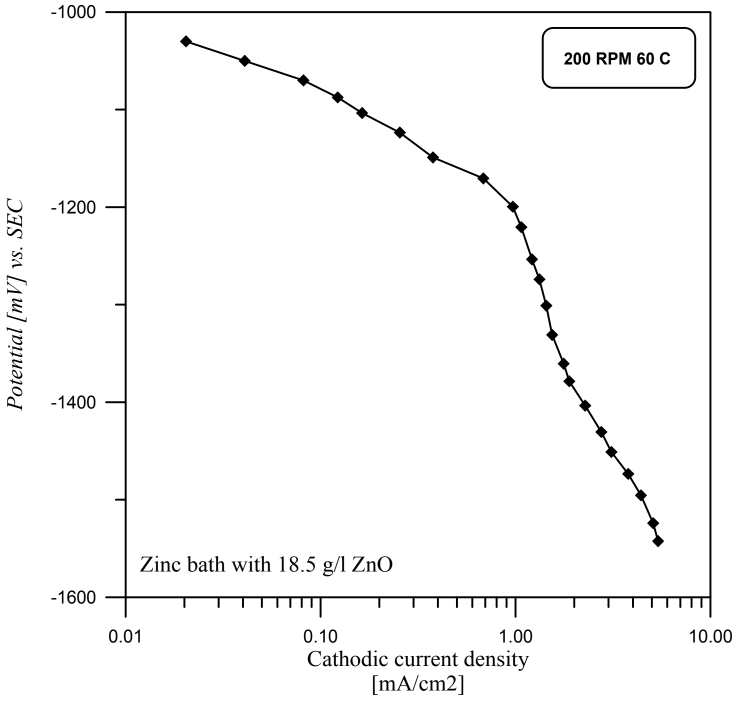

Fig4.10c Cathodic polarization curve on zinc

4.3.4 Individual anodes (copper and zinc) to plate brass alloy on graphite:

In previous chapter, section 3.6 we show how we plate with separated anodes, copper and zinc to obtain brass alloy plate with different percentage, Tables 4.7, 4.9 and 4.11 show the results of brass percentage plate from its elements (copper and zinc) and Tables 4.8, 4.10 and 4.12 show individual cathodic current efficiency for copper and zinc in brass alloy plating for different times and current densities.

Table 4.7 Cathodic current efficiency of plating brass alloy from its elements, with plating time 15 min., 200 RPM and temp.50 ^{0}C

Duration of plating (15 minutes)								
i_c (mA/cm^2)	i_z (mA/cm^2)	$\Delta W_{act.}$(g)	W_{tc} (g)	W_{tz} .(g)	W_{tcz}	Brass plate analysis*		Total Eff%
						W_{ac}%	W_{az}%	
0.4	0.12	0.0005	0.000480	0.000148	0.000628	75	25	79.61
0.55	0.55	0.0011	0.000660	0.000679	0.001339	49	51	82.15
0.7	1.8	0.0025	0.000840	0.002224	0.003064	27	73	81.59
1.84	1.84	0.0037	0.002210	0.002273	0.004483	49	51	82.53
5.5	2.7	0.0084	0.006605	0.003336	0.009941	66	34	84.49

*Brass plate was analyzed by *Abn-Sina Company for chemical industries*.

Table 4.8 Individual cathodic current efficiency for copper and zinc in brass alloy plating, with plating time 15 min., 200 RPM and temp.50 ^{0}C

Duration of plating (15 minutes)								
Copper deposit weight (g)	Zinc deposit weight (g)	$\Delta W_{act.}$(g)	W_{tc} (g)	W_{tz} .(g)	Brass plate analysis*		Eff% for copper	Eff% for zinc
					W_{ac}%	W_{az}%		
0.000375	0.000125	0.0005	0.000480	0.000148	75	25	78.12	84.45
0.000539	0.000561	0.0011	0.000660	0.000679	49	51	81.66	82.62
0.000675	0.001825	0.0025	0.000840	0.002224	27	73	80.35	82.05
0.001813	0.001887	0.0037	0.002210	0.002273	49	51	82.03	83.01
0.005544	0.002856	0.0084	0.006605	0.003336	66	34	83.93	85.61

*Brass plate was analyzed by *Abn-Sina Company for chemical industries*.

Table 4.9 Cathodic current efficiency of plating brass alloy from its elements, with plating time 20 min., 200 RPM and temp.50 ^{0}C

Duration of plating (20 minutes)								
i_c (mA/cm^2)	i_z (mA/cm^2)	$\Delta W_{act.}$(g)	W_{tc} (g)	W_{tz} .(g)	W_{tcz}	Brass plate analysis*		Total Eff%
						W_{ac}%	W_{az}%	
0.4	0.12	0.0007	0.00064	0.000197	0.000837	75.8	24.2	83.63
0.55	0.55	0.0015	0.00088	0.000902	0.001782	51.5	48.5	84.17
0.7	1.8	0.0034	0.001121	0.002965	0.004086	29.1	70.9	83.21
1.84	1.84	0.0050	0.002946	0.003031	0.005977	51.9	48.1	83.65
5.5	2.7	0.0111	0.008807	0.004448	0.013255	67.6	32.4	83.74

* Brass plate was analyzed by *Abn-Sina Company for chemical industries*.

Table 4.10 Individual cathodic current efficiency for copper and zinc in brass alloy plating, with plating time 20 min., 200 RPM and temp.50 ^{0}C

Duration of plating (20 minutes)								
Copper deposit weight (g)	Zinc deposit weight (g)	$\Delta W_{act.}$(g)	W_{tc} (g)	W_{tz} .(g)	Brass plate analysis*		Eff% for copper	Eff% for zinc
					W_{ac}%	W_{az}%		
0.000530	0.000169	0.0007	0.00064	0.000197	75.8	24.2	82.81	85.78
0.000772	0.000727	0.0015	0.00088	0.000902	51.5	48.5	87.72	80.59
0.000989	0.002410	0.0034	0.001121	0.002965	29.1	70.9	88.22	81.28
0.002595	0.002405	0.0050	0.002946	0.003031	51.9	48.1	85.61	79.34
0.007503	0.003596	0.0111	0.008807	0.004448	67.6	32.4	85.19	80.84

* Brass plate was analyzed by *Abn-Sina Company for chemical industries*.

Table 4.11 Cathodic current efficiency of plating brass alloy from its elements, with plating time 25 min., 200 RPM and temp.50 ^{0}C

Duration of plating (25 minutes)								
i_c (mA/cm^2)	i_z (mA/cm^2)	$\Delta W_{act.}$(g)	W_{tc} (g)	W_{tz} .(g)	W_{tcz}	Brass plate analysis*		Total Eff%
						W_{ac}%	W_{az}%	
0.4	0.12	0.0009	0.0008	0.000247	0.001047	76.1	23.9	85.95
0.55	0.55	0.0019	0.0011	0.001132	0.002232	50.5	49.5	85.12
0.7	1.8	0.0043	0.001401	0.003707	0.005108	29.5	70.5	84.18
1.84	1.84	0.0063	0.003683	0.003789	0.007472	50.9	49.1	84.31
5.5	2.7	0.0138	0.011009	0.00556	0.016569	67.2	32.8	83.28

*Brass plate was analyzed by *Abn-Sina Company for chemical industries*.

Table 4.12 Individual cathodic current efficiency for copper and zinc in brass alloy plating, with plating time 25 min., 200 RPM and temp.50 ^{0}C

Duration of plating (25 minutes)								
Copper deposit weight (g)	Zinc deposit weight (g)	$\Delta W_{act.}$(g)	W_{tc} (g)	W_{tz} .(g)	Brass plate analysis*		Eff% for copper	Eff% for zinc
					W_{ac}%	W_{az}%		
0.000684	0.000215	0.0009	0.0008	0.000247	76.1	23.9	85.5	87.04
0.000959	0.00094	0.0019	0.0011	0.001132	50.5	49.5	87.18	83.03
0.001268	0.003031	0.0043	0.001401	0.003707	29.5	70.5	90.5	81.76
0.003206	0.003093	0.0063	0.003683	0.003789	50.9	49.1	87.04	81.63
0.009273	0.004526	0.0138	0.011009	0.00556	67.2	32.8	84.23	81.40

* Brass plate was analyzed by *Abn-Sina Company for chemical industries*.

Chapter five

Discussion

5.1 Introduction:

Chapter Five introduces a large volume of experimental results. This is to be expected because of the number of variables involved in the present work, i.e, CuCN, ZnO concentrations, agitation, temperature, time of plating, and cathodic current density

The manner in which this chapter is presented is, therefore, similar to that used in Chapter Four. Section 5.2 deals with the effect of concentration on the deposition potential, cathodic, and anodic current efficiency. Section 5.3 explains the influence of agitation on the deposition potential, cathodic, and anodic current efficiency. Section 5.4 shows the effects of temperature on deposition potential, cathodic, and anodic current efficiency. Section 5.5 deals with the influence of plating time on cathodic and anodic current efficiency. Section 5.6 shows the effect of cathodic current density on cathodic and anodic current efficiency. Section 5.7 shows relationship between cathodic current efficiency and concentration in copper and zinc plating. Section 5.8 shows relationship between cathodic current efficiency and temperature of both copper and zinc plating. Section 5.9 shows relationship between cathodic current efficiency and time for copper and zinc plating. Section 5.10 shows relationship between cathodic current efficiency and cathodic current density in copper and zinc plating. Section 5.11 shows the brass plating from individual anodes (copper and zinc) and their analysis. Section 5.12 represents the statistical analysis between cooper current density and zinc current density with different percentage of brass alloy plating.

5.2 Effect of concentration:

5.2.1 on deposition potential:

It has been seen in chapter four which shows the results of the polarization curves as given in Figs.5.1 and 5.2, that deposition potential is less negative with increasing concentration of CuCN in copper bath and ZnO in zinc bath. The electrical conductivity increases markedly leading to higher deposit rates and lower deposition potential, so that deposition potential becomes less negative with increasing concentration of CuCN in copper bath and ZnO in zinc bath.

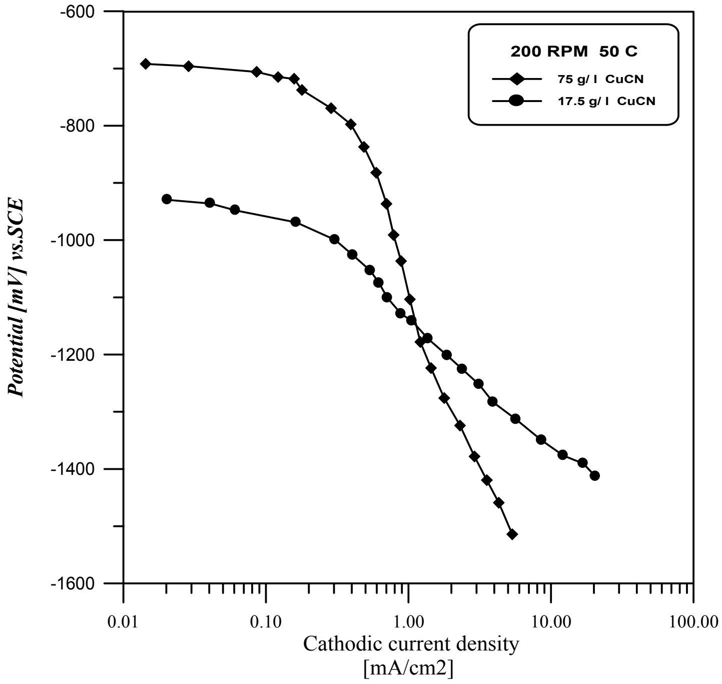

Fig.5.1 Cathodic polarization curves on copper

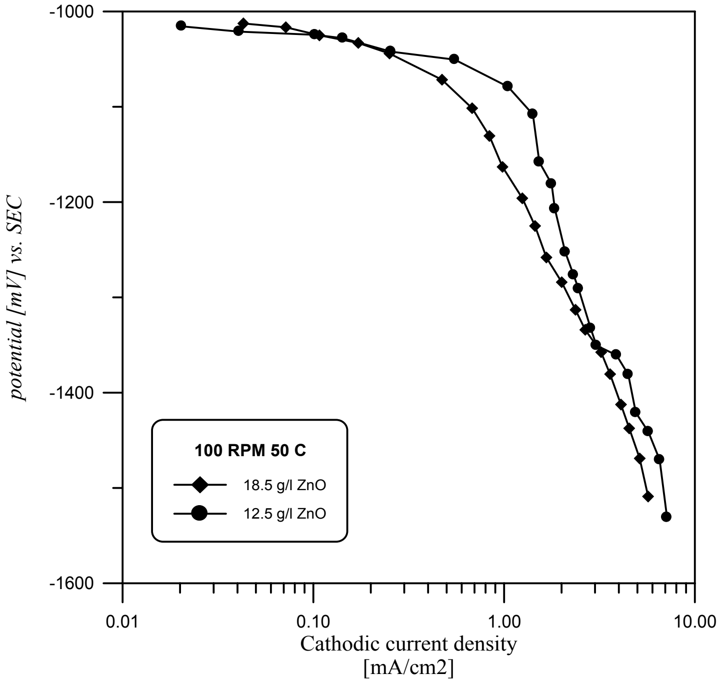

Fig.5.2 Cathodic polarization curves on zinc Zn

5.2.2 Cathodic and anodic current efficiency:

Figures 4.1a and 4.1b and Tables 4.5a and 4.6a show that the cathodic and anodic current efficiency, increase with increasing the concentration of CuCN in copper bath and ZnO in zinc bath. This could be attributed to the fact that increasing Cu^{2+} , Zn^{2+} ions content in the bath result due to a decrease in the Cu^{2+}, Zn^{2+} deposition in the diffusion layer and consequently decreases the concentration (diffusion) over potential[2].

5.3 Effect of agitation on deposition potential:

Figures 5.3, 5.4 it can be notice that copper(mass control) potential become less negative with increasing agitation for a given current density because the influence of velocity, whose primary effect is to increase the deposition rates of electrode process that are controlled by diffusion and little change in zinc(activation control) potential which may be negligible because it is activation controlled[19].

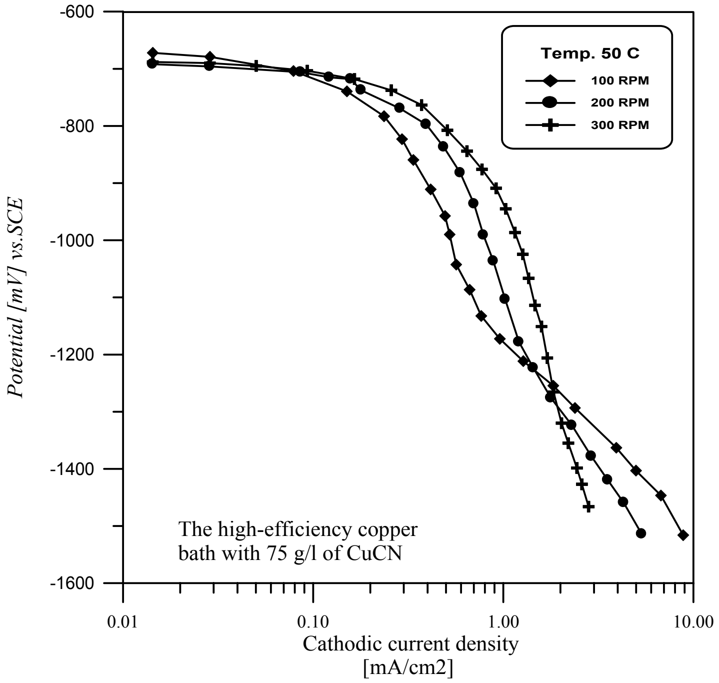

Fig.5.3 Cathodic polarization curves on copper

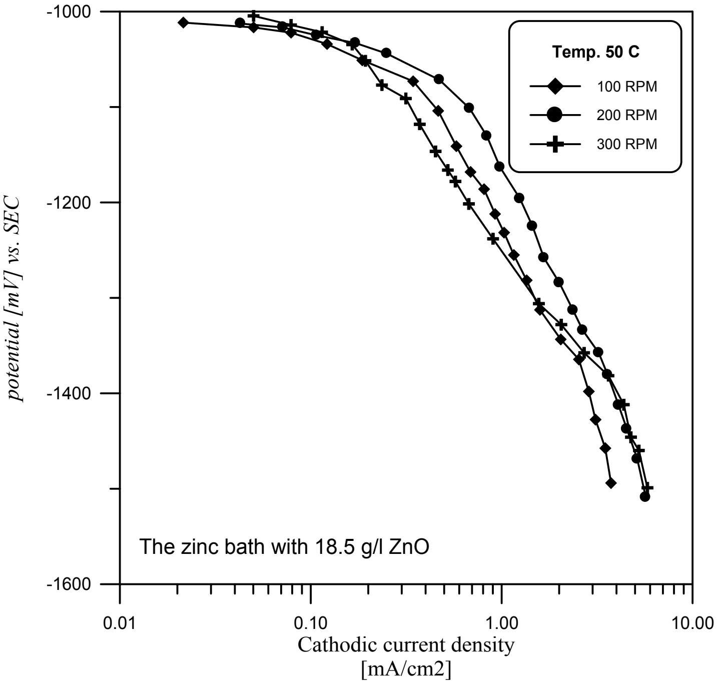

Fig.5.4 Cathodic polarization curves on zinc

5.4 Effect of temperature:

5.4.1 on deposition potential:

Figures 5.5, 5.6 which show that the curves of zinc are shifted to higher current densities with increasing of temperature and little change in copper because zinc controlled by the activation as temperature changes have the greatest effect when the rate determining step is the activation process [19]. In general, if diffusion rates are doubled for a certain increase in temperature, activation process may be increased by 10-100 times, depending on the magnitude of the activation energy [19].

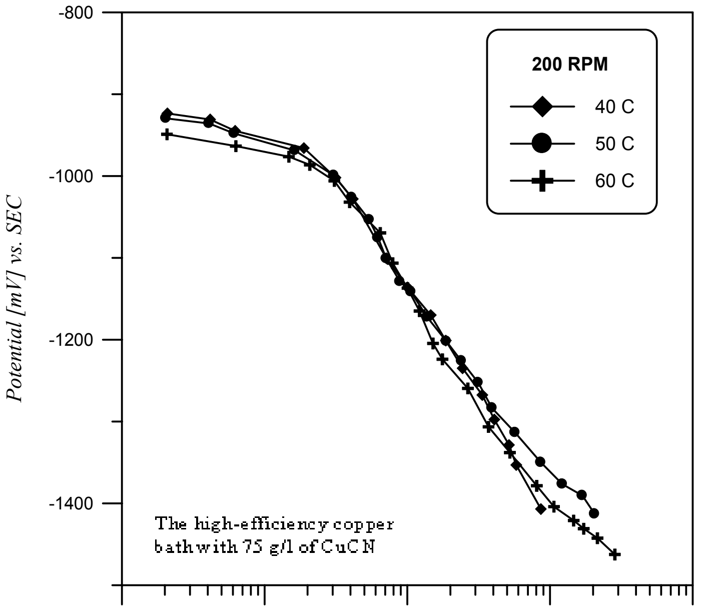

Fig.5.5 Cathodic polarization curves on copper

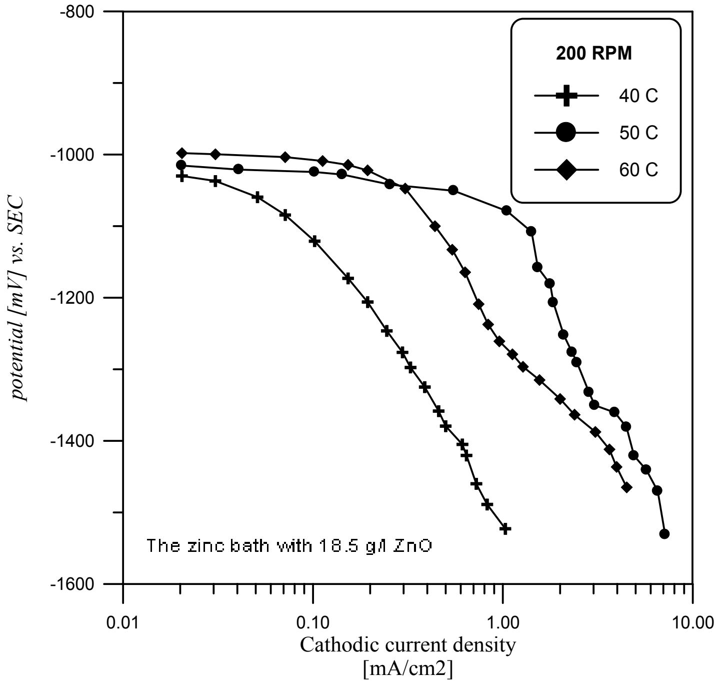

Fig.5.6 Cathodic polarization curves on zinc

5.4.2 Cathodic and anodic current efficiency:

It has to been seen from Figs. 4.2a and 4.2b and Tables 4.5b and 4.6b that an increase of temperature of copper bath and zinc bath will increase the cathodic current efficiency. This is due to the increased hydrolysis and oxidations which compensating by reduced dragout from less baths so that total cyanide consumption remains about the same [5].

5.5 Effect of time on cathodic and anodic current efficiency:

Figures 4.3a and 4.3b and Tables 4.5c and 4.6c show that the cathodic current efficiency increases with increasing the period of time. This indicates that the longer time results in better or higher efficiency [2].

5.6 Effect of cathodic current density on cathodic and anodic current efficiency:

Figures 4.4a and 4.4b and Tables 4.5d and 4.6d show that cathodic current efficiency decreases with increasing current density, this is perhaps because anode was polarized and became coated with an insulating film [5].

5.7 Relationships between cathodic current efficiency and concentration in individual copper and zinc plating:

Figures 4.1a, 4.1b one can notice the cathodic current efficiency increases with increasing concentration of CuCN in copper bath and ZnO in zinc bath. Using the best fit technique the following are obtained:

For copper

Eff% = 273.865 -72.2229*X+ 5.82389* X ^2 -0.133387* X ^3 ….5.1

with correlation coefficient C.C =99.99 %

For zinc

Eff% = 66.1275 +1.2031* X + 0.00670006* X ^2 ….5.2

with correlation coefficient C.C =99.98 %

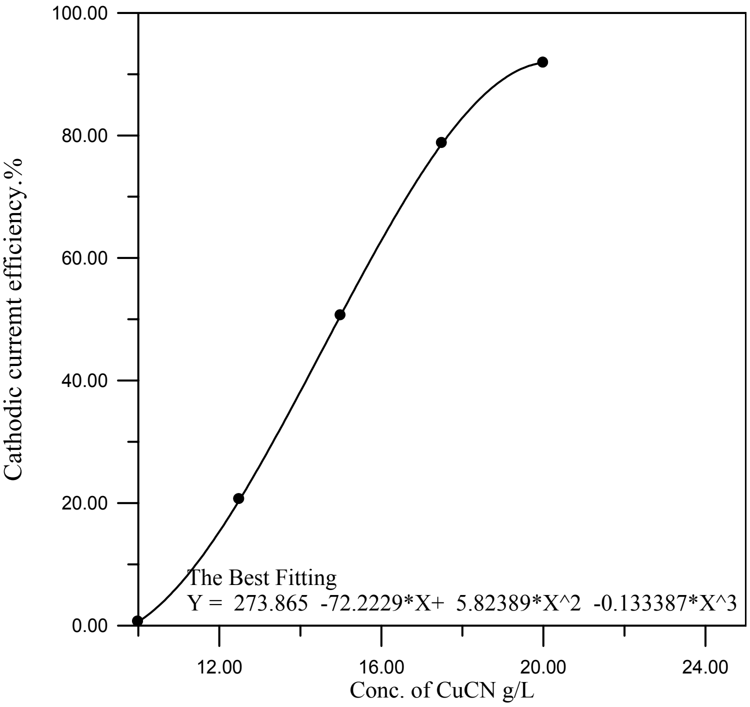

Fig.5.7 Cathodic current efficiency vs. conc.of CuCN g/l, temp.50 ^{0}C, i_c= 20 mA/cm^2, 200 RPM, time. 10 min.

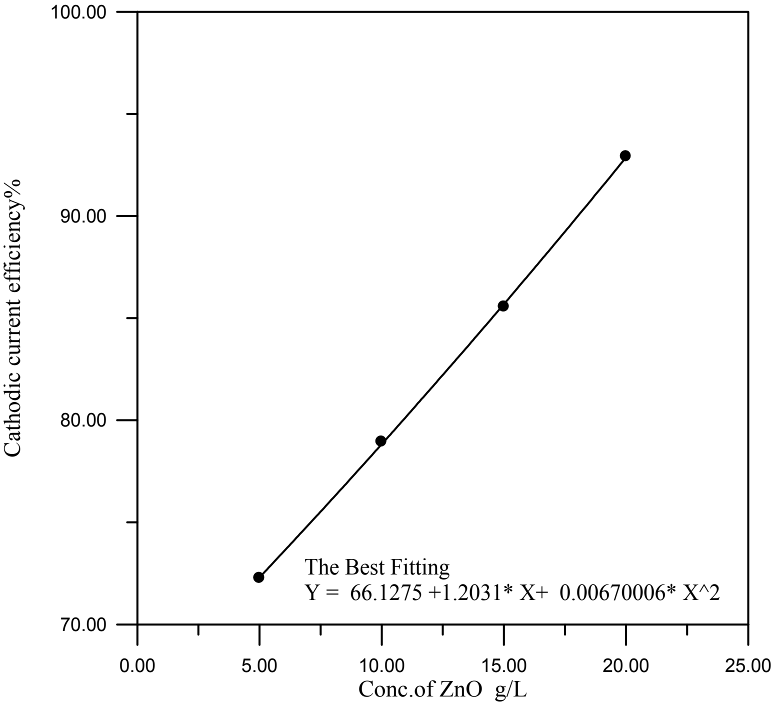

Fig.5.8 Cathodic current efficiency vs. conc.of ZnO g/l, temp.50 ^{0}C, i_c= 20 mA/cm^2, 200 RPM, time. 10 min.

5.8 Relationships between cathodic current efficiency and temperature in copper and zinc plating:

From Figs.4.2a, and 4.2b one can notice the increase of cathodic current efficiency with increased of bath temperature. The best fitting equations for these increases are:

For copper

$$Eff\% = 50.4299 + 0.101004 * T + 0.00929996 * T^2 \quad \ldots. 5.3$$

with correlation coefficient C.C =99.99 %

For zinc

$$Eff\% = 54.0401 + 0.0309967 * T + 0.00910004 * T^2 \quad \ldots. 5.4$$

with correlation coefficient C.C =99.99 %

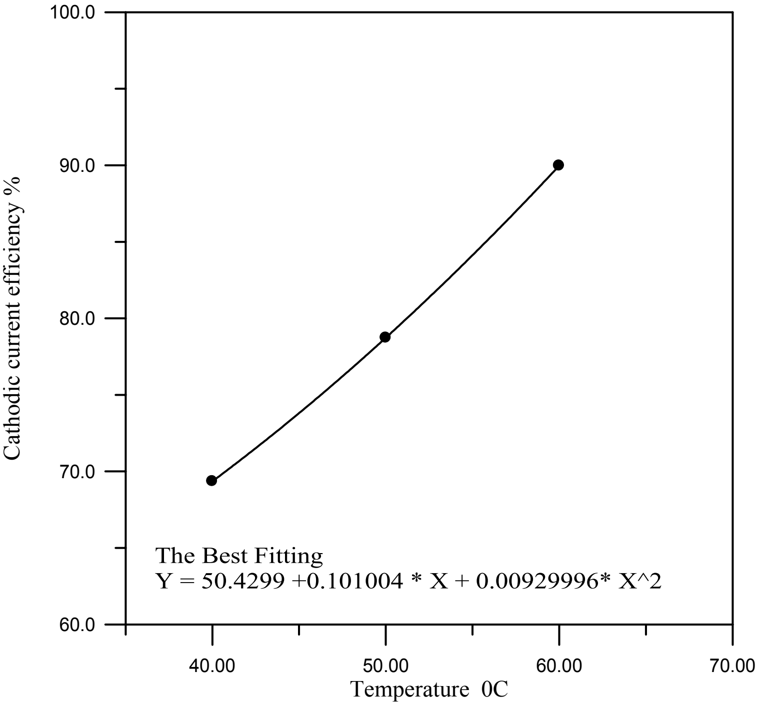

Fig.5.9 Cathodic current efficiency vs. temperature, conc.of CuCN 17.5 g/l, i_c= 20 mA/cm^2, 200 RPM, time. 10 min.

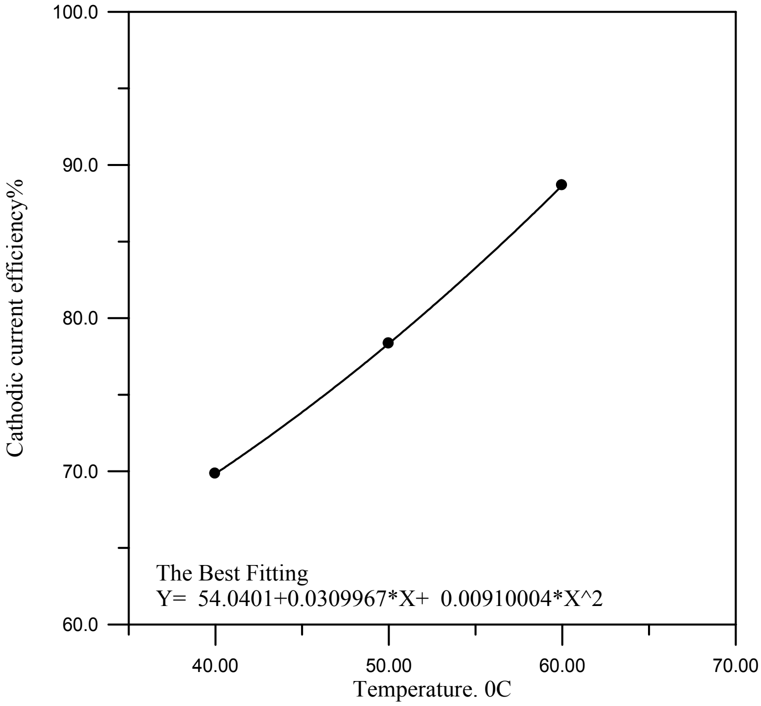

Fig.5.10 Cathodic current efficiency vs. temperature., conc.of ZnO 12.5 g/l, i_c= 20 mA/cm^2, 200 RPM, time. 10 min.

5.9 Relationships between cathodic current efficiency and time of copper and zinc plating:

From Figs.4.3a and 4.3b one can notice the cathodic current efficiency increases with increase time of copper and zinc plating. The best fitting of these are:

For copper

Eff% = 53.93 +2.44034 * t +0.0163994* t^2 -0.00249332* t^3 ….5.5

with correlation coefficient C.C =99.99 %

For zinc

Eff%= 46.7575+ 3.8871* t -0.0729 t^2 ….5.6

with correlation coefficient C.C =99.99 %

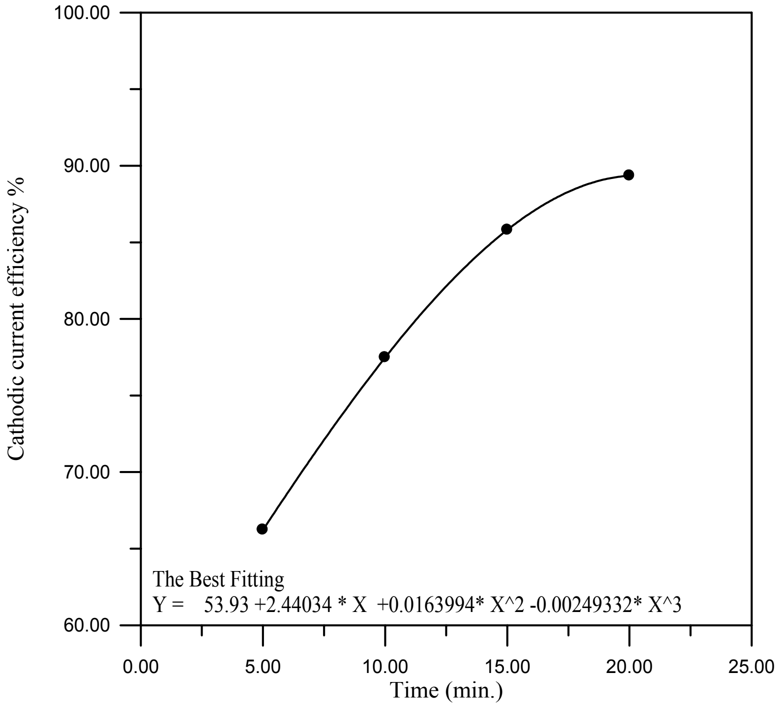

Fig.5.11 Cathodic current efficiency vs. time., conc.of CuCN 17.5 g/l, i_c= 20 mA/cm^2, 200 RPM, temp. 50 ^{0}C

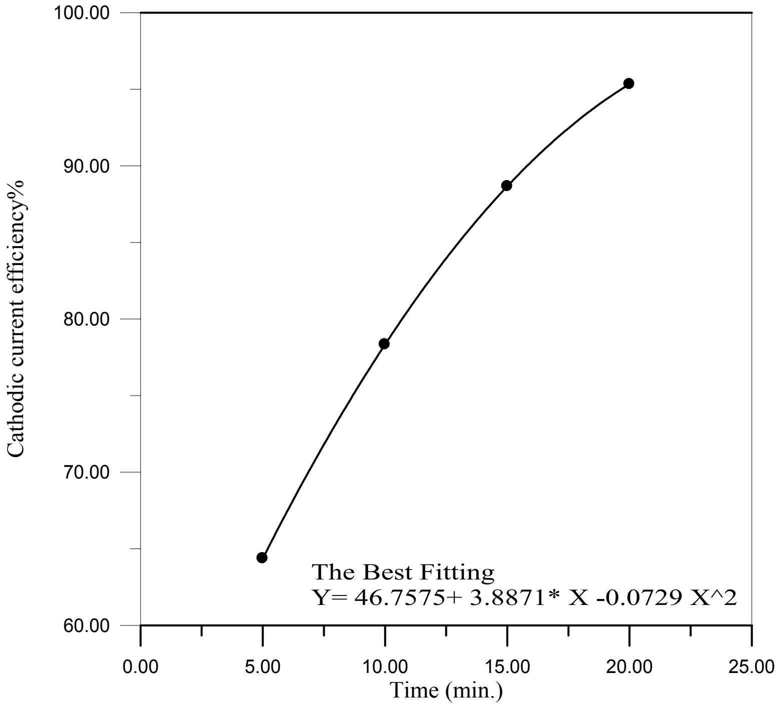

Fig.5.12 Cathodic current efficiency vs. time., conc.of ZnO12.5 g/l, i_c= 20 mA/cm^2, 200 RPM, temp. 50 ^{0}C

5.10 Relationships between cathodic current efficiency and cathodic current density of copper and zinc plating:

From Figs.4.4a and 4.4b one can notice the cathodic current efficiency decreases with increased cathodic current density of copper and zinc plating leading to the following equations:

For copper

Eff% = 94.43 +0.0828301* i_c+ -0.0635999* i_c^2 +0.000931665* i_c^3 ..5.7

with correlation coefficient C.C =99.99 %

For zinc

Eff%=73.94+2.62383* i_z -0.1631* i_z^2+0.00222167*i_z^3 ….5.8

with correlation coefficient C.C =99.99 %

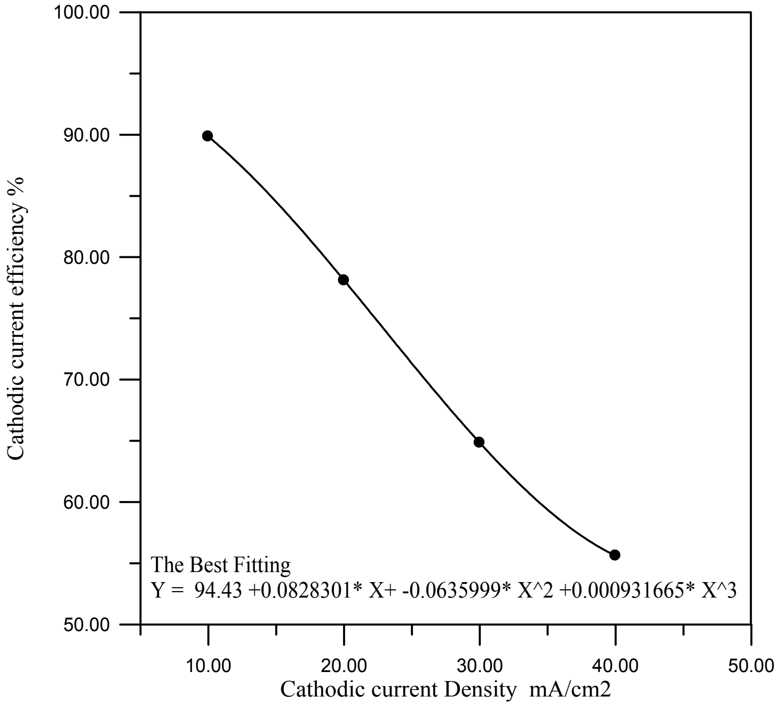

Fig.5.13 Cathodic current efficiency vs. current density, conc.of CuCN 17.5 g/l, time 10 min., 200 RPM, temp. 50 ^{0}C

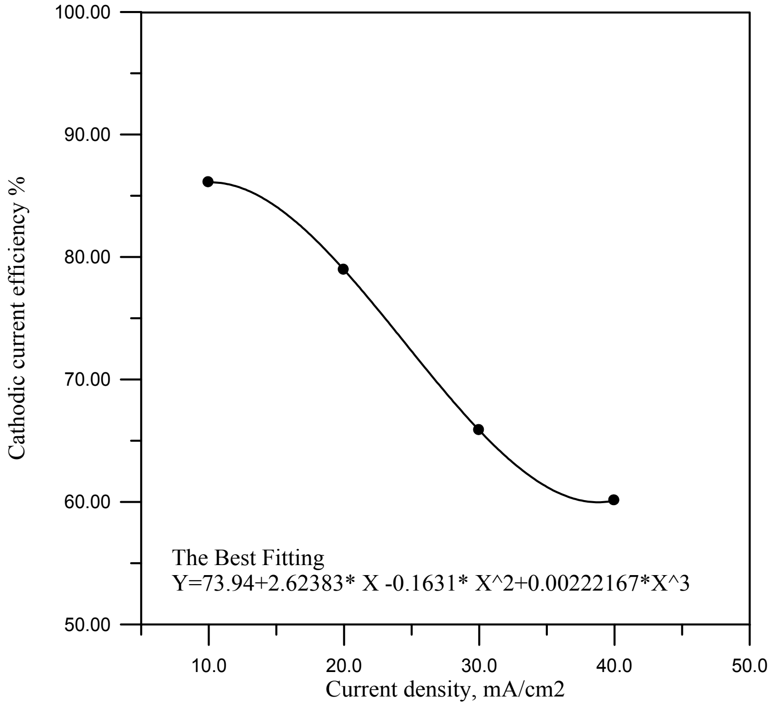

Fig.5.14 Cathodic current efficiency vs. current density , conc.of ZnO 12.5 g/l, time 10 min., 200 RPM, temp. 50 ^{0}C

5.11 Brass plating from individual anodes (copper and zinc):

Electrodeposits from solutions containing complex ions tend to be finer grained, smoother and more adherent than those formed from simple ion solutions [6]. Another advantage of modification is shifting of electrode potential by complexation that is possible to bring the potential of two metals closer together even though the standard potentials may be widely separated [6].

Perhaps one of most striking instance of alloy deposition is that brass. We have here two metals of widely disparate standard potential Table (E-1) and yet, by suitable complexing[20], it is possible to bring the polarization curves close together[20]. Alkaline cyanide solution is employed Fig. 5.14, for deposition at cathode potential E^{-}, copper and zinc can plate out simultaneously in comparable proportions [20].

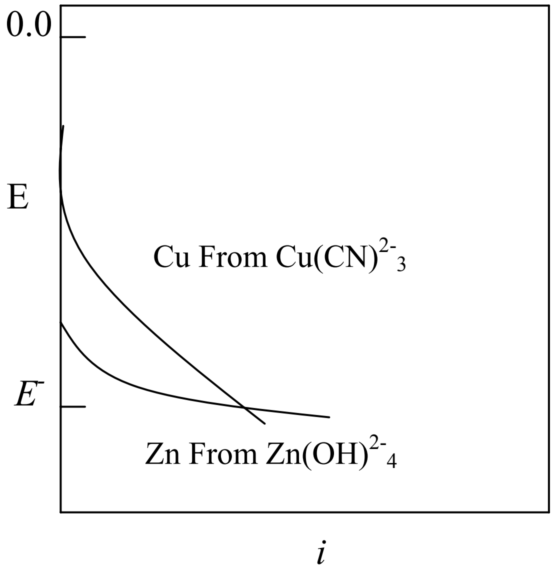

Fig. 5.14 Deposition of Brass from Cyanide bath [20]

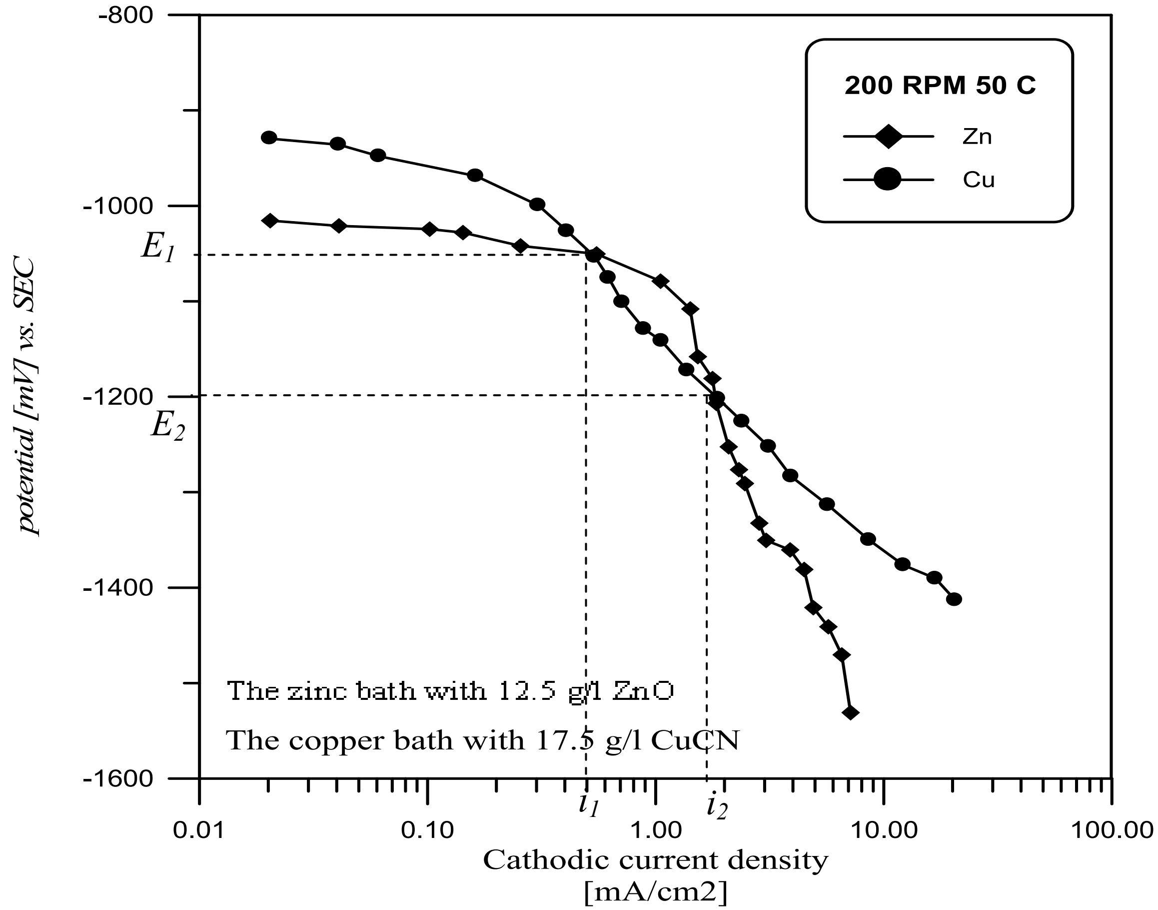

Fig. 5.15 Cathodic polarization curves for both of zinc and copper

Figure 5.15 shows two intersection points. Under these conditions there will be simultaneous and equal deposition of copper and zinc at the intersection potentials E_1 and E_2. At potentials more noble than E_1 the proportion of copper deposition will exceed that of zinc, whilst at potentials active or negative to E_1, a greater proportion of zinc will be deposited [6].

From Tables 4.7 to 4.12 one can see the weight percentages of zinc and copper in brass alloy are like the theoretical weight percentages with little difference which means when applying different currents on both zinc and copper (as separated anodes in brass electroplating) depending on Fig.5.15, we can obtain different percentages of brass alloy.

5.12 Relationship between copper current density and zinc current density with different percentage of brass alloy plating:

An important relationship between copper current density and zinc current density was found for different percentages of brass (copper and zinc) alloy plating. By applying certain percentages (as show in appendix D) of copper and zinc in the following empirical equation which is found from statistical analysis of results, one can find the ratio of current density (i_{Cu}/i_{Zn})

$$\mathbf{i_{Cu}/i_{Zn} = 0.719735+0.005395 *\exp (0.082058*Cu\ \%) -0.001086* \exp (0.082123*Zn\ \%)} \qquad \mathbf{....5.9}$$

with correlation coefficient C.C= 99.818% and mean error=4.8651%

The conditions of above equation are bath temperature 50 ^{0}C, 200RPM, and solution of 17.5 g/l CuCN, 12.5 g/l ZnO, 38 g/l NaCN and 96.1 g/l NaOH.

Thus for a given deposition potential, we can find both currents of copper and zinc which should be used for certain alloy percentages (that be wanted for certain purpose) from Fig.5.15.

Chapter Six

Conclusions and Recommendations for Future Work

6.1 Introduction:

The present work has been mainly aimed to find a relationship between current densities of individual copper and zinc anodes with percentages of brass alloy plating in certain solutions, also to study the influence of variables on cathodic current efficiency on copper and zinc electroplating, such as concentration of CuCN on copper and ZnO on zinc electroplates, bath temperature, electroplating time, and current density.

6.2 Conclusions:

1. Cathodic current efficiency increases with increasing concentration, bath temperature, and electroplating time.
2. Cathodic current efficiency decreases with increasing current density.
3. A relationship is obtained between current densities of individual anodes of copper and zinc with percentages of brass alloy plating, i.e., by applying certain percentages of copper and zinc in empirical equation, one can find the ratio of current densities (i_{Cu}/i_{Zn}) as follows.

$$\mathbf{i_{Cu}/i_{Zn} = 0.719735 + 0.005395 * \exp(0.082058 * Cu\ \%) - 0.001086 * \exp(0.082123 * Zn\ \%)}$$

with correlation coefficient C.C= 99.818% and mean error=4.8651%

The conditions of equation above are bath temperature 50 ^{0}C, 200RPM, and solution of 17.5 g/l CuCN, 12.5 g/l ZnO, 38 g/l NaCN and 96.1 g/l NaOH.

6.3 Recommendations for Future Work:

The following suggestions are to be considered or to be examined in greater detail for future work:

1) Plating a terne alloy or lead-tin coating from fluborate solution.
2) Plating a bronze or copper - tin from cyanide solution.
3) Studying in more detail the influence of variables to increase cathodic current efficiency.

References

1) Introduction of electroplating, htt://www.efunda.com.
2) Electroplating , http://www.faculty.kfupm.edu.sa.
3) The Baghdad Battery, http://www.unmuseum.org.
4) Definition of Electroplating, http://www.wordiq.com.
5) Lowenheim, F.A., Modern Electroplating,2nd ed., Chapman and Hall, London, (1962).
6) Von Fraunhofer., J. A., Basic Metal Finishing, Paul Elek , (1976).
7) Electroplating, http://www.metal-mart.com.
8) Plating history, http://www.artisanplating.com.
9) Pauling, L., the Nature of the chemical bond, 3rd ed., Cornell University Press, Ithaca, NewYork, (1960), chap. 11.
10) Mattson E., and Bockris, J.O'M., Electrochim. Acta, 3, 340 (1961).
11) Bockris, J.O'M., in Modren Aspects of electrochemistry, Vol. I Bockris, J.O'M., and Conway, B.E., Eds.Butterworth's, Washington, D.C.(1954), p. 217.
12) Brenner, A., electrodeposition of alloy, Vol. I, Acadimic Press, New York, (1963), P. 551.
13) Du Rose, A.H., in ASTM special tech. Publ.197(1956).
14) International Lead-Zinc Research Orgnazation, Inc., Project LE-36, Rep. 28, Dec. (1968).
15) American Electroplaters Society, (1973).
16) A new Cyanide-Free Alkaline High Performance Bright Zinc Bath ,Finishing Industries Journal, May (1977).
17) Introduction to the Nernst Equation, http://www.psigate.ac.uk.

18) Lawrance J. Durney, Electroplating Engineering Handbook, Van Nostrand Reinhold Company, (1987).

19) Shreir L. L., Corrosion, Volume 1, Newnes-Butterworths, (1976).

20) West J.M. ,Electrodeposition and Corrosion Processes, William Clowes and Sons,(1971).

APPENDIX A

Tables of cathodic polarization results of copper with different conditions

Table A-1 Cathodic polarization results at 40^{o}C.

RPM	*$A_{cath.}$ (cm^2)*	*Conc. (g/l)CuCN*
100	**4.0526**	**75**

Exp.No.(1).

E(V)vs. SCE	*i(mA/cm^2)*	*I(mA)*
-1771	14.5228	58.855
-1655	11.6296	47.130
-1570	9.4813	38.424
-1515	8.0921	32.794
-1471	7.0037	28.383
-1438	6.1871	25.074
-1410	5.4997	22.288
-1387	4.9556	20.083
-1356	4.1677	16.890
-1330	3.6093	14.627
-1310	3.1651	12.827
-1281	2.6067	10.564
-1260	2.2201	8.997
-1252	2.0624	8.358
-1246	1.9193	7.778
-1232	1.6900	6.849
-1210	1.4322	5.804
-1184	1.1457	4.643
-1156	0.9596	3.889
-1132	0.8306	3.366
-1110	0.7304	2.960
-1082	0.6445	2.612
-1060	0.5730	2.322
-1012	0.4725	1.915
-982	0.4153	1.683
-952	0.3580	1.451
-909	0.3151	1.277
-871	0.2435	0.987
-843	0.1720	0.697
-821	0.1145	0.464
-790	0.0143	0.058

Exp.No.(2)

E(V) vs. SCE	*i(mA/cm^2)*	*I(mA)*
-1560	15.3963	62.395
-1493	12.5463	50.845
-1435	10.0972	40.920
-1403	8.3643	33.897
-1376	7.2040	29.195
-1354	6.3305	25.655
-1333	5.6287	22.811
-1311	4.6548	18.864
-1290	3.8955	15.787
-1270	3.1794	12.885
-1257	2.7642	11.202
-1230	2.1912	8.880
-1200	1.7186	6.965
-1185	1.5326	6.211
-1180	1.3749	5.572
-1156	1.1027	4.469
-1123	0.9453	3.831
-1093	0.7876	3.192
-1060	0.6875	2.786
-1029	0.6159	2.496
-992	0.5300	2.148
-960	0.4296	1.741
-930	0.4010	1.625
-900	0.3580	1.451
-873	0.3008	1.219
-836	0.2292	0.929
-807	0.1431	0.580
-787	0.0716	0.290
-770	0.0143	0.058

Table A-2 Cathodic polarization results at 40°C.

RPM	*$A_{cath.}$ (cm^2)*	*Conc. (g/l)CuCN*
200	**4.0526**	**75**

Exp.No.(1).

E(V)vs. SCE	*i(mA/cm^2)*	*I(mA)*
-1505	6.4164	26.003
-1468	5.7146	23.159
-1418	4.6834	18.980
-1379	3.8955	15.787
-1345	3.2081	13.001
-1311	2.5924	10.506
-1287	2.1626	8.764
-1260	1.8188	7.371
-1243	1.5898	6.443
-1216	1.3320	5.398
-1190	1.1600	4.701
-1165	1.0169	4.121
-1131	0.8881	3.599
-1105	0.7876	3.192
-1071	0.6875	2.786
-1043	0.6159	2.496
-1010	0.5730	2.322
-876	0.3294	1.335
-855	0.3008	1.219
-827	0.2292	0.929
-803	0.1574	0.638
-780	0.0716	0.290
-758	0.0143	0.058

Exp.No.(2)

E(V) vs. SCE	*i(mA/cm^2)*	*I(mA)*
-1524	5.4997	22.288
-1477	4.5114	18.283
-1443	3.8240	15.497
-1406	3.1365	12.711
-1374	2.6353	10.680
-1348	2.2487	9.113
-1330	1.9908	8.068
-1303	1.6185	6.559
-1275	1.3177	5.340
-1248	1.0455	4.237
-1221	0.8594	3.483
-1199	0.7304	2.960
-1160	0.5873	2.380
-1123	0.5012	2.031
-1100	0.4582	1.857
-1054	0.4010	1.625
-998	0.3580	1.451
-952	0.3151	1.277
-915	0.2865	1.161
-905	0.2722	1.103
-865	0.2435	0.987
-820	0.2006	0.813
-790	0.1574	0.638
-763	0.1002	0.406
-740	0.0572	0.232
-716	0.0143	0.058

Table A-3 Cathodic polarization results at 40°C.

RPM	*$A_{cath.}$ (cm^2)*	*Conc. (g/l)CuCN*
300	**4.0526**	**75**

Exp.No.(1).

E(V)vs. SCE	*$i(mA/cm^2)$*	*I(mA)*
-1490	2.1912	8.880
-1475	2.0338	8.242
-1459	1.8906	7.662
-1440	1.7759	7.197
-1417	1.6185	6.559
-1385	1.5037	6.094
-1364	1.3892	5.630
-1337	1.3034	5.282
-1303	1.1886	4.817
-1272	1.0884	4.411
-1247	1.0169	4.121
-1204	0.9310	3.773
-1165	0.8449	3.424
-1113	0.7876	3.192
-1056	0.7018	2.844
-1006	0.6302	2.554
-958	0.5873	2.380
-930	0.5300	2.148
-903	0.4868	1.973
-865	0.4296	1.741
-828	0.3580	1.451
-800	0.3151	1.277
-771	0.2292	0.929
-740	0.1574	0.638
-728	0.1288	0.522
-710	0.0716	0.290
-700	0.0286	0.116
-695	0.0143	0.058

Exp.No.(2)

E(V) vs. SCE	*$i(mA/cm^2)$*	*I(mA)*
-1500	7.0895	28.731
-1471	6.3734	25.829
-1450	5.5283	22.404
-1430	5.0128	20.315
-1411	4.5114	18.283
-1385	3.8812	15.729
-1365	3.3371	13.524
-1348	2.9648	12.015
-1325	2.5492	10.331
-1301	2.2487	9.113
-1290	1.9908	8.068
-1270	1.8188	7.371
-1247	1.6042	6.501
-1209	1.3177	5.340
-1189	1.1743	4.759
-1157	1.0312	4.179
-1123	0.9453	3.831
-1110	0.9024	3.657
-1086	0.8306	3.366
-1054	0.7876	3.192
-1020	0.7304	2.960
-985	0.6875	2.786
-951	0.6445	2.612
-928	0.6016	2.438
-907	0.5730	2.322
-892	0.5443	2.206
-866	0.5012	2.031
-832	0.4296	1.741
-803	0.3580	1.451
-777	0.3151	1.277
-747	0.2435	0.987
-736	0.2006	0.813
-714	0.1288	0.522
-705	0.1002	0.406
-692	0.0286	0.116
-688	0.0143	0.058

Table A-4 Cathodic polarization results at 50^{o}C.

RPM	*$A_{cath.}$ (cm^2)*	*Conc. (g/l)CuCN*
100	**4.0526**	**75**

Exp.No.(1).

E(V)vs. SCE	*i(mA/cm^2)*	*I(mA)*
-1507	4.7263	19.154
-1445	3.7381	15.149
-1409	3.1079	12.595
-1359	2.4061	9.751
-1307	1.8475	7.487
-1264	1.4179	5.746
-1217	1.0598	4.295
-1175	0.8306	3.366
-1115	0.6588	2.670
-1053	0.5443	2.206
-1005	0.4725	1.915
-940	0.4010	1.625
-900	0.3724	1.509
-852	0.3008	1.219
-812	0.2435	0.987
-780	0.2006	0.813
-743	0.1574	0.638
-703	0.0716	0.290
-689	0.0286	0.116
-678	0.0143	0.058

Exp.No.(2)

E(V) vs. SCE	*i(mA/cm^2)*	*I(mA)*
-1525	12.9616	52.528
-1448	9.7535	39.527
-1397	6.8746	27.860
-1367	5.4567	22.114
-1280	2.9218	11.841
-1245	2.2487	9.113
-1206	1.4894	6.036
-1170	1.0884	4.411
-1150	0.8738	3.541
-1120	0.7876	3.192
-1080	0.6588	2.670
-1040	0.6445	2.612
-1015	0.6159	2.496
-970	0.5300	2.148
-907	0.4296	1.741
-866	0.3867	1.567
-823	0.3151	1.277
-776	0.2292	0.929
-719	0.1288	0.522
-680	0.0429	0.174
-672	0.0143	0.058

Table A-5 Cathodic polarization results at 50°C.

RPM	*$A_{cath.}$ (cm^2)*	*Conc. (g/l)CuCN*
200	**4.0526**	**75**

Exp.No.(1).

E(V)vs. SCE	*i(mA/cm^2)*	*I(mA)*
-1528	3.6236	14.685
-1470	3.0363	12.305
-1420	2.5492	10.331
-1383	2.1626	8.764
-1320	1.6900	6.849
-1275	1.4035	5.688
-1211	1.1314	4.585
-1160	0.9883	4.005
-1070	0.8306	3.366
-1007	0.7304	2.960
-960	0.6445	2.612
-901	0.5443	2.206
-844	0.4296	1.741
-798	0.3151	1.277
-750	0.2149	0.871
-730	0.1145	0.464
-700	0.0286	0.116
-693	0.0143	0.058

Exp.No.(2)

E(V) vs. SCE	*i(mA/cm^2)*	*I(mA)*
-1500	7.0895	28.731
-1448	5.5712	22.578
-1419	4.5544	18.457
-1373	3.6522	14.801
-1328	2.9075	11.783
-1277	2.1626	8.764
-1236	1.7473	7.081
-1196	1.4322	5.804
-1137	1.2175	4.934
-1066	1.0455	4.237
-1022	0.9310	3.773
-972	0.8594	3.483
-920	0.7590	3.076
-876	0.6588	2.670
-845	0.5730	2.322
-809	0.4582	1.857
-775	0.3294	1.335
-737	0.2292	0.929
-718	0.1574	0.638
-706	0.0859	0.348
-696	0.0286	0.116
-692	0.0143	0.058

.

Table A-6 Cathodic polarization results at 50^{o}C.

RPM	*$A_{cath.}$ (cm^2)*	*Conc. (g/l)CuCN*
300	**4.0526**	**75**

Exp.No.(1).

E(V)vs. SCE	*i(mA/cm^2)*	*I(mA)*
-1432	3.1222	12.653
-1404	2.7928	11.318
-1388	2.6497	10.738
-1335	2.2916	9.287
-1287	2.0767	8.416
-1224	1.8618	7.545
-1178	1.7186	6.965
-1140	1.6185	6.559
-1096	1.5037	6.094
-1046	1.4035	5.688
-1004	1.3034	5.282
-964	1.2032	4.876
-930	1.0741	4.353
-895	0.9739	3.947
-866	0.8306	3.366
-828	0.6875	2.786
-790	0.5300	2.148
-747	0.3580	1.451
-725	0.2292	0.929
-709	0.1431	0.580
-699	0.0859	0.348
-690	0.0286	0.116
-687	0.0143	0.058

Exp.No.(2)

E(V) vs. SCE	*i(mA/cm^2)*	*I(mA)*
-1500	2.5063	10.157
-1450	2.3918	9.693
-1409	2.2344	9.055
-1375	2.1053	8.532
-1353	1.9765	8.010
-1307	1.8188	7.371
-1234	1.6900	6.849
-1162	1.5612	6.327
-1132	1.4322	5.804
-1087	1.3177	5.340
-1045	1.2318	4.992
-1009	1.1027	4.469
-960	0.9883	4.005
-923	0.8594	3.483
-886	0.7161	2.902
-860	0.6016	2.438
-825	0.4868	1.973
-780	0.3867	1.567
-750	0.2865	1.161
-727	0.1863	0.755
-708	0.1002	0.406
-700	0.0716	0.290
-693	0.0429	0.174
-690	0.0286	0.116
-688	0.0143	0.058

Table A-7 Cathodic polarization results at 60^{o}C.

RPM	*$A_{cath.}$ (cm^2)*	*Conc. (g/l)CuCN*
100	**4.0526**	**75**

Exp.No.(1).

E(V)vs. SCE	*i(mA/cm^2)*	*I(mA)*
-1464	4.1963	17.006
-1426	3.6665	14.859
-1402	3.2656	13.234
-1364	2.7355	11.086
-1323	2.3346	9.461
-1290	1.9908	8.068
-1250	1.5612	6.327
-1210	1.2604	5.108
-1165	1.0598	4.295
-1110	0.9024	3.657
-1060	0.7876	3.192
-1007	0.7018	2.844
-952	0.6016	2.438
-919	0.5587	2.264
-868	0.4582	1.857
-823	0.3437	1.393
-778	0.2292	0.929
-730	0.1145	0.464
-712	0.0716	0.290
-709	0.0286	0.116
-700	0.0143	0.058

Exp.No.(2)

E(V) vs. SCE	*i(mA/cm^2)*	*I(mA)*
-1530	2.5638	10.390
-1486	2.2201	8.997
-1456	2.0051	8.126
-1423	1.7759	7.197
-1379	1.5612	6.327
-1338	1.4322	5.804
-1305	1.2890	5.224
-1260	1.2318	4.992
-1213	1.1171	4.527
-1157	1.0169	4.121
-1107	0.9310	3.773
-1075	0.8738	3.541
-1030	0.7876	3.192
-993	0.6445	2.612
-950	0.6302	2.554
-919	0.5443	2.206
-890	0.4725	1.915
-852	0.3867	1.567
-813	0.2865	1.161
-768	0.1863	0.755
-738	0.1002	0.406
-727	0.0716	0.290
-712	0.0286	0.116
-709	0.0143	0.058

Table A-8 Cathodic polarization results at 60^{o}C.

RPM	*$A_{cath.}$ (cm^2)*	*Conc. (g/l)CuCN*
200	**4.0526**	**75**

Exp.No.(1).

E(V)vs. SCE	*i(mA/cm^2)*	*I(mA)*
-1495	4.3683	17.703
-1445	3.6522	14.801
-1430	3.2224	13.059
-1400	2.9218	11.841
-1356	2.4634	9.983
-1306	2.2201	8.997
-1258	2.0338	8.242
-1210	1.9049	7.720
-1169	1.7759	7.197
-1146	1.6900	6.849
-1100	1.6328	6.617
-1049	1.4608	5.920
-1005	1.3320	5.398
-958	1.1743	4.759
-909	1.0026	4.063
-868	0.7733	3.134
-830	0.6016	2.438
-804	0.4582	1.857
-772	0.3294	1.335
-746	0.2292	0.929
-726	0.1002	0.406
-720	0.0716	0.290
-714	0.0286	0.116
-710	0.0143	0.058

Exp.No.(2)

E(V) vs. SCE	*i(mA/cm^2)*	*I(mA)*
-1505	3.3371	13.524
-1476	3.0077	12.189
-1426	2.6210	10.622
-1392	2.3489	9.519
-1348	2.0481	8.300
-1308	1.9336	7.836
-1257	1.7902	7.255
-1225	1.6471	6.675
-1160	1.4751	5.978
-1100	1.3892	5.630
-1045	1.2461	5.050
-1015	1.1743	4.759
-975	1.0455	4.237
-925	0.9167	3.715
-903	0.8163	3.308
-860	0.6588	2.670
-818	0.4868	1.973
-770	0.2865	1.161
-752	0.2292	0.929
-733	0.1431	0.580
-726	0.1002	0.406
-720	0.0572	0.232
-713	0.0286	0.116
-709	0.0143	0.058

Table A-9 Cathodic polarization results at 60°C.

RPM	*$A_{cath.}$ (cm^2)*	*Conc.(g/l)CuCN*
300	**4.0526**	**75**

Exp.No.(1).

E(V)vs. SCE	*i(mA/cm^2)*	*I(mA)*
-1537	4.5830	18.573
-1488	3.5232	14.278
-1451	3.6236	14.685
-1415	3.2369	13.118
-1387	2.9361	11.899
-1350	2.7069	10.970
-1226	2.1339	8.648
-1170	2.0194	8.184
-1100	1.9336	7.836
-1075	1.7759	7.197
-1045	1.7043	6.907
-1015	1.5898	6.443
-973	1.4608	5.920
-935	1.3177	5.340
-900	1.1743	4.759
-857	0.9453	3.831
-813	0.6731	2.728
-780	0.4439	1.799
-753	0.3437	1.393
-723	0.1863	0.755
-714	0.1145	0.464
-708	0.0716	0.290
-702	0.0286	0.116
-698	0.0143	0.058

Exp.No.(2)

E(V) vs. SCE	*i(mA/cm^2)*	*I(mA)*
-1535	3.9960	16.194
-1490	3.5232	14.278
-1468	3.1794	12.885
-1436	3.0506	12.363
-1398	2.7785	11.260
-1360	2.6497	10.738
-1330	2.4777	10.041
-1290	2.4061	9.751
-1230	2.2773	9.229
-1184	2.1339	8.648
-1145	2.0194	8.184
-1109	1.9479	7.894
-1068	1.7759	7.197
-1030	1.6185	6.559
-990	1.5037	6.094
-950	1.3177	5.340
-920	1.1600	4.701
-879	1.0026	4.063
-835	0.7304	2.960
-800	0.5157	2.090
-753	0.3437	1.393
-728	0.2149	0.871
-720	0.1574	0.638
-712	0.1145	0.464
-709	0.0716	0.290
-701	0.0429	0.174
-698	0.0143	0.058

Table A-10 Cathodic polarization results at 40^{o}C.

RPM	*$A_{cath.}$ (cm^2)*	*Conc. (g/l)CuCN*
200	**4.0526**	**17.5**

Exp.No.(1).

E(V)vs. SCE	*i(mA/cm^2)*	*I(mA)*
-1404	8.5715	34.737
-1351	5.7756	23.406
-1327	5.1224	20.759
-1290	4.0409	16.376
-1260	3.2858	13.316
-1225	2.3469	9.511
-1196	1.7754	7.195
-1172	1.4082	5.707
-1132	0.9796	3.970
-1096	0.6939	2.812
-1026	0.4081	1.654
-995	0.3062	1.241
-962	0.1836	0.744
-940	0.0612	0.248
-930	0.0407	0.165
-925	0.0205	0.083

Exp.No.(2)

E(V) vs. SCE	*i(mA/cm^2)*	*I(mA)*
-1410	8.6673	35.1251
-1355	5.8284	23.62017
-1330	5.1880	21.02489
-1305	4.1038	16.63106
-1275	3.4287	13.89515
-1245	2.5292	10.24984
-1206	1.9449	7.881902
-1168	1.5121	6.127936
-1140	1.0272	4.162831
-1105	0.7319	2.966098
-1030	0.4207	1.704929
-1009	0.3213	1.3021
-970	0.1930	0.782152
-950	0.0632	0.256124
-932	0.0422	0.17102
-922	0.0212	0.085915

Table A-11 Cathodic polarization results at 50°C.

RPM	*$A_{cath.}$ (cm^2)*	*Conc. (g/l)CuCN*
200	**4.0526**	**17.5**

Exp.No.(1).

E(V)vs. SCE	*i(mA/cm^2)*	*I(mA)*
-1416	20.7346	84.029
-1391	16.8164	68.150
-1376	12.1838	49.376
-1352	8.6734	35.150
-1312	5.6734	22.992
-1282	3.8775	15.714
-1255	3.1020	12.571
-1227	2.3878	9.677
-1203	1.8980	7.692
-1170	1.3673	5.541
-1143	1.0613	4.301
-1128	0.8775	3.556
-1102	0.7144	2.895
-1076	0.6122	2.481
-1052	0.5305	2.150
-1028	0.4081	1.654
-999	0.3062	1.241
-968	0.1634	0.662
-946	0.0612	0.248
-935	0.0407	0.165
-928	0.0205	0.083

Exp.No.(2)

E(V) vs. SCE	*i(mA/cm^2)*	*I(mA)*
-1410	20.4082	82.706
-1390	16.9388	68.646
-1377	12.2449	49.624
-1348	8.5714	34.737
-1315	5.7143	23.158
-1285	3.9796	16.128
-1250	3.1837	12.902
-1225	2.4082	9.759
-1201	1.8571	7.526
-1175	1.3878	5.624
-1140	1.0612	4.301
-1130	0.8980	3.639
-1100	0.7143	2.895
-1075	0.6327	2.564
-1055	0.5510	2.233
-1025	0.4082	1.654
-1000	0.3061	1.241
-970	0.1633	0.662
-950	0.0612	0.248
-937	0.0408	0.165
-931	0.0204	0.083

Table A-12 Cathodic polarization results at 60°C.

RPM	*$A_{cath.}$ (cm^2)*	*Conc. (g/l)CuCN*
200	**4.0526**	**17.5**

Exp.No.(1).

E(V)vs. SCE	*i(mA/cm^2)*	*I(mA)*
-1460	28.3265	114.796
-1445	21.3878	86.676
-1433	17.1633	69.556
-1424	14.3468	58.142
-1406	10.8163	43.834
-1377	7.9389	32.173
-1336	5.2041	21.090
-1303	3.5918	14.556
-1264	2.5714	10.421
-1223	1.7347	7.030
-1207	1.5101	6.120
-1160	1.1430	4.632
-1132	0.9591	3.887
-1103	0.7756	3.143
-1063	0.5917	2.398
-1028	0.3877	1.571
-1002	0.3062	1.241
-988	0.2041	0.827
-976	0.1429	0.579
-963	0.0612	0.248
-950	0.0205	0.083

Exp.No.(2)

E(V) vs. SCE	*i(mA/cm^2)*	*I(mA)*
-1465	28.5876	115.854
-1440	21.6286	87.652
-1429	17.3096	70.149
-1418	14.9339	60.521
-1402	10.4908	42.515
-1380	8.2061	33.256
-1340	5.2717	21.364
-1310	3.8193	15.478
-1255	2.7456	11.127
-1225	1.7900	7.254
-1202	1.5185	6.154
-1170	1.2932	5.241
-1142	1.0497	4.254
-1110	0.8034	3.256
-1076	0.7020	2.845
-1036	0.4002	1.622
-1010	0.3094	1.254
-985	0.2102	0.852
-977	0.1527	0.619
-964	0.0644	0.261
-948	0.0210	0.085

APPENDIX B

Tables of cathodic polarization results of zinc with different conditions

Table B-1 Cathodic polarization results at 40^{o}C.

RPM	*$A_{cath.}$ (cm^2)*	*Conc. (g/l) ZnO*
100	**4.0526**	**18.5**

Exp.No.(1).

E(V)vs. SCE	*i(mA/cm^2)*	*I(mA)*
-1445	0.9596	3.889
-1505	0.7734	3.134
-1476	0.7161	2.902
-1455	0.6445	2.612
-1426	0.6015	2.438
-1394	0.5156	2.090
-1364	0.3867	1.567
-1325	0.3581	1.451
-1298	0.3008	1.219
-1270	0.2292	0.929
-1251	0.2005	0.813
-1208	0.1575	0.638
-1183	0.1289	0.522
-1146	0.0859	0.348
-1127	0.0716	0.290
-1093	0.0430	0.174
1066	0.0286	0.116
-1042	0.0143	0.058

Exp.No.(2)

E(V) vs. SCE	*I(mA/cm^2)*	*I(mA)*
-1523	0.8593	3.483
-1492	0.7591	3.076
-1470	0.7018	2.844
-1438	0.6445	2.612
-1397	0.5586	2.264
-1358	0.4726	1.915
-1310	0.4440	1.799
-1283	0.4010	1.625
-1241	0.3294	1.335
-1213	0.2864	1.161
-1185	0.2578	1.045
-1139	0.2292	0.929
-1111	0.2005	0.813
-1090	0.1432	0.580
-1068	0.1146	0.464
-1050	0.0859	0.348
-1032	0.0430	0.174
-1002	0.0143	0.058

Table B-2 Cathodic polarization results at 40^{o}C.

RPM	*$A_{cath.}$ (cm^2)*	*Conc. (g/l) ZnO*
200	**4.0526**	**18.5**

Exp.No.(1).

E(V)vs. SCE	*I(mA/cm^2)*	*I(mA)*
-1497	3.3657	13.640
-1448	2.9647	12.015
-1423	2.6353	10.680
-1400	2.4634	9.983
-1377	1.8332	7.429
-1354	1.5325	6.211
-1328	1.2604	5.108
-1303	0.9596	3.889
-1288	0.8450	3.424
-1272	0.7161	2.902
-1243	0.6302	2.554
-1230	0.5586	2.264
-1187	0.4726	1.915
-1140	0.4010	1.625
-1125	0.3437	1.393
-1070	0.2721	1.103
-1024	0.1432	0.580
-1018	0.1289	0.522
-1011	0.0859	0.348
-1007	0.0716	0.290
-1000	0.0286	0.116
-998	0.0143	0.058

Exp.No.(2)

E(V) vs. SCE	*i(mA/cm^2)*	*I(mA)*
-1450	2.9360	11.899
-1425	2.6066	10.564
-1401	2.4777	10.041
-1375	1.8476	7.487
-1350	1.5182	6.152
-1329	1.2747	5.166
-1302	0.9309	3.773
-1290	0.8307	3.366
-1270	0.7304	2.960
-1250	0.6302	2.554
-1232	0.5442	2.206
-1188	0.4870	1.973
-1142	0.4153	1.683
-1126	0.3581	1.451
-1075	0.2721	1.103
-1025	0.1575	0.638
-1020	0.1289	0.522
-1011	0.0859	0.348
-1007	0.0716	0.290
-1000	0.0286	0.116
-999	0.0143	0.058

Table B-3 Cathodic polarization results at 40°C.

RPM	***$A_{cath.}$ (cm^2)***	***Conc. (g/l) ZnO***
300	**4.0526**	**18.5**

Exp.No.(1).

E(V)vs. SCE	***i(mA/cm^2)***	***I(mA)***
-1504	0.7734	3.134
-1465	0.7304	2.960
-1435	0.6302	2.554
-1401	0.5729	2.322
-1370	0.5299	2.148
-1352	0.5013	2.031
-1308	0.4010	1.625
-1271	0.3151	1.277
-1237	0.2721	1.103
-1206	0.2148	0.871
-1186	0.1862	0.755
-1157	0.1146	0.464
-1110	0.0573	0.232
-1078	0.0301	0.122
-1042	0.0143	0.058

Exp.No.(2)

E(V) vs. SCE	***i(mA/cm^2)***	***I(mA)***
-1475	0.7448	3.018
-1432	0.6159	2.496
-1401	0.5872	2.380
-1375	0.5299	2.148
-1345	0.4726	1.915
-1302	0.3867	1.567
-1280	0.3581	1.451
-1243	0.2864	1.161
-1210	0.2292	0.929
-1180	0.1719	0.697
-1147	0.1003	0.406
-1112	0.0716	0.290
-1080	0.0286	0.116
-1030	0.0143	0.058

Table B-4 Cathodic polarization results at 50°C.

RPM	*$A_{cath.}$ (cm^2)*	*Conc. (g/l) ZnO*
100	**4.0526**	**18.5**

Exp.No.(1).

E(V)vs. SCE	*i(mA/cm^2)*	*I(mA)*
-1458	3.4516	13.988
-1425	3.3227	13.466
-1389	3.0506	12.363
-1364	2.8358	11.492
-1328	2.4634	9.983
-1306	2.0051	8.126
-1275	1.5754	6.385
-1253	1.3033	5.282
-1230	1.1458	4.643
-1209	1.0169	4.121
-1186	0.8880	3.599
-1170	0.7877	3.192
-1153	0.6731	2.728
-1136	0.5729	2.322
-1098	0.4583	1.857
-1054	0.3294	1.335
-1034	0.1862	0.755
-1028	0.1289	0.522
-1022	0.1003	0.406
-1020	0.0716	0.290
-1015	0.0286	0.116
-1011	0.0143	0.058

Exp.No.(2)

E(V) vs. SCE	*i(mA/cm^2)*	*I(mA)*
-1530	4.0389	16.368
-1490	3.6665	14.859
-1466	3.1652	12.827
-1432	2.8931	11.724
-1401	2.6210	10.622
-1381	2.0767	8.416
-1350	1.6041	6.501
-1310	1.4036	5.688
-1280	1.1744	4.759
-1254	1.0455	4.237
-1238	0.9596	3.889
-1202	0.8307	3.366
-1183	0.7018	2.844
-1146	0.5872	2.380
-1110	0.4726	1.915
-1092	0.3581	1.451
-1068	0.1862	0.755
-1040	0.1146	0.464
-1022	0.0573	0.232
-1013	0.0286	0.116
-1008	0.0143	0.058

Table B-5 Cathodic polarization results at 50°C.

RPM	*$A_{cath.}$ (cm^2)*	*Conc. (g/l) ZnO*
200	**4.0526**	**18.5**

Exp.No.(1).

E(V)vs. SCE	*i(mA/cm^2)*	*I(mA)*
-1528	5.0701	20.547
-1471	4.5258	18.341
-1442	4.0245	16.310
-1419	3.4660	14.046
-1381	2.9074	11.783
-1360	2.7069	10.970
-1345	2.1626	8.764
-1330	1.9765	8.010
-1298	1.7187	6.965
-1280	1.5754	6.385
-1247	1.4609	5.920
-1206	1.3033	5.282
-1180	1.2317	4.992
1151	1.1171	4.527
-1111	0.9596	3.889
1076	0.6875	2.786
-1046	0.3581	1.451
-1036	0.2435	0.987
-1029	0.1432	0.580
-1024	0.1003	0.406
-1022	0.0716	0.290
-1016	0.0286	0.116
-1014	0.0143	0.058

Exp.No.(2)

E(V) vs. SCE	*i(mA/cm^2)*	*I(mA)*
-1490	6.3161	25.597
-1467	5.7575	23.333
-1433	5.0414	20.431
-1406	4.7406	19.212
-1380	4.2823	17.355
-1355	3.7524	15.207
-1323	3.1652	12.827
-1296	2.7642	11.202
-1270	2.2915	9.287
-1236	1.7616	7.139
-1203	1.4465	5.862
-1186	1.1887	4.817
-1146	0.7304	2.960
-1110	0.5586	2.264
-1092	0.4010	1.625
-1067	0.2578	1.045
-1042	0.1432	0.580
-1030	0.1003	0.406
-1021	0.0716	0.290
-1009	0.0430	0.174
-1003	0.0143	0.058

Table B-6 Cathodic polarization results at 50^{o}C.

RPM	*A$_{cath.}$ (cm^2)*	*Conc. (g/l) ZnO*
300	**4.0526**	**18.5**

Exp.No.(1).

E(V)vs. SCE	*i(mA/cm^2)*	*I(mA)*
-1476	5.6000	22.694
-1440	4.8266	19.560
-1425	4.0532	16.426
-1402	3.6378	14.743
-1370	2.7928	11.318
-1348	2.0194	8.184
-1328	1.4895	6.036
-1310	1.2460	5.050
-1290	0.9023	3.657
-1250	0.6731	2.728
-1217	0.5872	2.380
-1209	0.5586	2.264
-1183	0.5013	2.031
-1146	0.4440	1.799
-1112	0.3867	1.567
-1092	0.2864	1.161
-1060	0.2578	1.045
-1042	0.2292	0.929
-1030	0.1575	0.638
-1018	0.1146	0.464
-1008	0.0859	0.348
-1001	0.0286	0.116
-998	0.0143	0.058

Exp.No.(2)

E(V) vs. SCE	*i(mA/cm^2)*	*I(mA)*
-1522	6.0153	24.378
-1480	5.6573	22.927
-1467	5.4711	22.172
-1422	5.0987	20.663
-1393	4.4685	18.109
-1367	3.3944	13.756
-1328	2.6210	10.622
-1302	1.8905	7.662
-1186	1.2747	5.166
-1139	0.5586	2.264
-1123	0.4870	1.973
-1110	0.4010	1.625
-1090	0.3008	1.219
-1070	0.2435	0.987
-1062	0.1862	0.755
-1043	0.1289	0.522
-1027	0.1003	0.406
1013	0.0716	0.290
-1010	0.0430	0.174
-1001	0.0143	0.058

Table B-7 Cathodic polarization results at 60^{o}C.

RPM	*$A_{cath.}$ (cm^2)*	*Conc.(g/l) ZnO*
100	**4.0526**	**18.5**

Exp.No.(1).

E(V)vs. SCE	*i(mA/cm^2)*	*I(mA)*
-1570	9.4813	38.424
-1515	8.0920	32.794
-1471	7.0035	28.383
-1438	6.1872	25.074
-1410	5.4997	22.288
-1387	4.9555	20.083
-1356	4.1678	16.890
-1330	3.6092	14.627
-1310	3.1652	12.827
-1281	2.6066	10.564
-1260	2.2199	8.997
-1252	2.0624	8.358
-1246	1.9192	7.778
-1232	1.6900	6.849
-1210	1.4322	5.804
-1184	1.1458	4.643
-1156	0.9596	3.889
-1132	0.8307	3.366
-1110	0.7304	2.960
-1082	0.6445	2.612
-1060	0.5729	2.322
-1012	0.4726	1.915
-982	0.4153	1.683
-952	0.3581	1.451
-909	0.3151	1.277
-871	0.2435	0.987
-843	0.1719	0.697
-821	0.1146	0.464
-790	0.0143	0.058

Exp.No.(2)

E(V) vs. SCE	*i(mA/cm^2)*	*I(mA)*
-1560	15.3963	62.395
-1493	12.5462	50.845
-1435	10.0971	40.920
-1403	8.3642	33.897
-1376	7.2041	29.195
-1354	6.3304	25.655
-1333	5.6286	22.811
-1311	4.6547	18.864
-1290	3.8956	15.787
-1270	3.1795	12.885
-1257	2.7642	11.202
-1230	2.1913	8.880
-1200	1.7187	6.965
-1185	1.5325	6.211
-1180	1.3749	5.572
-1156	1.1028	4.469
-1123	0.9453	3.831
-1093	0.7877	3.192
-1060	15.3963	62.395
-1029	12.5462	50.845
-992	10.0971	40.920
-960	8.3642	33.897
-930	7.2041	29.195
-900	6.3304	25.655
-873	5.6286	22.811
-836	4.6547	18.864
-807	3.8956	15.787
-787	3.1795	12.885
-770	2.7642	11.202

Table B-8 Cathodic polarization results at 60^{o}C.

RPM	*$A_{cath.}$ (cm^2)*	*Conc. (g/l) ZnO*
200	**4.0526**	**18.5**

Exp.No.(1).

E(V)vs. SCE	*I(mA/cm^2)*	*I(mA)*
-1545	5.408163	21.91712
-1523	5.102041	20.67653
-1501	4.387755	17.78182
-1477	3.795918	15.38334
-1452	3.102041	12.57133
-1431	2.755102	11.16533
-1405	2.285714	9.263085
-1379	1.877551	7.608963
-1361	1.755102	7.112726
-1330	1.55102	6.285664
-1302	1.44898	5.872136
-1276	1.326531	5.3759
-1251	1.204082	4.879663
-1221	1.081633	4.383426
-1198	0.959184	3.887188
-1170	0.714286	2.894714
-1148	0.367347	1.48871
-1123	0.244898	0.992474
-1103	0.163265	0.661649
-1090	0.122449	0.496237
-1070	0.081633	0.330824
-1050	0.040816	0.165412
-1030	0.020408	0.082706

Exp.No.(2)

E(V) vs. SCE	*i(mA/cm^2)*	*I(mA)*
-1540	5.367347	21.75171
-1525	5.061224	20.51112
-1490	4.408163	17.86452
-1470	3.77551	15.30063
-1450	3.102041	12.57133
-1430	2.755102	11.16533
-1402	2.265306	9.180379
-1378	1.897959	7.691669
-1360	1.77551	7.195432
-1332	1.530612	6.202958
-1300	1.428571	5.789427
-1272	1.326531	5.3759
-1256	1.22449	4.962368
-1220	1.061224	4.300716
-1201	0.979592	3.969894
-1171	0.653061	2.646596
-1150	0.387755	1.571416
-1124	0.265306	1.07518
-1104	0.163265	0.661649
-1085	0.122449	0.496237
-1070	0.081633	0.330824
-1050	0.040816	0.165412
-1030	0.020408	0.082706

Table B-9 Cathodic polarization results at 60°C.

RPM	***$A_{cath.}$ (cm^2)***	***Conc. (g/l) ZnO***
300	**4.0526**	**18.5**

Exp.No.(1).

E(V)vs. SCE	***i(mA/cm^2)***	***I(mA)***
-1488	5.4567	22.114
-1440	5.0701	20.547
-1436	4.7406	19.212
-1408	4.1821	16.948
-1383	3.7524	15.207
-1370	3.3944	13.756
-1350	2.6496	10.738
-1335	2.2915	9.287
-1326	1.8762	7.604
-1309	1.4895	6.036
-1278	1.0742	4.353
-1260	0.9309	3.773
-1214	0.7734	3.134
-1191	0.6875	2.786
-1162	0.6302	2.554
-1132	0.5872	2.380
-1110	0.5442	2.206
-1074	0.4726	1.915
-1045	0.3581	1.451
-1029	0.2435	0.987
-1018	0.1432	0.580
-1013	0.1003	0.406
-1010	0.0716	0.290
-1005	0.0286	0.116
-1003	0.0143	0.058

Exp.No.(2)

E(V) vs. SCE	***i(mA/cm^2)***	***I(mA)***
-1525	5.9151	23.971
-1470	5.2276	21.185
-1443	5.0414	20.431
-1420	4.3110	17.471
-1390	3.8956	15.787
-1349	2.5780	10.448
-1320	2.1054	8.532
-1310	1.5754	6.385
1270	1.0312	4.179
-1253	0.8737	3.541
-1210	0.7018	2.844
-1188	0.6588	2.670
-1158	0.6015	2.438
-1113	0.5442	2.206
-1078	0.4870	1.973
-1050	0.3867	1.567
-1030	0.2578	1.045
-1020	0.1719	0.697
-1014	0.1146	0.464
-1009	0.0859	0.348
-1006	0.0716	0.290
-1001	0.0286	0.116
-997	0.0143	0.058

Table B-10 Cathodic polarization results at 40^{o}C.

RPM	***$A_{cath.}$ (cm^2)***	***Conc. (g/l) ZnO***
200	**4.0526**	**12.5**

Exp.No.(1).

E(V)vs. SCE	***i(mA/cm^2)***	***I(mA)***
-1480	4.7959	19.436
-1448	4.2245	17.120
-1423	3.7551	15.218
-1400	3.5102	14.225
-1377	2.6122	10.586
-1354	2.1837	8.850
-1328	1.7959	7.278
-1303	1.3673	5.541
-1288	1.2041	4.880
-1272	1.0204	4.135
-1243	0.8980	3.639
-1230	0.7959	3.226
-1187	0.6735	2.729
-1140	0.5714	2.316
-1125	0.4898	1.985
-1070	0.3878	1.571
-1024	0.2041	0.827
-1018	0.1837	0.744
-1011	0.1224	0.496
-1007	0.1020	0.414
-1000	0.0408	0.165
-998	0.0204	0.083

Exp.No.(2)

E(V) vs. SCE	***i(mA/cm^2)***	***I(mA)***
-1450	4.1837	16.955
-1425	3.7143	15.053
-1401	3.5306	14.308
-1375	2.6327	10.669
-1350	2.1633	8.767
-1329	1.8163	7.361
-1302	1.3265	5.376
-1290	1.1837	4.797
-1270	1.0408	4.218
-1250	0.8980	3.639
-1232	0.7755	3.143
-1188	0.6939	2.812
-1142	0.5918	2.398
-1126	0.5102	2.068
-1075	0.3878	1.571
-1025	0.2245	0.910
-1020	0.1837	0.744
-1011	0.1224	0.496
-1007	0.1020	0.414
-1000	0.0408	0.165
-999	0.0204	0.083

Table B-11 Cathodic polarization results at 50°C.

RPM	*$A_{cath.}$ (cm^2)*	*Conc. (g/l) ZnO*
200	**4.0526**	**12.5**

Exp.No.(1).

E(V)vs. SCE	*i(mA/cm^2)*	*I(mA)*
-1532	7.1633	29.030
-1471	6.5306	26.466
-1440	5.7143	23.158
-1422	4.9184	19.932
-1382	4.4694	18.113
-1360	3.8776	15.714
-1351	3.0612	12.406
-1333	2.8367	11.496
-1292	2.4694	10.007
-1278	2.2857	9.263
-1255	2.0816	8.436
-1208	1.8367	7.444
-1182	1.7755	7.195
-1156	1.5306	6.203
-1107	1.4082	5.707
-1078	1.0204	4.135
-1051	0.5510	2.233
-1040	0.2449	0.992
-1027	0.1429	0.579
-1024	0.1020	0.414
-1020	0.0408	0.165
-1016	0.0204	0.083

Exp.No.(2)

E(V) vs. SCE	*i(mA/cm^2)*	*I(mA)*
-1530	7.1429	28.947
-1470	6.5510	26.549
-1442	5.7143	23.158
-1420	4.8980	19.849
-1380	4.4898	18.195
-1361	3.8980	15.797
-1350	3.0408	12.323
-1332	2.8571	11.579
-1290	2.4490	9.925
-1275	2.3469	9.511
-1250	2.1020	8.519
-1206	1.8571	7.526
-1180	1.7755	7.195
-1160	1.5306	6.203
-1109	1.4286	5.789
-1080	1.0816	4.383
-1050	0.5510	2.233
-1044	0.2653	1.075
-1029	0.1429	0.579
-1025	0.1020	0.414
-1022	0.0408	0.165
-1015	0.0204	0.083

Table B-12 Cathodic polarization results at 60°C.

RPM	*$A_{cath.}$ (cm^2)*	*Conc. (g/l) ZnO*
200	**4.0526**	**12.5**

Exp.No.(1).

E(V)vs. SCE	*i(mA/cm^2)*	*I(mA)*
-1501	0.9184	3.722
-1473	0.7551	3.060
-1445	0.6735	2.729
-1408	0.6122	2.481
-1400	0.5714	2.316
-1371	0.4490	1.820
-1345	0.4082	1.654
-1310	0.3469	1.406
-1280	0.2857	1.158
-1245	0.2449	0.992
-1203	0.1837	0.744
-1172	0.1429	0.579
-1140	0.1020	0.414
-1092	0.0816	0.331
-1070	0.0612	0.248
-1044	0.0408	0.165
-1033	0.0204	0.083

Exp.No.(2)

E(V) vs. SCE	*i(mA/cm^2)*	*I(mA)*
-1545	1.1429	4.632
-1505	0.8980	3.639
-1475	0.7755	3.143
-1433	0.6735	2.729
-1410	0.6531	2.647
-1388	0.5510	2.233
-1372	0.5102	2.068
-1340	0.4286	1.737
-1315	0.3673	1.489
-1308	0.3469	1.406
-1290	0.3061	1.241
-1240	0.2449	0.992
-1206	0.2041	0.827
-1150	0.1224	0.496
-1099	0.0816	0.331
-1075	0.0612	0.248
-1041	0.0408	0.165
-1030	0.0204	0.083

APPENDIX C

Sample of Calculations

Calculations of cathodic current efficiency for zinc and copper:

By using equation

$$\text{Eff \%} = w/w_t \times 100 \qquad \ldots 2.1$$

where (w) is the experimental weight of the deposit and (w_t) is the theoretical weight of the deposit. The theoretical weight of the individual metal deposited can be calculated as follows:

$$w_t = \frac{Q}{Faraday's} \times Equivalent\ Weight\ of\ metal \qquad \ldots.\ 2.2$$

Where ($Q = I \times t$) is the amount of electricity passed through the cell and expressed in ampere second and Faraday's constant is 96485 [2]. Equivalent weight of copper 31.773 and 32.69 for zinc [5].

For Zinc

Total current I = 81 mA, time = 10 min, Temp. 50^{O}C, 200 RPM, 12.5 g/l ZnO and equivalent weight of zinc=32.69

For zinc plating	
w_{z1}(cathode weigh before electroplating)(g)	**w_{z2} (cathode weigh after electroplating)(g)**
5.2132	5.2262

$w = w_{z2} - w_{z1}$

$w = 5.2262 - 5.2132$

$w = 0.013$ g

$Q= 81 * 10^{-3} * 10 * 60$

Q= 48.6 A.sec (= Coulomb)

w_{tZn}= 48.6 * 32.69/96485

w_{tZn}=0.016466g

Eff%= (0.013 / 0.016466) *100

=78.95% cathodic current efficiency for zinc at Temp. 50^{O}C, 200 RPM and 12.5g/l ZnO.

For Copper

Total current I = 81 mA, time = 10 min, Temp. 50^{O}C, 200 RPM, 17.5g/l CuCN and equivalent weight of zinc=31.773

For Copper Plating	
w_{c1}(cathode weigh before electroplating)	**w_{c2} (cathode weigh after electroplating)**
5.1854	5.198

$w=w_{c2}- w_{c1}$

w=5.198 – 5.1854

w=0.0126 g

$Q= 81 * 10^{-3} * 10 * 60$

Q= 48.6 A.sec (= Coulomb)

w_{tCu}= 48.6 * 31.773/96485

w_{tCu}=0.016004 g

Eff%= (0.0126 / 0.016004) *100

=78.73% cathodic current efficiency for copper at Temp. 50^{O}C, 200 RPM and 17.5 g/l CuCN

APPENDIX D

Sample of Calculations

To Obtain Current Density for Copper and Zinc for Certain Percentage of Brass Electroplating

To evaluate the current densities for copper and zinc to obtain 60% of copper and 40% of zinc as an alloy electroplating (brass):

From equation 5.9 we find the ratio of i_{Cu}/i_{Zn} as follows:

i_{Cu}/i_{Zn}= 0.719735+0.005395* exp(0.082058*60)-0.001086*exp(0.082123*40)

= 1.49

and C.C= 99.818% then i_{Cu}/i_{Zn} =1.487.

If we take i_{Zn} = 5 mA/cm^2 then i_{Cu} =7.43 mA/cm^2

To insure that current densities will lead to same percentage, from equations 2.2 so:

For cathode area A= 4 cm^2, and plating time 10 min.

Theoretical weight of copper $$w_{tCu} = \frac{7.43*4*10^{-3}*10*60*31.773}{96485}$$

$$=0.005872 \text{ g}$$

Theoretical weight of zinc $$w_{tZn} = \frac{5*4*10^{-3}*10*60*32.69}{96485}$$

$$= 0.004065 \text{ g}$$

Total theoretical weight = 0.009937

w_{tCu}% = (0.005872 /0.009937) *100

= 59.09

w_{tZn}% = (0.004065 /0.009937)*100

= 40.90

APPENDIX E

Table E-1 Electrochemical Series of Common Metals

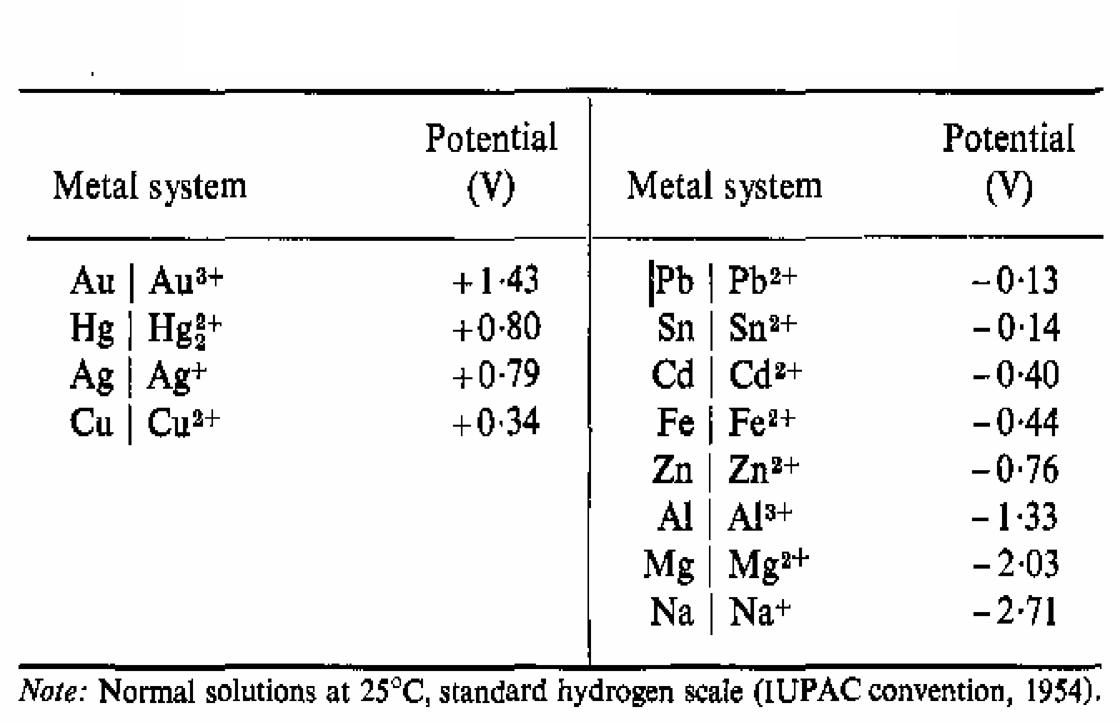

Metal system	Potential (V)	Metal system	Potential (V)
Au | Au^{3+}	+1·43	Pb | Pb^{2+}	−0·13
Hg | Hg_2^{2+}	+0·80	Sn | Sn^{2+}	−0·14
Ag | Ag^{+}	+0·79	Cd | Cd^{2+}	−0·40
Cu | Cu^{2+}	+0·34	Fe | Fe^{2+}	−0·44
		Zn | Zn^{2+}	−0·76
		Al | Al^{3+}	−1·33
		Mg | Mg^{2+}	−2·03
		Na | Na^{+}	−2·71

Note: Normal solutions at 25°C, standard hydrogen scale (IUPAC convention, 1954).

الخلاصة

إنّ الهدفَ من العملِ هو الحْصول على علاقة بين نسبٍ مئويةٍ مختلفةٍ منْ طلاءِ سبيكةِ النحاس الاصفر(البراص) المتكونة من عنصري النحاس و الخارصين وذلك بتَطبيق الكثافات المختلفة من التيارات على كلٍ مِنَ النحاس والخارصين (كأقطاب موجبة) في محلولٍ سيانيدي. وكذلك دراسةُ تأثيرِ المتغيّراتِ المُخْتَلِفةِ لطلاءِ النحاسِ والخارصين(كأقطاب موجبة) على قضيبٍ منَ الجرافايت (كقطب سالب). وايضا دراسةُ سلوكِ كفاءةِ التيارِ الكاثودي بحالاتٍ مختلفةٍ من درجات الحرارة ، والوقت، و كثافات التيار الكاثودي ، وتركيز سيانيد النحاس(CuCN) في الحمّامِ النحاسي وتركيز اوكسيد الخارصين(ZnO) في الحمّامِ الخارصيني.

إنّ جهدَ الترسيبِ عاملٌ مهمٌ في طلاءِ السبيكةِ الذي يُحدّدُ من قبلِ عملياتِ الإستقطابِ الكاثودي بدلاً مِنْ ان يُحددَ من قبلِ سلسلةِ e. m. f. إنّ فائدةَ إستعمالُ المحاليلِ المعقّدةِ (سيانيد)هوتقليلُ الفارقِ الحاصل بين جهود الترسيب لمعدنين مختلفين و الذي لايحصلُ في المحاليل المائية.

و قد اختبرتْ كفاءةُ التيارِ الكاثودي لأربعة عواملِ رئيسيةِ والتي تُؤثرُ على عمليةِ الطلاءِ. وهي درجاتَ الحرارة، وقت عمليةِ الطلاء ، كثافة التيار الكاثودي وتركيز سيانيد النحاس(CuCN) في طلاء النحاس و تركيز اوكسيد الخارصين(ZnO) في طلاء الخارصين.

ودلتِ النَتائِجُ بأنّ كفاءةَ التيار الكاثودي تزدادُ بزيادةِ درجة الحرارة، وقت عملية الطلاء و بزيادةِ تركيز كلٍ من سيانيد النحاس CuCN في طلاء النحاس و اوكسيد الخارصين ZnO في طلاءالخارصين وتنقصُ بزيادةِ كثافةِ التيار الكاثودي.

وقد وجدتْ صيغةٌ تُظهرُ العلاقة بين كثافة التيار المسلطِ على النحاس (i_{Cu}) وكثافة التيار المسلط على الخارصين (i_{Zn}) مع النسَب المئويةِ مِنْ طلاء سبيكة البراص (% Zn ,% Cu) كالتالي:

$$\mathbf{i_{Cu} / i_{Zn} = 0.719735 + 0.005395 * exp (0.082058 * Cu \%) - (0.001086*exp (0.082123 * Zn\%)}$$

إنّ شروطَ المعادلةِ المذكورة يجب ان تكون درجة حرارة المحلول ٥٠ C˚، و سرعة جهاز الخلط 200RPM، ومكونات محلول طلاء سبيكةالبراص هي CuCN ١٧,٥ g /l، ZnO 12.5 g /l، NaCN 38 g /l و NaOH ٩٦,١ g /l.

شكر و تقدير

اودُ أن أعبر عن خالص شكري وتقديري وَ امتناني العميق للمشرف الاستاذ الدكتور قاسم جبار محمد السليمان و الدكتور نصير الحبوبي لما بذلوه من جهد كبير و ارشادات سديدة و قيمة طوال فترة اعداد الرسالة.

أودُ أيضاً أن أشكر السيد رئيس القسم و موظفي قسم الهندسة الكيماوية لإبدائهم المساعدة اللازمة أثناء فترة البحث.

ولا أنسى أن أتقدم بالشكر و الامتنان إلى من لازمني طوال فترة البحث وخلال أصعب الظروف إلى أعز من في الوجود إلى أبي و أمي و جميع أفراد عائلتي فلهم جزيل الشكر و التقدير.

م. احمد يقظان موسى

الترسيب الكهروكيميائي المشترك للمعادن

رسالة

مقدمة الى كلية الهندسة في جامعة النهرين و هي جزء من متطلبات نيل

درجة ماجستير علوم في الهندسة الكيمياوية

من قبل

احمد يقظان موسى

(بكالوريوس في الهندسة الكيمياوية ٢٠٠٢)

ربيع الثاني ١٤٢٦

نيسان ٢٠٠٥